2020

Donor Age Effects on the Proliferative and Chondrogenic/ Osteogenic Differentiation Performance of Equine Bone Marrow- and Adipose Tissue Derived Mesenchymal Stem Cells in Culture

Jasmin Bagge
University of Kentucky, jasminbagge_lady@hotmail.com
Author ORCID Identifier:
https://orcid.org/0000-0002-8090-5074
Digital Object Identifier: https://doi.org/10.13023/etd.2020.054

STUDENT AGREEMENT:

I represent that my thesis or dissertation and abstract are my original work. Proper attribution has been given to all outside sources. I understand that I am solely responsible for obtaining any needed copyright permissions. I have obtained needed written permission statement(s) from the owner(s) of each third-party copyrighted matter to be included in my work, allowing electronic distribution (if such use is not permitted by the fair use doctrine) which will be submitted to UKnowledge as Additional File.

I hereby grant to The University of Kentucky and its agents the irrevocable, non-exclusive, and royalty-free license to archive and make accessible my work in whole or in part in all forms of media, now or hereafter known. I agree that the document mentioned above may be made available immediately for worldwide access unless an embargo applies.

I retain all other ownership rights to the copyright of my work. I also retain the right to use in future works (such as articles or books) all or part of my work. I understand that I am free to register the copyright to my work.

REVIEW, APPROVAL AND ACCEPTANCE

The document mentioned above has been reviewed and accepted by the student's advisor, on behalf of the advisory committee, and by the Director of Graduate Studies (DGS), on behalf of the program; we verify that this is the final, approved version of the student's thesis including all changes required by the advisory committee. The undersigned agree to abide by the statements above.

Jasmin Bagge, Student

Dr. James N. MacLeod, Major Professor

Dr. Daniel Howe, Director of Graduate Studies

DONOR AGE EFFECTS ON THE PROLIFERATIVE AND CHONDROGENIC/ OSTEOGENIC DIFFERENTIATION PERFORMANCE OF EQUINE BONE MARROW- AND ADIPOSE TISSUE DERIVED MESENCHYMAL STEM CELLS IN CULTURE

DISSERTATION

A dissertation submitted in partial fulfillment of the
requirements for the degree of Doctor of Philosophy in the
College of Agriculture, Food and Environment
at the University of Kentucky

By
Jasmin Bagge
Lexington, Kentucky
Director: Dr. James N. MacLeod, Professor of Veterinary Science
Lexington, Kentucky
2020

https://orcid.org/0000-0002-8090-5074

ABSTRACT OF DISSERTATION

DONOR AGE EFFECTS ON THE PROLIFERATIVE AND CHONDROGENIC/ OSTEOGENIC DIFFERENTIATION PERFORMANCE OF EQUINE BONE MARROW- AND ADIPOSE TISSUE DERIVED MESENCHYMAL STEM CELLS IN CULTURE

Orthopedic injuries are a major cause of lameness and morbidity in horses. Bone marrow (BM)- and adipose tissue (AT) derived mesenchymal stem cells (MSCs) have shown potential to facilitate the repair of orthopedic injuries and are being used increasingly in veterinary clinics. Presently, the use of MSCs as a therapy for equine patients is most commonly applied as autologous transplants, using BM- and AT-MSCs harvested from the patient shortly after the time of injury. Cell-based therapies are therefore delayed to enable primary cell numbers to be expanded in culture. Of concern, however, are human and rodent studies that have shown a sharp decline in MSC quantity and quality with increasing donor age. This may be problematic for the important equine demographic of older orthopedic patients due to current recommendations that often call for 10-100 million MSCs in treatment protocols.

This thesis, therefore, examines the critical gap of knowledge on the relationship between donor age and MSC parameters in horses and tests the hypothesis that increasing donor age is a major variable in equine BM- and AT-MSC proliferation and chondrogenic/osteogenic differentiation with decreasing capacities following non-linear kinetics.

To this end, BM- and AT-MSCs and dermal fibroblasts (biological negative control) were harvested immediately post mortem from horses in 5 different age groups, with 4 horses in each age group. The age groups were newborn (0 days), yearling (1-2 years), adult (5-8 years), middle-aged (12-18 years), and geriatric (≥ 22 years) horses.

In the first part of the study, the cellular proliferation of the cells was tested using an EdU incorporation assay and by targeted gene expression analysis of proliferation, aging and senescent biomarkers. The results showed that the cellular proliferation of equine MSCs declined with increasing donor age, but interestingly there were no significant difference in pairwise comparisons between age groups other than the geriatric horses. The cellular proliferation of the two MSC types was equally affected by donor age. Tumor suppressor gene expression was up-regulated with increasing donor age.

In the second part of the study, the same cells were grown in culture and stimulated separately to differentiate into both chondrocytes and osteocytes. The chondrogenic differentiation potential of the cells was compared quantitatively by measuring pellet size, matrix proteoglycan, and gene expression of articular cartilage biomarkers. The osteogenic differentiation potential of the cells was assessed quantitatively by measuring alkaline phosphatase activity, calcium deposition, and gene

expression of subchondral bone biomarkers. Overall, the data showed that the chondrogenic and osteogenic differentiation potential of equine MSCs decline with increasing donor age. The data further indicated that BM-MSCs have a larger chondrogenic pellet size and proteoglycan content, and a higher alkaline phosphatase activity compared to AT-MSCs, and that BM-MSCs calcium deposition was affected earlier by donor age. The chondrogenic and osteogenic differentiation performance of BM-MSCs declined already between newborn and yearlings. AT-MSCs showed minimal chondrogenic differentiation performance in all age groups. Gene expression of growth factors, chondrogenic and osteogenic biomarkers were down-regulated with increasing donor age.

Together, these results support the hypothesis that equine BM- and AT-MSCs proliferation and chondrogenic/osteogenic differentiation decline with increasing donor age following non-linear kinetics. Hence, the study highlights the importance of donor age considerations and MSC selection for autologous treatment of orthopedic injuries. This new knowledge has the potential to optimize autologous stem cell therapies of cartilage and bone injuries in horses, and will help advice owners on when to harvest and potentially cryopreserve the cells.

KEYWORDS: Horse, Mesenchymal Stem Cells, Donor Age, Proliferation, Cartilage, Bone

Jasmin Bagge

01/16/2020

Date

DONOR AGE EFFECTS ON THE PROLIFERATIVE AND CHONDROGENIC/ OSTEOGENIC DIFFERENTIATION PERFORMANCE OF EQUINE BONE MARROW- AND ADIPOSE TISSUE DERIVED MESENCHYMAL STEM CELLS IN CULTURE

By
Jasmin Bagge

Dr. James N. MacLeod
Director of Dissertation

Dr. Daniel Howe
Director of Graduate Studies

01/16/2020
Date

ACKNOWLEDGMENTS

The journey of this dual degree PhD program has been the mountain ride of a life time and would not have been possible without the tremendous support and guidance from many people. Firstly, I would like to give heartfelt thanks to my American mentor, Dr. James MacLeod, for his incredible guidance, encouragement, honesty, and profound dedication to making me succeed both on a professional and personal level. Dr. MacLeod exemplifies the high quality mentorship and wisdom to which I aspire. Secondly, I am very grateful to my Danish mentor, Dr. Lise Berg, for believing in me and for giving me the opportunity to pursue this unique dual degree PhD. Dr. Berg's positive guidance opened up my eyes to the life-changing wonders of stem cell research and supported me in keeping the clinically relevant questions in focus throughout this PhD.

I would also like to thank my Dissertation Committee; Drs. Amanda Adams, Jennifer Janes, and John McCarthy, whom each provided support, guidance, and research resources that substantially improved my thinking and project. My clinical mentor, Dr. Denis Verwilghen, was instrumental in defining the path of my research and in initiating this program. For this, I am extremely grateful. Thank you to Matthew Rutledge, Eva Loveland, and Dr. Arnold Stromberg for steering me straight in the world of statistics, and to Dr. Ashley Steuer and Jamie Norris for programming assistance.

I am very grateful for the friendship and assistance of previous and present lab members, particularly Bianca Ruspi, Emily Melcher, Simone Buchardt, Maria Rhod and ChanHee Mok for helping me when I needed it the most. I would also like to thank Tina Roust, Annie Ravn, Rachael Lowney, Nikolette Birky, Dr. Rashmi Dubey, Dr. Scotty

DePriest, Dr. Emma Adam, Dr. Parvathy Thampi, Dr. Line Thomsen, Dr. Louise Bundgaard, Dr. Bruno Menarim, Angela Mangine, and Kathryn Babiarz for their immense support and assistance in this research. A big shout out should also go to my study-buddy in crime, Jessica Hanneman, for keeping a good sense of humor after a long day of studying. I am truly grateful for the support and help of the faculty, office staff, lab technicians, and graduate students at Gluck Equine Research Center and the University of Copenhagen. I graciously acknowledge the help of Drs. Ball and Adams' laboratories and the Veterinary Diagnostic Lab to collect cells from newborn and geriatric horses, together with Dr. Kevin Murach's help in optimizing the EdU assay and Day Barker's help with control qPCR. I appreciate the research funding from the Independent Research Fund Denmark (NIH 133500133B), Hesteafgiftsfonden, The Lourie Family Foundation, and other funding sources that made this research possible.

None of this would have been possible without the love and support of the best family, friends, horse, and dog a girl could ask for. Thank you Mary Lou and Ernie Bailey for opening up your home and for making us feel like family. Thank you mom and dad for always believing in me and for showing me that through hard work you can do anything you set your mind to. Words cannot explain how grateful I am that you are always there for me. My heartfelt thanks to my brother for his loving support, scientific sparing, and for flying all the way to Lexington to lend a helping hand. Finally, I thank my lucky star for the day I met the love of my life and best friend, Martin, whom without I could not have done any of this, and for the light of my life, my son Felix, for being the greatest gift. Thank you both for embarking on this crazy journey with me –

I love you with all of my heart.

TABLE OF CONTENTS

LIST OF TABLES

LIST OF FIGURES

CHAPTER 1. INTRODUCTION

1.1 Orthopedic injuries in horses

Orthopedic injuries are a major cause of lameness and morbidity in horses worldwide, leading to substantial personal and financial losses for horse owners and the horse industry [1–3]. Articular cartilage injuries are particularly problematic since cartilage has a very limited intrinsic repair capacity, believed to be due in part to a lack of vasculature and low mitotic activity of the chondrocytes. Articular cartilage is present on opposing bone surfaces in diarthrodial synovial joints, where its main functions are to distribute load and provide a smooth and lubricated surface for articulation to minimize the load-friction of movement [4]. Lesions involving articular cartilage often progress and potentially involve subchondral bone, which leads to significant pain and loss of function, resulting in long periods of rest with a poor prognosis to return to full athletic function (Figure 1.1) [4,5].

One of the major orthopedic diseases responsible for retirement of horses is osteoarthritis [3]. Osteoarthritis is a degenerative joint disease that historically has been identified as a cartilage disease, but is now recognized as a disease of the whole osteochondral unit with alterations to the articular cartilage and subchondral bone, together with low-grade systemic and local inflammation as measured by an up-regulation in e.g. peripheral CD8+ T-cells, and synovial tumor necrosis factor-α, interleukin-1, and interleukin-6 [6–8]. Abnormalities in the subchondral bone include sclerosis, bone marrow lesions, and osteophyte formations [6,7]. In the horse, evidence furthermore suggests that subchondral bone injuries can be an important etiological variable leading to initial cartilage damage during osteoarthritis [3,9,10]. Unlike articular

cartilage, bone is vascularized and has access to progenitor cells which in general provides for healing capabilities. Nevertheless, a bone persistent reparative response with unmatched bone formation and resorption is reported in horses where architectural disruption leads to weak areas and is associated with some subchondral bone lesions, and dense bone may never remodel completely. Bone persistent resorption areas are therefore believed to be one of the contributing factors to osteoarthritis in horses [3].

Another major risk factor for developing osteoarthritis is an increase in age. It is recognized, however, that age is only one of many contributing factors and that aging and osteoarthritis are independent processes although osteoarthritis is a progressive disease [6,7]. An "adipogenic switch" has been reported in some studies where bone marrow (BM) derived mesenchymal stem cells (MSCs) from aged donors are more prone to adipogenic differentiation compared to osteogenic differentiation. As BM-MSCs are progenitors for the bone forming cell, osteoblasts, an age-related switch may potentially affect osteoblast formation and bone remodeling *in vivo*, and thus be a risk factor for bone diseases [11]. Intense athletic training, trauma, infection, and conformation deformities are amongst other risk factors of osteoarthritis, and the disease can hence be seen at all ages [12].

Current therapies for osteoarthritis in the horse include administration of anti-inflammatory and pain relieving drugs including intra-articular injections of corticosteroids and/or hyaluronic acid, and surgical debridement [13,14]. Unfortunately, none of the existing techniques have been able to fully restore articular cartilage structure and function with complete integration into the normal surrounding tissue, and fibrocartilage formation is often seen together with osteophyte formation after bone

involvement (Figure 1.1) [5,6,15–19]. Moreover, these therapies have the potential for unwanted systemic adverse effects like gastric ulcers and diarrhea, together with local side effects as corticosteroids have shown toxicity towards chondrocytes [13,14,20]. Consequently, there is a great need for new cartilage and bone restoration methods.

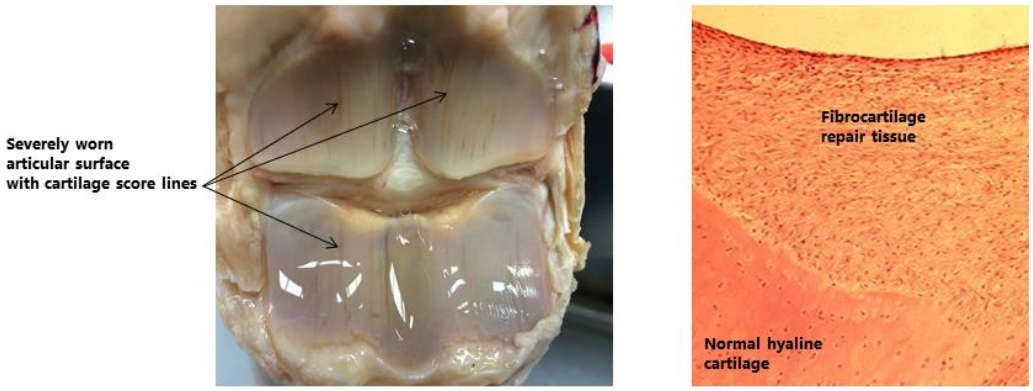

Figure 1.1*: Left: Joint surfaces of an equine fetlock with osteoarthritis where the cartilage is severely worn with score lines (arrows). Right: Safranin-O stained histological section of normal hyaline articular cartilage and fibrocartilage repair tissue illustrating the poor integration between the two. Images courtesy of Drs. MacLeod, Todhunter, and Fortier.*

1.2 Mesenchymal stem cells as a treatment of orthopedic injuries

Cell-based therapies with MSCs are an area of high scientific and clinical interest within the broad field of regenerative medicine, as MSCs have shown capacity to facilitate the repair of orthopedic injuries in addition to managing the symptoms [17,18,21–23].

MSCs are multipotent spindle-shaped stromal cells capable of plastic adherence, self-renewal, and differentiation into multiple mesodermal lineages including cartilage, bone, and adipose tissue. MSCs were first described in the 1960's and 1970's in a series of studies by Friedstein and coworkers as a plastic-adherent fibroblast-like population isolated from the bone marrow capable of osteogenic differentiation [24,25]. The term 'mesenchymal stem cell' was later popularized by Caplan in 1991 [26]. MSCs can be

isolated from multiple tissues such as adipose tissue, bone marrow, synovial fluid, peripheral blood, and umbilical cord blood [27–31]. The international Society of Cellular Therapy (ISCT) have suggested the following criteria for identification of human MSCs: 1) plastic-adherence when cultured under standard conditions, 2) *in vitro* tri-lineage differentiation into chondrocytes, osteoblasts, and adipocytes, and 3) expression of surface markers CD105, CD73, and CD90, and an absence of CD45, CD34, CD14, CD11b, CD79α, CD19, and HLA-DR [32].

Cell surface markers of equine MSCs are not exactly the same as those found in humans, and a limited availability of equine specific antibodies have made surface marker assessment and clarification challenging [33]. However, a recent study by Bundgaard *et al.* reported expression of CD29, CD44, CD90, CD105, and CD166 in equine BM- and AT-MSCs, and a lack of CD34, CD45, and CD79α when using mass spectrometry [34]. Nevertheless, there is still a lack of a uniform agreement on how to characterize equine MSCs. Furthermore, recently published studies no longer perform tri-lineage differentiation to verify stemness [34–37].

For the purpose of this dissertation, MSCs will be defined as spindle-shaped post-embryonic, bone-marrow- or adipose tissue derived cells, capable of plastic adherence and expansion when cultured under standard culture conditions, with an ability to undergo chondrogenic and osteogenic differentiation *in vitro*.

Clinically relevant equine tissue sources of MSCs include bone marrow (BM) and adipose tissue (AT), where published literature has reported a promising capacity to differentiate into chondrogenic and osteogenic lineages with the potential to restore orthopedic lesions [35,38–42]. Several studies have compared chondrogenic and

osteogenic *in vitro* differentiation in a range of MSCs [35,38,39,41,43], and most studies report a higher potential of BM-MSCs to treat cartilage and bone injuries compared to AT-MSCs [35,41,44–46]. This was supported by an *in vivo* equine osteoarthritis model, where Frisbie *et al*. noted a greater improvement when using BM-MSCs compared to AT-MSCs or placebo [46].

For successful therapies, a substantial number of cells are needed, which requires extensive *ex vivo* cell expansion. Generally, cell-based therapy protocols call for 10-100 x 10^6 MSCs per treatment depending on injury type [40,47–49]. MSC yield after primary isolation depends on cell type, donor age and gender, and inter-animal variation [42,50]. Vidal *et al.* reported a low frequency of BM-MSCs with a mean of 1.5 x 10^4 BM-MSCs per 10 mL bone marrow aspirate in young horses, whereas 1.3 x 10^6 AT-MSCs were found per 10 mL adipose tissue in young horses below the age of 5 [31,42]. Equine MSCs consequently need to be expanded *in vitro* for about 2-3 weeks prior to implantation [31,40]. However, this depends on injury type, aspirate/tissue volume, MSC frequency, proliferation rate, and expansion medium. Repeated MSC applications have shown beneficial effects *in vivo*, which also clearly necessitates additional cell numbers [51,52].

The first report on culture-expanded MSC treatment in horses dates back to 2003, where Smith *et al.* implanted autologous BM-MSCs into a spontaneous lesion in a superficial digital flexor tendon [53]. The cells were injected together with blood plasma and were assessed to result in an improvement in tendon healing and lameness. This finding could also be due to the growth factors in the plasma, but importantly, this study showed the ability to expand MSCs *in vitro* to obtain higher cell numbers without

producing adverse patient effects 10 days and 6 weeks post implantation. In 2007, Wilke *et al.* treated 6 horses with femoropatellar cartilage defects with autologous BM-MSCs combined with fibrin or with fibrin alone. They reported an improved cartilage healing in horses treated with the combined product 30 days after treatment compared to horses treated with fibrin alone, but observed no difference between the 2 groups 8 months after treatment [54]. This raises the possibility that multiple MSC treatments may be beneficial, which was later supported in osteoarthritis and meniscus regeneration studies [51,52]. In another study by McIlwraith *et al.*, 10 young adult horses with induced micro-fractured chondral defects were treated with 20 x 10^6 BM-MSCs and hyaluronan, and found no clinical improvement compared to horses treated with hyaluronan alone. They did, however, report an enhanced cartilage repair with improved tissue firmness and increased aggrecan content in the MSC treated horses [18]. A recent dose-response study highlighted the importance of MSC numbers for long-term success of knee osteoarthritis in humans. They noted an improved range of motion and lower pain score in patients treated with a single low dose (10 x 10^6) or high dose (100 x 10^6) of BM-MSCs at 6 months, but only saw improved cartilage healing and improved clinical symptoms in the high-dose group at 12 months [55]. A canine bone defect model showed that 15 x 10^6 BM-MSCs/mL of implant volume (total of 30 x 10^6 MSCs) was required to improve bone regeneration of a 21 mm long segment of the femoral diaphysis [56]. This study was supported by a mathematical model, which found that 70 x 10^6 osteoblasts were needed to produce 1 cm^3 of bone [57]. Timing of MSC treatment may also be a key factor as ter Huurne *et al.* showed reduced cartilage destruction in mice when implanting AT-MSCs 7 days after inducing experimental collagenase osteoarthritis, whereas no difference was

seen between MSC treated and control joints when applying AT-MSCs 14 days after osteoarthritis induction [58]. Together this exemplifies the importance of cell choice, dosage, timing, and the potential need for multiple treatments in order to optimize cell-based treatments of orthopedic lesions.

Previous studies using labeled MSCs have shown that MSCs have an affinity for injured joint tissue and that they localize and participate to a certain degree in repair of joint structures including articular cartilage [22,23]. In contrast, a recent study demonstrated that the primary localization of MSCs after intra-articular injection was in the synovial membrane and to a lesser extent in the articular cartilage [59]. The current understanding is thus that the major regenerative effect of MSCs primarily lies in their paracrine effects and that the persistence of intra-articular injected MSCs is limited in the joint [60,61]. To enhance retention of MSCs within the injury site and to promote tissue like morphology, MSCs are with recent techniques being incorporated into scaffolds like poly-ε-caprolactone (PCL), which is a synthetic porous biomaterial that is relative resistant to hydrolysis and support proliferation, viability, and differentiation of implanted MSCs. Differentiation capability is thereby becoming increasingly important [59,61–64].

1.3 Culture and cryopreservation of mesenchymal stem cells

In the body, MSCs remain predominantly in G0 of the cell cycle (quiescence) while maintaining their differentiation capacity. When plated *in vitro* they exit their quiescent state and begin to proliferate and to form individual colonies [65,66]. Ideal culture conditions preserve MSC phenotype and functional characteristics similar to *in vivo*

properties, with self-renewal and differentiation capacity. High cell density and long-term culture are known to cause a loss of differentiation potential in equine MSCs. Equine MSCs grow well in Dulbecco modified essential medium (DMEM) with glucose and glutamine, supplemented with 1% penicillin/streptomycin to minimize the risk of bacterial contamination. Such medium limits the growth of hematopoietic cells and macrophages. Serum (typically 10% fetal bovine serum) or other serum-mimicking supplements also has to be added to the expansion medium to provide e.g. mitogens essential for growth [67–69].

Equine MSCs have been cryopreserved in cryogenic medium containing 10% dimethyl sulfoxide (DMSO) for multiple years with no alteration in proliferation, multi-potency, or morphology. However, some cells are lost during the freezing and thawing process [68,70]. Cryopreservation allows for cells to be standardized for research purposes and for MSCs to be stored for autologous (same donor and recipient) or allogenic (donor and recipient are different) use in patients.

Medium can be modified to initiate differentiation, but despite much research there is still a lack of standardization and induction medium ingredients and concentrations varies between studies [34,35,38,41].

1.4 Chondrogenic differentiation and validation in culture

Induction of chondrogenesis of MSCs in culture has been more successful as 3D pellets than in monolayer cultures, as it appears that cell-cell interaction enhances chondrogenesis and chondrocyte survival [71,72]. Induction mediums of chondrogenesis typically consists of high glucose DMEM, penicillin/streptomycin, low levels of serum or

serum-supplement, growth factors from the transforming growth factor-β (TGF-β) superfamily, ascorbic acid, dexamethasone, non-essential amino acids, and insulin-transferrin-selenium-sodium pyruvate [34,35,39,71,73,74]. Addition of TGF-β has been demonstrated to induce chondrogenesis in 3D MSC pellets, with a significant increase in proteoglycans and collagen type II, which are essential components of the extracellular matrix of articular cartilage. Expression of collagen type I, which is a marker of biomechanically inferior fibrocartilage, was down-regulated [73–75]. TGF-β stabilizes SRY-box transcription factor 9 (SOX9) protein, which is a key transcriptional regulator of chondrogenesis [76]. An equine study reported that TGF-β_3 was more potent to induce chondrogenesis of MSCs compared to TGF-β_1 [77]. In contrast, a high throughput mRNA-profiling study concluded that TGF-β_1 induced superior chondrogenesis of human MSCs compared to TGF-β_3 [74]. Addition of dexamethasone to the medium has been shown to increase TGF-β signaling, which resulted in higher proteoglycan and collagen type II content [74,75,78]. High level glucose (4.5 g/L) DMEM has also been reported to increase TGF-β signaling and chondrogenic induction by enhancing recycling of TGF-β receptors [79]. Ascorbic acid is an essential co-factor for hydroxylation and stabilization of selected prolines and lysines, which are components of pro-collagen. Supplementing the chondrogenic induction medium with ascorbic acid is hence demonstrated to increase expression of collagen type II [80].

Chondrogenic induction can be evaluated in a variety of ways. Articular chondrocytes are elongated to cuboidal in shape depending on distance from the articular surface. Each chondrocyte is centered in a lacunae, which is a cavity within the extracellular matrix. The extracellular matrix of articular cartilage consists primarily of

water, proteoglycans, and collagen type II and to a minor extent of glycoproteins and non-collagenous proteins [4]. Morphological evaluation of chondrogenic induced pellets using Hematoxylin & Eosin staining is important to assess cell viability and structure, together with pellet composition [33,35]. Measurement of pellet size is another assessment, as production of extracellular matrix has been shown to be positively correlated with an increase in pellet size instead of cell proliferation [35,38,81]. Chondrogenic differentiation can be further validated by assessing proteoglycan content in the extracellular matrix using Safranin-O or Toludine Blue staining. Safranin-O is an orange to red stoichiometric orthochromatic dye that adheres to the sulfate groups of proteoglycan molecules in a 1:1 manner [82]. Safranin-O staining has hence been shown to be proportional to the proteoglycan content present in articular cartilage, whereas Toludine Blue is a more intense staining due to higher affinity for sulfur in cartilage [83]. Sulfated glycosaminoglycans (GAGs) (attached to the protein core in proteoglycans like aggrecan) and glycoproteins can furthermore be identified with an Alcian Blue staining. GAGs are however also found in skin [84]. Masson's Trichrome staining and immunohistochemistry can be used to identify collagen content, where immunohistochemistry can locate collagen type II and collagen type I specifically [33,71,85]. Gene expression of cartilage markers like SOX9, aggrecan, and collagen type II are also commonly applied to validate chondrogenesis [33,35,71].

1.5 Osteogenic differentiation and validation in culture

Osteogenic differentiation of MSCs is typically done in monolayer cultures in osteogenic induction medium containing low glucose DMEM, serum, penicillin/streptomycin,

dexamethasone, ascorbic acid, and β-glycerophosphate [42,86,87]. Addition of dexamethasone has been shown to induce osteogenesis by up-regulating runt-related transcription factor 2 (RUNX2) expression, which is an essential early transcription factor for osteogenesis [88]. RUNX2 is amongst others a transcription factor for osteogenic alkaline phosphatase (ALP), and dexamethasone has thereby shown to enhance ALP activity in osteogenic induced MSCs [87]. Ascorbic acid is an essential co-factor for hydroxylation and stabilization of selected prolines and lysines, which are components of pro-collagen. Supplementing the osteogenic induction medium with ascorbic acid has hence demonstrated to increase expression of collagen type I, which is an essential component in bone extracellular matrix [86,88]. β-glycerophosphate provides phosphate, which is essential for hydroxyapatite ($Ca_{10}(PO_4)6(OH_2)_2$). Hydroxyapatite is the main inorganic component of bone and is hence a crucial bone crystalline mineral [89]. Addition of β-glycerophosphate has thereby shown to enhance osteogenic mineralization and to facilitate phosphorylation of intracellular signaling molecules required to activate RUNX2 [88].

Osteogenic differentiated cells show a change in morphology from spindle-shaped fibroblast-like cells to mainly polygonal cells with an overlaying mineral deposition making the cells hard to see [39]. Osteogenesis is typically validated by Alizarin Red S staining and Van Kossa staining, which stain calcium deposits and phosphate deposits respectively [33]. Alizarin Red S staining is highly specific for bone, as approximately 99% of calcium in the body is localized in bone [84]. Measuring of ALP activity is another important validation method, as ALP activity is an early marker of osteogenesis and highly expressed in bone [89,90]. Gene expression of osteogenic markers like

RUNX2, ALP, osterix, collagen type I and osteocalcin are also commonly used to evaluate osteogenic differentiation of MSCs [33,87].

1.6 Autologous versus allogenic mesenchymal stem cell treatment

Historically, MSCs are said to be free of or to have very low levels of major histocompatibility complex (MHC) class II on their cell surface, which would make them capable of avoiding/minimizing T-cell recognition and allow for allogenic treatments where cells from one donor are applied to another recipient [60,91]. Recent studies have shown that that is not entirely true. In 2014, Schnabel *et al.* [92] demonstrated that equine BM-MSCs are heterogeneous in expression of MCH class II, and that an MCH class II mismatch could cause *in vitro* immune reactions. They also showed that MHC class II-negative BM-MSCs were able to up-regulate MHC class II expression *in vitro* if exposed to inflammatory stimuli, which problematize the idea of purely using established MHC class II-negative stem cells for allogenic treatment. The same research group showed that intradermal injection of allogenic MHC class II mismatched BM-MSCs cause strong antibody responses *in vivo* [93]. A repeated intra-articular study by Joswig *et al.* later showed that immunological adverse effects occurred already after the second intra-articular injection in horses with allogenic MSCs [94]. As repeated MSC treatments have shown beneficial effects *in vivo* [51,52], this emphasizes the potential issues with allogenic treatments. Advantages of allogenic treatments are a more standardized unit that could be applied fast in cases where it is impossible to obtain quality MSCs from the patient. Advantages of autologous cell transplants are decreased risk of host-versus-graft reactions, no need to screen potential donors for compatibility, and less risk of infection

[95]. Furthermore, reduced osteoarthritis progression has been reported in horses when autologous chondro-progenitor cells were applied but not when using allogenic cells [96]. Clinical application of allogenic MSCs is regulated by national authorities [40]. Due to the risk of immunological reactions mentioned above, the current application of MSCs in equine practice is usually autologous, using cells harvested from the patient shortly after the time of injury [43].

1.7 Mesenchymal stem cells in regeneration

The normal function of MSCs in the body is to perform organ specific self-renewal and to be responsible for tissue regeneration through direct differentiation, immunomodulatory- and growth factor excreting properties [21,22,97–99]. An overview of these properties is shown in Figure 1.2. However, a reduced tissue regenerative capacity is seen *in vivo* with increasing age. This is believed to be strongly correlated with an age-related decline in adult MSCs quantity with increasing donor age [7,97]. *In vitro* studies suggest that an age-related decrease in MSC functionality might also be a contributing factor, although this factor is still debated [7,97,100]. A recent study by Khong *et al*. used single-cell sequencing to determine a loss in MSC quiescence with increasing donor age, which could explain the reported stem cell depletion with aging and an imbalance of progenitor cells [66]. In support of this, induction of quiescence in BM-MSCs has shown to enhance stemness both *in vitro* and *in vivo* [101]. The important issue about age-related changes in MSC functionality in horses is the focus of my dissertation as described below.

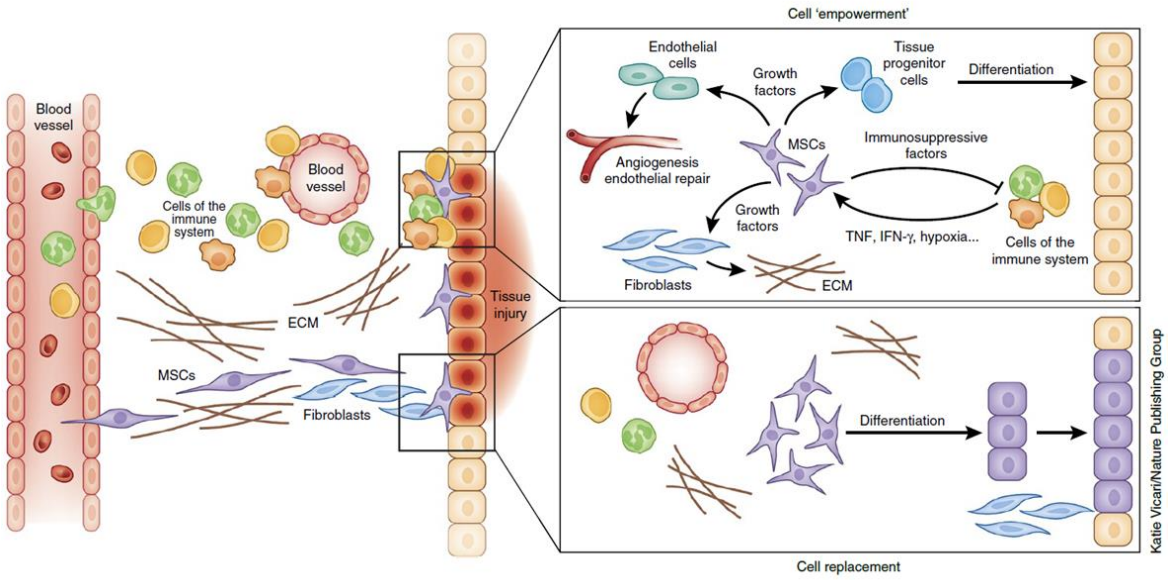

Figure 1.2**:** *Overview of mesenchymal stem cell properties – cell replacement versus cell empowerment. When tissue is damaged, inflammation occurs and MSCs are attracted to the injury site. Due to their multipotent differentiation capacity, the recruited MSCs can differentiate themselves into functional cells to replace the damaged cells, which is called cell replacement or direct differentiation. In response to inflammatory cytokines, MSCs also have the capacity to produce immunoregulatory factors that modulate the progression of inflammation, which is beneficial for the inflammatory process occurring during osteoarthritis. Lastly, MSCs excrete large amounts of growth factors, which stimulate fibroblasts, endothelial cells, and importantly progenitor cells in situ, which facilitate tissue repair through extracellular matrix remodeling, angiogenesis, and differentiation of progenitor cells. The two later properties are collected called cell empowerment. Reprinted by permission from Springer Nature: Nature Immunology,* [99]*, copyright 2014.*

1.8 Definition of age and aging

Age and aging can be defined in multiple ways depending on the scientific area investigated and the research questions asked. Chronological age describes the age of an individual from the calendar time that has passed since date of birth and hence follows a stable curve. Biological age describes the functional capability age and depends on the biological state of the individual/organism, which can be impacted by endogenous and exogenous stress factors. The biological age does not have to correlate perfectly with the

chronological age [102]. Recent studies have shown that DNA methylation is the most promising molecular estimator of biological age, also known as the epigenetic clock [102,103].

For the purpose of this study, chronological age will be used as age and donor-age, and aging will be defined as "a gradual process marked by the deterioration of functionality in living multicellular organisms with the passage of time" as described by Ganguly *et al.* [7]. Using this definition emphasizes the importance of MSCs in cell renewal and thus in impacting lifespan. Furthermore, aging relates to a multicellular organism, and can be distinguished from mitotic age and cellular senescence/aging, which refers to the number of cell divisions and to the related irreversible arrest of cell division on a cellular level [104,105].

1.9 Cellular senescence

Normal somatic cells have a limited proliferative capability due to a process called cellular senescence. One of the mechanisms responsible for cellular senescence is shortening and eventual dysfunction of the telomeres. Telomeres in mammals are the TTAGGG repetitive DNA sequences and associated cap proteins at the ends of chromosomes that stabilize the ends of linear chromosomes and thus prevent their fusion and degradation [106–109]. Due to the nature of lagging-strand DNA synthesis, DNA polymerase cannot completely replicate the 3' end of the telomeres. Native DNA polymerase only replicate DNA in a 5' to 3' direction, and synthetize the leading strand in a continuous manner. The lagging strand is however made in a discontinuous manner with a short set of Okazaki fragments each requiring a new primer. During discontinuous

lagging strand DNA synthesis the most distal primer in the 3' end cannot be replaced. Telomeric DNA is therefore lost with each cell cycle, which leads to a progressive telomere shortening unless the cell expresses telomerase [104,107,110].

Telomerase is an enzyme that adds the telomeric sequence to the chromosome end and prevents shortening of the telomeres. Most normal cells do not express this enzyme and develops short telomeres that signal for the cell to cease proliferation by inducing cellular growth arrest. When the telomeres are critically shortened and have lost their protective cap protein, the exposed chromosome ends are recognized as DNA damage, which trigger a p53/p21 induced cell cycle arrest [104,107,110]. p53 is a tumor suppressor and transcription factor for p21. p21 inhibit cyclin dependent kinases, which is necessary for the cell to progress from G1- to S-phase during cell cycle, leading to growth arrest [107]. Senescent cells can also activate the p16/Retinoblastoma (Rb) pathway independent of p53. p16 is a tumor suppressor that inhibits DNA replication by inhibiting cyclin dependent kinases 4/6 necessary for phosphorylating and inactivating Rb family members. Non-phosphorylated Rb thereby binds E2F transcription factor 1 resulting in G1-arrest (Figure 1.3) [107,111]. Cellular senescence hence occurs via one or both of these pathways, with p53/21 mediated senescence being primarily due to telomere dysfunction and DNA damage, and the p16/Rb pathway being primarily due to chromatin disruption, oncogenes, and oxidative stress (Figure 1.3) [105,111].

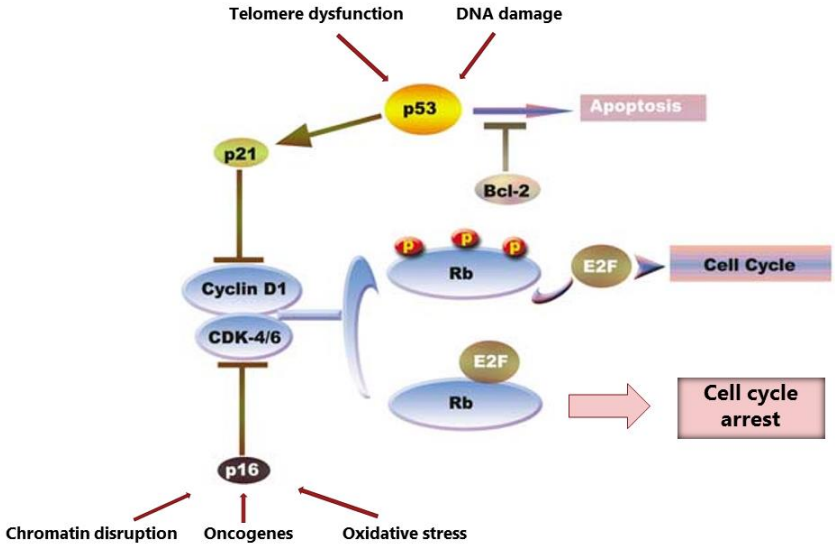

Figure 1.3: *Flow diagram showing the role of major components of the p53/p21 and the p16/RB pathway in cell cycle regulation. Modified figure from Jayasurya et al.* [112]. *Reprinted by permission from Springer Nature: Modern Pathology,* [112], *copyright 2005.*

The two independent processes are believed to be an evolutionary protective mechanism to prevent excessive cell growth. When a senescent cell is arrested in G1 it is irreversible if the p53 and p16 pathways are intact and the cell cannot be stimulated to proliferate by mitogens [107]. Fibroblasts from normal human tissue have the capability to go through 20-50 population doublings when cultured in growth medium containing mitogens before undergoing cellular senescence [110]. The process by which cultured normal mammalian cells have limited capacity to divide and become senescent are known as the Hayflick limit [104].

Most if not all cancer cells have recovered the capability to produce telomerase, and have mutations in p53 and/or p16/RB making them immortal with unlimited proliferative capacity [105,110,111]. Besides cancer cells, telomerase activity is documented in germ-line cells [113], embryonic stem cells [114], and to a lower degree

in some adult stem cells [115,116]. In MSCs, the expression of telomerase is still debated as some studies report low levels of telomerase while others find no expression or activity [105,117–119]. Differences may be caused by measurement techniques with various sensitivity levels and different cut-offs for telomerase presence. It has furthermore been speculated that telomerase-active MSCs might be a minor subpopulation [105]. In horses, a telomere shortening of 70-116 base pairs per population doubling has been reported in MSCs [120], which correlate with a 30-120 base pair shortening seen in human MSCs [105,109]. Senescent cells remain alive in a metabolically altered state and are morphologically enlarged and flattened [105,121]. It is important to remember that different cell lines proliferate at various rates and hence reach cellular senescence at different time points if measured on a chronological scale. Proliferation is furthermore faster during growth and development, and multiple studies have shown that the cellular proliferation rate decreases with increasing donor age [27,42,50,97,102,120,122–124]. Accumulation of senescent cells is thereby said to drive aging and age-related diseases [121].

1.10 Donor age effects on mesenchymal stem cells

Multiple studies have shown a sharp decline in MSC quantity and quality with increasing donor age, which may be problematic for the important demographic of older equine orthopedic patients with regards to autologous treatments [65,85,97,122,123,125–127]. Below are some of these donor age effects discussed.

1.10.1 Donor age effects on MSC frequency

The frequency of MSCs when harvested can be determined by utilizing a colony forming unit-fibroblast (CFU-F) assay. MSCs are rare and can be found in 0.001% to 0.01% of bone marrow aspirates [128] and in near 2% of adipose tissue stromal vascular fraction in humans [129]. However, most human and rodent studies agree on a decline in MSC frequency with increasing donor age [50,105,124,130]. This change has been suggested to be caused by an increased predisposition to cellular senescence and a decrease in quiescence [27,66,131]. Species and gender may also be important determinants of MSC frequency. A human study by Siegel *et al.* [130] reported a general decline in BM-MSC frequency with increasing age when mixing both genders, but only found a significant age-related decline within females, even though they produced more CFU-Fs than seen in males. Likewise, Katsara *et al.* [50] reported a 3.5 fold higher BM-MSC frequency in young mice compared to old mice, but found a higher frequency of BM-MSCs in males compared to females in all age groups. In contrast, Guercio *et al.* [125] found no difference in AT-MSC frequency in young and old canines. Likewise, Justesen *et al.* [100] reported no significant correlation between donor age and total number of colonies in human BM-MSCs. Some of these variances may be due to difference in isolation and culture methods.

1.10.2 Donor age effects on MSC proliferation in culture

Multiple assays exist to determine cellular proliferation. These include cell doubling methods, 5-bromo-2'-deoxyuridine (BrdU) assays, 5-ethynyl-2'-deoxyuridine (EdU) assays, and fluorescence activated cell sorting (FACS) [110,132]. The cell doubling

method is fast and cheap, but has a low specificity, is investigator-dependent, includes potential cells without plastic adherence, and is potentially affected by trypsinization. Advantages of the BrdU and the EdU assays are that they can detect cells that have gone through the S-phase by applying markers that are incorporated in the DNA during replication. EdU is a thymidine analog and is readily incorporated into cellular DNA during the S-phase. Advantages of the EdU assay over the BrdU assay are no requirement for cell denaturation, more time-efficient, more specific, and less investigator dependent [132]. Advantages of a FACS approach is a location of the cells within the cell cycle and determination of apoptotic cells, while disadvantages include a high cost and complex equipment [110]. Gene expression of markers of proliferation, growth factors, and senescence are also commonly included.

As shown in Table 1.1., the vast majority of studies report a decline in MSC proliferation with increasing donor age. Some studies however found no difference in cellular proliferation between young and old MSCs. It should be noticed that those studies compared age groups closer in age than some of the others. An equine study by Schröck *et al.* [133] reported a heterogeneous population of equine BM-MSCs with a decreasing population of cells with maximum proliferation speed with increasing donor age. However, the study had a limited study population and was not designed to provide kinetics or clinically relevant thresholds with regards to donor age. On the other hand, Vidal *et al*. [42] found no effect of donor age on the proliferative capacity of equine BM-MSCs, but Vidal's study only included horses below 5 years of age (mean 2.4 years old), which could explain the different conclusions. Chen *et al.* [134] furthermore reported that the proliferative capacity of AT-MSCs was less affected by donor age than BM-MSCs.

Donor age effects on telomere length is more ambiguous as some studies show no difference in telomere length [27,105,131], whereas others show a shortening of telomere length with increasing age [105,135]. At the same time Asumda *et al.* [97] reported a higher telomerase activity in BM-MSCs from young rats, whereas other studies found no telomerase activity in human BM-MSCs [130,131]. An equine study by Wilson *et al.* tested telomerase activity in BM-MSCs from young horses aged 3-5 years, and found only 1 sample positive for telomerase activity at day 2 after collection and all the samples negative on day 10 [119]. With regards to senescence markers, studies have shown an increase in β-galactosidase activity, and p16, p21, and p53 expression with increasing donor age [27,37,122–124]. It should however be noted, that β-galactosidase activity is not a specific marker of donor age, but considered a reliable marker of cellular senescence as shown by Stenderup *et al.* where β-galactosidase activity was up-regulated in late passages, but not between BM-MSCs from young and old donors [105,131]. It has however been suggested that accelerated senescence is seen in old MSCs [27,131]. Multiple studies have shown a down-regulation in growth factors in old MSCs [37,97]. An age-related increase in expression of tumor suppressors and a down-regulation of growth factors may very well cause the lower *in vitro* cellular proliferation described in old MSCs in most studies. These studies were supported by a recent proteomics study, where the majority of MSC age-related changes were seen in proteins related to cell survival and death, and cellular proliferation [85].

Table 1.1: Mesenchymal stem cell proliferation characteristics as a function of donor age

Species	Cell type	Young ("Y")	Middle-aged ("M")	Old ("O")	Sample size	Assay	Donor age effect	Notes	Ref.
Horse	BM-MSC	17-51 d.		9 mo.-5 yo.	Y=3, O=5	Cell doubling	No effect of donor age		[42]
Horse	BM-MSC	2 w. premature – 28 yo. (no defined age groups)			n=9 total	eFlour 670 flow cytometry	Decline with aging		[133]
Human	BM-MSC	<50 yo.		>55 yo.	Y=3, O=16	Cell doubling, Gene expression	Decline with aging	Doubling time was 1.7-fold longer in old MSCs. ↑ p53, p21, BAX, β-GAL in old MSCs	[122]
Human	BM-MSC AT-MSC	19-54 yo.		68-75 yo.	Y=14, O=8	Cell doubling, Gene expression	Decline with aging in BM-MSCs. No effect of donor age in AT-MSCs	AT-MSCs are less affected then BM-MSCs. p21 and β-GAL lower in old AT-MSCs than old BM-MSCs	[134]
Human	BM-MSC	7-18 yo.	19-40 yo.	>40 yo.	n=57 total	Cell doubling, Gene expression	Decline with aging	↑ p21 and p53 in old MSCs	[123]
Human	BM-MSC	<45 yo.	45-65 yo.	>65 yo.	Y=11, M=26, O=13	Cell doubling	No effect of donor age		[130]
Human	AT-MSC	<30 yo.	35-50 yo.	>60 yo.	Y=8, M=10, O=11	Cell doubling, Gene expression	Decline with aging	↑ p16, p21, and β-GAL in old MSCs. Lower frequency of BM-MSCs in old donors	[124]
Human	BM-MSC	18-29 yo.		68-81 yo.	Y=6, O=5	Cell doubling	Decline with aging	Accelerated senescence in old MSCs	[131]
Rhesus macaque	BM-MSC	< 5 yo.	8-10 yo.	>12 yo.	Y=9, M=4, O=9	Cell doubling, FACS	Decline with aging	↑ β-GAL, p53, p21 in old MSCs. Telomere length not affected. Aging increases cell senescence	[27]
Dog	AT-MSC	1-4 yo.		8-14 yo.	n=20 total	Cell doubling	Decline with aging	MSC frequency was not affected by donor age	[125]
Rat	BM-MSC	4 mo.		15 mo.	n=4/ group	Cell doubling, Gene expression	Decline with aging	Higher telomerase activity in young MSCs. ↓ VEGF, EGF, and IGF in old MSCs	[97]
Mouse	BM-MSC	6 d.	6 w.	1 yo.	n=3/ group	Cell doubling	Decline with aging		[136]
Mouse	BM-MSC	<4 w.	5-12 w.	13-34 w.	n= at least 3/ group	Cell doubling	Decline with aging	Lower frequency in females	[50]
Mouse	BM-MSC	2-3 mo.		23-24 mo.	?	Cell doubling, Gene expression	Decline with aging	↑ p53, p21, BAX, p16 and ↓ VEGF in old MSCs	[37]

*Y: young age group, M: middle-aged age group, O: old age group, d: days old, w: weeks old, mo: months old, yo: years old, ↑: up-regulated gene expression, ↓: down-regulated gene expression.

1.10.3 Donor age effects on MSC differentiation in culture

Donor age also appears to be a major factor altering the chondrogenic and osteogenic differentiation performance of BM- and AT-MSCs in culture. Currently, most work has been performed on assessing the osteogenic differentiation potential as a function of age. As shown in Table 1.2 and Table 1.3 most studies report a decline in chondrogenic and osteogenic differentiation potential of MSCs with increasing donor age. A study by Asumda *et al.* [97] found that BM-MSCs from 15 months old rats had lost their chondrogenic and osteogenic differentiation potential altogether, which was supported by a 76% decline in osteogenic alkaline phosphatase activity in adult human BM-MSCs [65], and a 82% decline in proteoglycan content of chondrogenic induced BM-MSC pellets from 1 year old rats compared to 1 week old rats [127]. Previous studies have reported, that AT-MSCs osteogenic differentiation capacity was less affected by donor age than BM-MSCs [134,137]. It should be noted that most of the studies reporting no effect of donor age compare age groups that are relatively closer to each other as seen in Table 1.2 and Table 1.3. On a gene level, most studies also report a down-regulation in expression of chondrogenic (e.g. SOX9, aggrecan, collagen type II) and osteogenic markers (e.g. RUNX2, alkaline phosphatase, osteocalcin) with increasing donor age after culture in induction medium [122,124,127].

An "adipogenic switch" has been reported in some studies where BM-MSCs from aged donors are more prone to adipogenic differentiation compared to osteogenic differentiation [11,105]. This observation may be explained by Kretlow *et al.'s* finding that chondrogenic and osteogenic differentiation performance decline earlier than adipogenic differentiation in BM-MSCs [136].

Table 1.2: Mesenchymal stem cell chondrogenic differentiation performance as a function of donor age

Species	Cell type	Young ("Y")	Middle-aged ("M")	Old ("O")	Sample size	Assay	Donor age effect	Notes	Ref.
Human	AT-MSC	<30 yo.	35-50 yo.	>60 yo.	Y=8, M=10, O=11	Alcian Blue, Gene expression	Decline with aging	↓ aggrecan and collagen type II in old MSCs	[124]
Human	BM-MSC	<45 yo.	45-65 yo.	>65 yo.	Y=11, M=26, O=13	Safranin-O, Gene expression	No effect of donor age	No effect of gender	[130]
Human	BM-MSC	7-18 yo.	19-40 yo.	>40 yo.	n=57 total	Toluidine blue, Alcian Blue	Declined with aging, but did not reach significance		[123]
Rat	BM-MSC	1 w.	12 w.	1 yo.	n= 3-5/ group	Safranin-O, Gene expression	Decline with aging	Pellets from M and O were largely negative for proteoglycans, collagen type II, aggrecan and SOX9	[127]
Rat	BM-MSC	4 mo.		15 mo.	n=4/ group	Immuno-cytochemistry (anti-aggrecan)	Decline with aging	No chondrogenic potential in old MSCs	[97]
Mouse	BM-MSC	6 d.	6 w.	1 yo.	n=3/ group	Immuno-histochemistry (COL2), Alcian blue, Safranin-O	Decline with aging		[136]

*Y: young age group, M: middle-aged age group, O: old age group, d: days old, w: weeks old, mo: months old, yo: years old, ↓: down-regulated gene expression.

Table 1.3: Mesenchymal stem cell osteogenic differentiation performance as a function of donor age

Species	Cell type	Young ("Y")	Middle-aged ("M")	Old ("O")	Sample size	Assay	Donor age effect	Notes	Ref.
Human	BM-MSC	3-36 yo.		41-70 yo.	n=41 total	Alkaline phosphatase activity	Decline with aging	No effect of gender. A 76% decline in ALP between age groups	[65]
Human	BM-MSC	18-42 yo.		66-78 yo.	Y=34, O=20	Alkaline phosphatase activity, Gene expression	No effect of donor age		[100]
Human	BM-MSC AT-MSC	19-54 yo.		68-75 yo.	Y=14, O=8	Alizarin Red S, Gene expression	Decline with aging in BM-MSCs. No donor age effect in AT-MSCs	AT-MSCs are less affected by donor age than BM-MSCs	[134]
Human	BM-MSC	7-18 yo.	19-40 yo.	>40 yo.	n=57 total	Alkaline phosphatase activity	Decline with aging		[123]
Human	AT-MSC	<30 yo.	35-50 yo.	>60 yo.	Y=8, M=10, O=11	Von kossa, Gene expression	Decline with aging	↓ ALP and osteocalcin in old MSCs	[124]
Human	BM-MSC	<50 yo.		>55 yo.	Y=3, O=7	Alkaline phosphatase activity, Gene expression	Decline with aging	↓ RUNX2, osterix, ALP, osteocalcin in old MSCs	[122]
Human	BM-MSC	18-29 yo.		68-81 yo.	Y=6, O=5	Alizarin Red S	No effect of donor age		[131]
Human	BM-MSC	<45 yo.	45-65 yo.	>65 yo.	Y=11, M=26, O=13	Alizarin Red S, Gene expression	No effect of donor age	No effect of gender	[130]
Rhesus macaque	BM-MSC	<5 yo.	8-10 yo.	>12 yo.	Y=9, M=4, O=9	Alizarin Red S	Decline with aging		[27]
Rat	BM-MSC	4 mo.		15 mo.	n=4/ group	Alizarin Red S, Immuno-cytochemistry (osteocalcin)	Decline with aging	No osteogenic potential in old MSCs	[97]
Mouse	BM-MSC	2 mo.	8 mo.	26 mo.	n=4/ group	Alkaline phosphatase activity, Gene expression	Decline with aging	↓ osteoadherin, osteoglycin, osteonectin in old MSCs	[126]
Mouse	BM-MSC	6 d.	6 w.	1 yo.	n= at least 3/ group	Alizarin Red S	Decline with aging		[136]
Mouse	AT-MSC	6 d.		60 d.	n=3/ group	Alkaline phosphatase activity, Von Kossa	No effect of donor age		[137]

*Y: young age group, M: middle-aged age group, O: old age group, d: days old, w: weeks old, mo: months old, yo: years old, ↓: down-regulated gene expression

1.11 Priority knowledge gaps and hypotheses

As reported in other species, the age of the horse may be an important variable for orthopedic injuries treated with autologous cells. Very little is however known about donor age effects on MSCs in horses, and no donor age related equine MSC proliferative, and chondrogenic and osteogenic differentiation studies have been designed with multiple age groups or sufficient donors to provide thresholds relevant for clinical practice. It is furthermore unknown if the cellular proliferation and chondrogenic and osteogenic differentiation performance of equine BM- and AT-MSCs are equally affected by donor age. Ultimately, age-associated alterations may impact the efficacy of autologous transplanted MSCs in aged horses resulting in poorer regenerative results.

The studies described in this dissertation were designed to address these priority questions using 2 clinically relevant stem cell types from 5 clinically relevant and well distinguished age groups. Experiments reported in chapter 2 test the hypothesis that increasing donor age is a major variable impacting equine BM- and AT-MSC proliferation with decreasing capacities following non-linear kinetics. These data are further expanded in chapter 3, where the reported experiments tests the hypothesis that increasing donor age is a major variable impacting equine BM- and AT-MSC chondrogenic and osteogenic differentiation performance with decreasing capacities following non-linear kinetics. Finally, chapter 4 reflects on the combined dissertation work and elaborates on the clinical importance of donor age, together with proposed future study directions.

CHAPTER 2. DONOR AGE EFFECTS ON THE CELLULAR PROLIFERATION OF EQUINE MESENCHYMAL STEM CELLS IN CULTURE

2.1 INTRODUCTION

Musculoskeletal injuries are the leading cause of lost training days and early retirement of horses, and can affect horses at all ages [1,2,138]. Current treatment options aiming at restoring the inherent function of cartilage, tendon, ligament, and some bone injuries and enhancing the long term prognosis are however of limited availability [17]. Fortunately, mesenchymal stem cells (MSCs) have shown potential to facilitate the repair of musculoskeletal injuries including bone, cartilage, and tendon injuries through immunomodulatory-, differentiating-, and growth factor excreting properties [21,22,38,47,48,98,139], and are hence being used increasingly in equine practice. Bone marrow (BM)- and adipose tissue (AT) derived MSCs are currently the choice of therapy, where BM-MSCs have shown higher potential to treat cartilage and bone injuries [35,41,44,45]. Nevertheless, Vidal *et al.* reported a low frequency of BM-MSCs with a mean of 1.5 x 10^4 BM-MSCs per 10 mL bone marrow aspirate in young horses, whereas a mean of 1.3 x 10^6 AT-MSCs was found per 10 mL adipose tissue in young horses [31,42]. Notably, MSC frequency depends on cell type, donor age, donor sex, and inter-animal variation [42,50]. For successful therapies, a substantial number of cells are needed, which requires extensive *ex vivo* cell expansion. Generally, cell-based therapy protocols require 10-100 x 10^6 MSCs per treatment [40,47–49], and equine MSCs consequently need to be expanded *in vitro* for about 2-3 weeks prior to implantation [31,40]. However, this depends on injury type, aspirate/tissue volume, MSC frequency, proliferative rate, and expansion medium. A canine bone defect model showed that 15 x 10^6 MSCs/mL of implant volume (total of 30 x 10^6 MSCs) was required to improve bone

regeneration of a 21 mm long segment of the femoral diaphysis [56]. This study was supported by a mathematical model, which found that 70 x 10^6 osteoblasts were needed to produce 1 cm^3 of bone [57]. Additionally, repeated MSC applications have shown beneficial effects *in vivo*, which increases the need for cells [51].

Unfortunately, human and rodent studies have shown a decline in frequency and *in vitro* proliferative capacity of BM- and AT-MSCs with increasing donor age [27,37,50,97,122–124,131]. A human study performed on donors from the age of 17 to 90 years old, revealed a doubling rate that was almost twice as long in BM-MSCs from old donors (≥ 55 years old) [122]. It has furthermore been determined that MSCs from aged human, non-human primate, and rodent donors have increased levels of cell cycle arrest genes like p21 and p53 [27,122,123], and decreased expression of growth factors like vascular endothelial growth factor (VEGF) and insulin-like growth factor (IGF) [97].

Very little is, however, known about these age-dependent relationships in horses, and no equine MSC proliferative age studies have been designed with multiple age groups or sufficient donors to provide thresholds relevant for clinical practice [36,42,133]. A lack of direct age correlating models between horses and other species highlights the importance of equine studies to investigate the potential donor age issue further. Expansion issues cause in best case a delay of treatment, which may be an issue for some applications where early treatment has been shown to be of essence [58], but can be devastating if the cells cannot be expanded. Together, this may limit the clinical potential of MSCs from aged horses, as the ability to expand the cells is vital to obtain sufficient numbers for autologous treatment, and cellular proliferation has been shown to be positively correlated with regenerative potential [140]. Presently, autologous treatment

is preferred over allogenic treatment due to the potential risk of immunological reactions associated with allogenic treatments in equine models [40,92–94,141]. This is problematic as many patients with osteoarthritis are aged [142]. The need for regenerative medicine in equine practice is thus believed to increase tremendously partly due to the progressively aging equine population [143]. Together, this emphasizes the significance of understanding the changes in the proliferative capacity of equine MSCs as a function of donor age.

The studies reported in this chapter were therefore designed to test the hypothesis that increasing donor age is a major variable impacting equine BM- and AT-MSC proliferation with decreasing capacities following non-linear kinetics. Specific aims were to 1) compare the cellular proliferation of BM- and AT- MSCs from horses in different age groups using an EdU proliferation assay, and to 2) assess the expression of targeted biomarkers of cellular proliferation, cellular senescence, and proliferation related markers that have shown age-dependent variation in other species.

2.2 MATERIALS AND METHODS

2.2.1 Experimental samples

BM-MSCs, AT-MSCs, and dermal fibroblasts (DF) (biological control) were harvested immediately post-mortem from horses of mixed breeds in 5 different clinically relevant and well-distinguished age groups with 4 horses in each age group. The age groups were newborn (0 days old), yearling (1-2 year old), adult (5-8 year old), middle aged (12-18 year old), and geriatric (≥ 22 year old) horses. All horses were euthanized due to reasons unrelated to this study. The study was conducted according to the ethical guidelines of

animal research at the University of Copenhagen and the University of Kentucky. A written consent was obtained from all privately-owned horses prior to collection.

Sample size was determined by power analysis. Two-sample t-test power calculations were performed in R (version 3.6.0) using pilot study data (not shown) to assess BM- and AT-MSC cellular proliferation using cells from newborn foals and geriatric horses (n=2 horses per age group per cell type) and the following equation:

$$n = 2 * \frac{(z1 - \frac{\alpha}{2} + z1 - \beta)^2}{(\delta/\sigma)^2}$$

where σ is the standard deviation for the outcome, α is the significance level, $1 - \beta$ is the power, $z1 - \frac{\alpha}{2} = 1.96$ for $\alpha = 0.05$, $z1 - \beta = 0.84$ for $1 - \beta = 0.80$, and δ was set to 10% as the minimum relevant difference. The estimated sample size to achieve a power of 0.80 was determined as 4 horses per age group per cell type. An overview of the biological replicates used in this study is outlined in Table 2.1.

Table 2.1: Overview of biological replicates used as study population

Age group	Age	Breed	Sex	Horse ID	BM-MSCs	AT-MSCs	DF	Reason for euthanasia
Newborn	0 d.	Pony	M	EQF1701	x	x	x	Research
Newborn	0 d.	Pony	M	EQF1703	x	x	x	Research
Newborn	0 d.	Pony	M	EQF1704	x	x	x	Research
Newborn	0 d.	Pony	F	EQF1705	x	x	x	Research
Yearling	16 mo.	Thoroughbred	F	EQA1504	x	x	x	Research
Yearling	16 mo.	Thoroughbred	F	EQA1505	x	x	x	Research
Yearling	15.5 mo.	Thoroughbred	M	EQA1506	x			Research
Yearling	15 mo.	Thoroughbred	M	EQA1507	x		x	Research
Yearling	15 mo.	Thoroughbred	M	EQA1508		x	x	Research
Yearling	16 mo.	Thoroughbred	M	EQA1509		x		Research
Adult	8 yo.	Warmblod	M	O115	x	x		Unknown
Adult	5 yo.	Standardbred	F	1607	x	x		Research
Adult	7 yo.	Standardbred	F	1608	x	x		Research
Adult	6 yo.	Standardbred	F	V1804			x	Research
Adult	6 yo.	Standardbred	F	V1805			x	Research
Adult	5 yo.	Standardbred	F	V1806			x	Research
Adult	7 yo.	Standardbred	M	V1807	x	x	x	Research
Middle-aged	16 yo.	Thoroughbred	F	S1702	x		x	Research
Middle-aged	18 yo.	Thoroughbred	F	S1703	x		x	Weight loos
Middle-aged	12 yo.	Standardbred	F	S1704			x	Research
Middle-aged	12 yo.	Standardbred	F	S1705			x	Research
Middle-aged	16 yo.	Fjord horse	M	O315		x		Unknown
Middle-aged	14 yo.	Pony	M	O415		x		Unknown
Middle-aged	13 yo.	Standardbred	F	1606	x	x		Research
Middle-aged	15 yo.	Standardbred	F	O916		x		Research
Middle-aged	15 yo.	Standardbred	F	1116	x			Research
Geriatric	25 yo.	Coldblood	M	O314	x	x		Unknown
Geriatric	22 yo.	Thoroughbred	F	G1609	x	x	x	Research
Geriatric	32 yo.	Thoroughbred	F	G1610			x	Research
Geriatric	25 yo.	Thoroughbred	F	G1801	x	x	x	Lymphoma
Geriatric	31 yo.	Thoroughbred	F	G1802	x	x	x	Colic

**d.=days old, mo.=months old, yo.=years old, M=Male, F=Female, BM= Bone marrow, AT= Adipose tissue, MSC= Mesenchymal stem cells, DF= Dermal fibroblasts.*

2.2.1.1 Bone marrow derived MSC collection and isolation

BM or BM aspirates were collected immediately post-mortem from the sternum of 12 female and 8 male horses, with the following age distribution; newborn (mean=0 days, range=0-0 days), yearling (mean=15.7 months, range=15.3-16 months), adult (mean=6.8 years, range=5-8 year), middle aged (mean=15.5 years, range=13-18 year), and geriatric (mean=25.8 years, range=22-31 year).

For the newborns, BM was collected as described by Vidal *et al.* [42] with few modifications. Briefly, BM was collected from the 4^{th}-6^{th} sternebrae by sterile curettage after splitting the sternum in midline. The marrow trabecular bone was transported on ice to the laboratory in ice cold sterile Dulbecco's phosphate buffered saline (dPBS, Gibco, Cat# 14190144) with 2% (v/v) amphotericin B (Gibco, Cat# 15290026), and 2% (v/v) penicillin/streptomycin (P/S, Gibco, Cat#15070063) (isolation juice) and processed within 2 hours of collection. In the cell laboratory, the marrow trabecular bone was rinsed twice in 37°C pre-warmed isolation juice and crushed before being grown as an explant culture in 2 T75 cm^2 culture flasks (Cellstar BioGreiner, VWR, Cat# 82050-856) with 12 mL/flask Dulbecco's modified Eagle's medium (DMEM, 1 g/L glucose, with phenol red, GlutaMAX, and pyruvate, Gibco, Cat# 10567-022), 10% (v/v) fetal bovine serum (FBS), 1% (v/v) P/S, and 1% amophotericin B (isolation medium). After 48 hours, BM crusts and non-adherent cells were aspirated along with the isolation medium, and the medium was changed to expansion medium containing 1 g/L DMEM, 10% FBS, and 1% P/S. The cells were cultured at 37°C in a humidified atmosphere containing 5% CO_2 and expansion medium was changed every 2-3 days.

For the four latter age groups, BM was aspirated from the 4^{th}-6^{th} sternebrae as previously described [34,42]. In short, the area over the sternum was clipped and surgically prepared with 2% chlorohexidine medical scrub and 70% ethanol. A total of 20 mL of BM was collected using a 10 cm, 11 G Jamshidi® bone biopsy needle (Henry Schein Vet, Cat# DJ4011X) and two 20 mL Luer-Lock syringes preloaded with 1000 IU sodium heparin (Henry Schein Vet, Cat# 4327680) per 10 mL BM aspirate. The BM aspirate was transferred to a 50 mL falcon tube and gently inverted, before being transported on ice to the laboratory and further processed within 2 hours of collection. In the cell laboratory, the BM aspirate was layered slowly onto Ficoll-Paque® PREMIUM (GE Healthcare, Cat# 17-5442-02) in a 1:1 (v/v) manner and centrifuged for 30 minutes at 600 g. The mononuclear cell layer containing BM-MSCs was collected and washed twice in sterile dPBS and centrifuged for 5 minutes at 200 g between the washes. The supernatant was removed and the pellet was re-suspended in 24 mL isolation medium and equally divided into two T75 cm^2 culture flasks. After 48 hours, allowing the BM-MSCs to adhere to the bottom of the flasks, the first medium change occurred and isolation medium was replaced with expansion medium. The cells were incubated at 37^oC and 5% CO_2.

2.2.1.2 Adipose tissue derived MSC collection and isolation

AT was collected from the gluteal region above the biceps femoris muscle next to the tail base of 10 female and 10 male horses as previously described [34], with the following age distribution; newborn (mean=0 days, range=0-0 days), yearling (mean=15.8 months, range=15.3-16.1 months), adult (mean=6.8 years, range=5-8 year), middle aged (mean=14.5 years, range=13-16 year), and geriatric (mean=25.8 years, range=22-31

year). Briefly, the gluteal area next to the tail base was surgically clipped and prepared as described for BM-MSCs, and 10 grams of AT was collected through a ~8 x 8 cm surgical window. The AT was transferred to a 50 mL falcon tube with ice cold isolation juice and transported on ice to the laboratory where the tissue was further processed within 2 hours of collection. In the cell laboratory, the AT was washed two times in isolation juice and dissected into smaller pieces where visible blood vessels were removed. The AT was digested in sterile filtered (0.2 µm) AT enzyme medium consisting of DMEM (1 g/L), 1% P/S, 50 µg/mL gentamycin (Sigma-Aldrich, Cat# G1264-1G), and 1 mg/mL collagenase type I (Worthington, Cat# X7H9763A) for 3 hours at 37^{o}C and 30 rpm. The enzyme medium containing released cells was transferred through a 70 µm cell strainer and the pellet with AT-MSCs was washed twice in sterile dPBS and centrifuged at 500 g for 5 minutes between the washes. The pellet was re-suspended in 24 mL isolation medium supplemented with 50 µg/mL gentamycin and distributed into 2 T75 cm^2 culture flasks. The first medium change occurred 48 hours after isolation, where fresh expansion medium was added. The cells were grown at 37^{o}C in air with 5% CO_2 with medium change every 2-3 days.

2.2.1.3 Dermal fibroblast collection and isolation

DFs (biological control) were harvested from the gluteal region above the biceps femoris muscle next to the tail base of 14 female and 6 male horses as previously described [35], with the following age distribution; newborn (mean=0 days, range=0-0 days), yearling (mean=15.6 months, range=15.3-16 months), adult (mean=6 year, range=5-7 year), middle aged (mean=14.5 years, range=12-18 year), and geriatric (mean=27.5 years, range=22-32 year). Briefly, 6 grams of dermal tissue was collected from the surgical

window made to collect AT-MSCs. The dermis was transferred to a 50 mL falcon tube with ice cold isolation juice and transported on ice to the laboratory where the tissue was further processed within 2 hours of collection. In the cell laboratory, the dermal tissue was washed two times in isolation juice and dissected into smaller pieces. The dermis was digested in sterile filtered (0.2 µm) DF enzyme medium consisting of dPBS, 1% P/S, 1% bovine serum albumin (BSA – Sigma, Cat# A9418-10G), 50 µg/mL gentamycin, and 1 mg/mL collagenase type I for 2 hours at 37°C and 30 rpm. The enzyme medium containing released cells was transferred through a 70 µm cell strainer and the pellet with DFs was washed twice in sterile dPBS and centrifuged at 1000 g for 4 minutes between the washes. The pellet was re-suspended in 24 mL isolation medium supplemented with 50 µg/mL gentamycin and distributed into 2 T75 cm^2 culture flasks and grown at 37°C in air with 5% CO_2. The first medium change occurred 48 hours after isolation, where fresh expansion medium was added. Expansion medium was changed every 2-3 days.

Figure 2.1: *Representative images showing collection sites for sternal bone marrow from newborn foals (A) and adult horses (C), adipose tissue (B) and dermal tissue (E). Some of the materials needed for tissue collection are shown in image D. *Modified anatomy horse from: www.rainbowresource.com.*

2.2.2 Cell expansion and storage

At approximately 80% confluence, the cells were passaged with 1 mL 0.25% Trypsin/1 mM EDTA (Gibco, Cat# 11560626) per T75 cm^2 culture flask. Cell counting was performed manually using tryphan blue (Fisher Scientific, Cat# 11538886) and a hemocytometer. The cells were grown with a seeding density of 500,000 cells per T75 cm^2 culture flask. At passage 2 (P2), the cells were cryopreserved with Recovery-Cell Culture Freezing Medium® (Gibco, Cat# 11560446, containing 10% DMSO) at a concentration of 2-3 x 10^6 cells per 1 mL freezing medium in cryogenic vials (Nalgene, Thermo Scientific, Cat# 5000-0020). The cells were thawed in 37^{o}C pre-warmed expansion medium and washed three times in dPBS to remove leftover freezing medium before being grown in expansion medium and incubated at 37^{o}C and 5% CO_2 with medium change every 2-3 days. Proliferation assays were performed at passage 4.

2.2.3 Assessment of cellular proliferation

Cellular proliferation was quantified by determining levels of incorporated 5-ethynyl-2'-deoxyuridine (EdU) after pulse labeling. EdU is a thymidine analog that is integrated into newly synthetized DNA when the cell goes through the synthesis (S) phase of the cell cycle. Using Click-iT chemistry, EdU incorporated proliferating cells can be fluorescently labeled and visualized through fluorescence microscopy. EdU pulsing, fluorophore labeling, and subsequent visualization was done as described previously [36,132], and by the manufacturer using a Click-iT Plus Alexa Fluor 594 EdU Imaging Kit® (Life Technologies, Cat# C10639).

In short, passage 4 cells were seeded at a density of 25,000 cells per well in a 24-well plate (Nunc, Thermo Scientific, Cat# 10604903) and cultured in expansion medium

for 48 hours. Seeding density and expansion duration was determined based on a pilot study to avoid overlapping of cells (data not shown). The cells were then pulsed for 24 hours with 8 µM EdU (Jena Bioscience, Cat# CLK N001-25). A total of 8 technical replicate wells were pulsed with EdU, and 1 control well was kept under normal expansion medium without pulsing. Next, the cells were fixed in 4% methanol-free paraformaldehyde (Fisher Scientific, Cat# 11586711, in dPBS) and washed with 3% BSA (Sigma, Cat# A7906, in dPBS) before being permeabilized with 0.1% Triton-X (Sigma, Cat# T9284). For EdU label detection, the cells were incubated for 30 minutes with 250 µL kit cocktail containing Alexa 594 per well. The staining cocktail was removed and the cells were washed with 3% BSA and dPBS before being counterstained with 300 µL 4', 6-diamidino-2-phenylindole dihydrochloride (DAPI - Invitrogen, Life Technologies, Cat# D1306) per well for 15 minutes at a concentration of 1µg/mL. The fluorophore staining cocktail was prepared fresh for each assay and the cells were incubated protected from light.

Images of the cells were taken in the dark using a fluorescence microscope with DAPI and Texas Red (equivalent to Alexa 594) filters using exposure times between 100-150 ms. A total of 3 random images were taken per well for each fluorophore. The total number of cell nuclei (DAPI stained) and the number of proliferating cells (EdU labeled and Alexa 594 stained) were counted using automated imaging software (NIH Image-J version 1.48). The cellular proliferation rate was calculated as the number of EdU labeled nuclei as a percentage of total cell nuclei in each image. The proliferation percentage was calculated for all 3 images per well and then averaged.

2.2.4 Differential gene expression

2.2.4.1 RNA isolation and reverse transcription

Passage 4 cells were grown as monolayer cultures in T75 cm^2 flasks with expansion medium. At approximately 80% confluence, the cells were extracted with QIAzol® (Qiagen, Cat# 79306), a guanidinium thiocynate-phenol-chloroform lysis reagent, and snap frozen in liquid nitrogen before being stored at -80°C prior to RNA isolation. The cells were homogenized in 2 mL of QIAzol® using a PowerGen 125 homogenizer (Fisher Scientific, Cat# 15120247). Total RNA was isolated using a spin column-based Qiagen RNeasy Mini Kit® (Qiagen, Cat# 74104) with modifications as previously described [144]. RNA quantity was determined immediately after RNA isolation using a NanoDrop ND 1000 spectrophotometer. The samples then underwent ethanol precipitation to remove processing contaminants. Quantification of the purified RNA was performed using the Qubit BR Assay (Life Technologies, Cat# Q10210) and NanoDrop ND 1000 spectrophotometer. The quality of the purified RNA was assessed with a Bioanalyzer 2100 (Agilent Technologies, Eukaryotic Total RNA Nano & Pico Series II). All purified RNA samples met the following quality thresholds; 260/280 ratios of 1.9-2.1, 260/230 ratios of 1.8-2.28, and an Agilent RNA integrity number (RIN) of ≥ 8.0, with the exception of one sample (Appendix 1) that behaved as expected in down-stream analyses and thus were not excluded from the study.

Removal of potential genomic DNA contamination and reverse transcription of total RNA to cDNA was achieved using a commercially available kit as per manufacturer's protocol (Maxima First Strand cDNA Synthesis Kit® for RT-qPCR with

dsDNase, Life Technologies, Cat# K1672). All cDNA samples were diluted with nuclease-free water to 13.9 ng/uL and stored at -80^{o}C.

2.2.4.2 Real-time quantitative PCR

Forty-seven biomarkers were selected for the gene expression panel based on functional annotation to have biological relevance important for cell proliferation, cellular senescence, or evidence in the literature of age-dependent variation related to proliferation. The biomarker panel e.g. included known mitogens, cell cycle regulators, tumor suppressors, anti- and pro-apoptotic genes, and markers of cellular senescence (Genes and annotations are shown in Appendix 2).

Commercially available, validated equine-specific TaqMan® primer-probe sets (FAM dye-labeled MGB probes - Thermo Fisher) for all biomarkers were used to quantitate the steady state mRNA levels. Details on the primer-probe sets are listed in Table 2.2. The functionality of all primer-probe sets was tested against a positive control equine sample containing mixed cDNA consisting of a 43-sample pool of various tissue [145], day 35 whole fetus, and neonatal epiphyseal cartilage. Negative controls of RNase-free water and minus-template was incorporated, and each sample was run in duplicate.

Real-time quantitative PCR (RT-qPCR) reactions were conducted in a 384-well plate with a total reaction volume of 10 µL using 62.55 ng cDNA per reaction. A robotic ViiA™ RT-qPCR System (Thermo Fisher Scientific) was used to perform the reactions. LinRegPCR was used to measure reaction amplification efficiencies and cycle threshold (Ct) values were calculated [146]. All targets amplified with amplification efficiencies close to 2 except for the negative controls that showed no amplification (data not shown).

Three commercially available equine-specific endogenous control TaqMan® primer-probe sets were tested against all samples. The endogenous controls consisted of β-2-microglobulin (B2M), β-glucoronidase (GUSB), and ribosomal protein lateral stalk subunit P0 (RPLP0). Using NormFinder software [147], GUSB was determined as having the most uniform performance across all cell types and age groups (data not shown).

The gene expression of the experimental samples were analyzed by RT-qPCR using the BIOMARK HD System (Fluidigm) as previously described [148]. Fluidigm is an automated nanofluidic RT-qPCR system that uses microfluidic technology in which dynamic arrays of integrated fluidic circuits are used, allowing for samples and reagents to be mixed in a variety of patterns. Hence, little sample quantity is needed to be tested against multiple (e.g. 96) targets, making it less time-consuming and more cost-effective compared to standard qPCR [148].

Briefly, all experimental cDNA samples were shipped at a concentration of 13.9 ng/µL (middle of positive standard curve), together with the positive control (7 three-fold dilutions to detect high and low expressed genes), negative controls, and primer-probe sets (including endogenous controls) to The Carver Biotechnology Center, University of Illinois, IL, USA, where the Fluidigm was performed. A total of 7 µL of cDNA and 25 µL of primer-probe sets were shipped per sample or target, respectively. The Fluidigm was carried out using 96.96 dynamic arrays (Fluidigm Corporation, CA, USA) according to manufacturer's instructions.

The data were analyzed with Fluidigm Real-Time PCR Analysis Software in the BIOMARK instrument (Fluidigm Corporation, CA, USA) where Ct values were

calculated. Delta Ct values were determined for each sample by subtracting the corresponding Ct value of the endogenous control (GUSB). The positive control was used as a calibrator to calculate ΔΔCt values. Relative expression (RQ) of the gene targets were calculated using the $2^{-\Delta\Delta Ct}$ method [149]. RQ levels were used for graphical bar/boxplot presentations made in GraphPad Prism 8.0.1, and Ln(RQ) values were used for heatmap and statistical analysis to linearize the data again and to avoid right-shifting of data. Gene expression heatmap visualization was done on averaged Ln(RQ) levels for each study group, grouping the samples according to cell type and donor age, and genes according to biological function. Heatmap was generated in RStudio 3.6.0 using the *heatmap ggplot* function.

2.2.5 Inter-laboratory control

The study was performed in two different laboratories (University of Copenhagen (UCPH) and University of Kentucky (UK)). To control for potential inter-laboratory differences, an inter-assay control was included. BM-MSCs from the same cell line was shipped on dry-ice from UK to UCPH and tested using the same procedures in both laboratories. Plastic ware, mediums, reagents, commercially available kits, and protocols were kept constant throughout the entire study for all samples. The inter-laboratory control was tested using the EdU proliferation assay and by Fluidigm RT-qPCR. Isolated RNA was shipped on dry-ice from UCPH to UK to allow for all RNA and cDNA samples to be analyzed on the same machines. Laboratory was furthermore added as a variable in the statistical model used for data analysis. All inter-laboratory controls showed no indication of significant differences between laboratories (data not shown).

Table 2.2: Overview of TaqMan primer-probe sets used in RT-qPCR reactions.

Gene ID	Gene name(s)	ThermoFisher Assay ID
ABI3BP	ABI family member 3 binding protein	Ec06625599_m1
AQP1	Aquaporin	Ec06625425_m1
AREG	Amphiregulin	Ec06992855_m1
BARD1	BRCA1-associated RING domain 1	Ec07061151_m1
BAX	BCL2 associated X apoptosis regulator	Ec07016716_s1
BCL2	B-cell lymphoma 2	Ec07005800_g1
BMP3	Bone morphogenic factor 3	Ec07037656_m1
BRCA1	Breast cancer type 1	Ec07017862_s1
CASP3	Caspase 3	Ec03470391_m1
CASP8	Caspase 8	Ec06959413_m1
CAVIN1	Caveolae associated protein 1	Ec07036873_m1
CCND1	Cyclin D1	Ec07036996_m1
CDKN1A	p21, Cyclin-dependent kinase inhibitor 1A	Ec06955195_m1
CLU	Clusterin	Ec03468575_m1
COMP	Cartilage oligomeric matrix protein	Ec03468062_m1
CSF2	Colony stimulating factor 2	Ec03468208_m1
CTGF	Connective tissue growth factor	Ec06625777_gH
CTNNB1	Beta-catenin	Ec00991819_m1
EPGN	Epithelial mitogen	Ec06992859_m1
FGF1	Fibroblast growth factor 1	Ec01092738_m1
FGF5	Fibroblast growth factor 5	Ec04656774_m1
FGF18	Fibroblast growth factor 18	Ec03248217_g1
GDF6	Growth differentiation factor 6	Ec07097112_m1
GLB1	Beta-galactosidase	Ec06954363_m1
GLI3	GLI family zinc finger 3	Ec06625512_m1
HDGF	Hepatoma-derived growth factor	Ec07037751_m1
HGF	Hepatocyte growth factor	Ec07000054_m1
IGF1	Insulin-like growth factor 1	Ec03468689_m1
IGFBP5	Insulin-like growth factor binding protein 5	Ec03470296_m1
LOC100146270	p16, Cyclin-dependent kinase 4 inhibitor B	Ec07037471_mH
MET	MET proto-oncogene, receptor tyrosine kinase	Ec02622441_m1
MYC	c-myc	Ec07007511_m1
PCNA	Proliferating cell nuclear antigen	Ec06974312_m1
PDGFD	Platelet-derived growth factor subunit D	Ec06997714_m1
PHB	Prohibitin	Ec07055990_m1
PTCH2	Patched 2	Ec06625424_g1
S100A1	S100 calcium binding protein A1	Ec03470173_g1

Table 2.2: (Continued)

Gene ID	Gene name(s)	ThermoFisher Assay ID
SNAI2	Snail family transcriptional repressor 2	Ec06625397_m1
SOST	Scherostin	Ec07036868_m1
TERT	Telomerase reverse transcriptase	Ec06972692_m1
TGFA	Transforming growth factor alpha	Ec06949183_m1
TGFB1	Transforming growth factor beta 1	Ec06625477_m1
TGFB2	Transforming growth factor beta 2	Ec07074189_g1
TGFB3	Transforming growth factor beta 3	Ec00682163_m1
TIMP2	Metallopeptidase inhibitor 2	Ec03470558_m1
TP53	Tumor protein 53	Ec03470648_m1
VEGFA	Vascular endothelial growth factor A	Ec03467879_m1
B2M	Beta-2-microblobulin	Ec03468699_m1
GUSB	Beta-glucoronidase	Ec03470630_m1
RPLP0	Ribosomal protein lateral stalk subunit P0	Ec04947733_g1

2.2.6 Statistical analysis

The cellular proliferation data, comparing age-groups within cell types and across cell types, were analyzed with a generalized linear mixed model using The GLIMMIX Procedure in SAS 9.4 with Tukey-Kramer's *post hoc* modifications for multiple comparisons. Gene expression data were analyzed in 2 steps. Initially, one-way analysis of variance (ANOVA) using SAS 9.4 was applied individually to all 47 gene targets within each cell type to look for donor age effects. Next, targets showing significant difference on the ANOVA and more than 5-fold difference between study groups on the heatmap (Figure 2.6) were analyzed using The GLIMMIX Procedure with Tukey-Kramer's *post hoc* modifications for multiple comparisons to compare across tissue types. Statistical analysis of Fluidigm RT-qPCR results was performed on individual extracted Ln(RQ) values. Genes with missing data points (as visualized on Figure 2.6) were removed from the statistical analysis for the given cell type. To control for non-paired samples and potential inter-laboratory variables, horse number and laboratory were added to the statistical models as additional factors. Due to age-clustering within age groups, statistical linear regression analyses were not feasible and kinetics were determined based on graphical presentations. Data were considered statistically significant if the p-values were <0.05.

2.3 RESULTS

2.3.1 EdU proliferation assay

All cell lines were able to be expanded to ~80% confluence at passage 4. When assessing the effect of donor age within one cell type, there was a significant decrease in cellular proliferation with increasing donor age for BM-MSCs ($p=0.0154$), AT-MSCs ($p=0.0003$), and DFs ($p<0.0001$) (Table 2.3 and Figure 2.3). For BM-MSCs, there was a significant difference in pair-wise comparisons between newborn and geriatric ($p=0.0234$), yearling and geriatric ($p=0.0352$), and adult and geriatric ($p=0.0247$) horses. Representative images of proliferating BM-MSCs from horses in different age groups are shown in Figure 2.2. Similarly for AT-MSCs, there was a significant difference between newborn and geriatric ($p=0.0007$), yearling and geriatric ($p=0.0015$), adult and geriatric ($p=0.001$), and middle-aged and geriatric ($p=0.0016$) horses (Figure 2.3). Hence, there is interestingly no difference in pairwise comparisons between age groups other than geriatric horses for BM- and AT-MSCs. For DFs, there was a significant difference in pair-wise comparisons between newborn and middle-aged ($p=0.0453$), newborn and geriatric ($p<0.0001$), yearling and middle-aged ($p=0.0275$), yearling and geriatric ($p<0.0001$), adult and geriatric ($p<0.0001$), and middle-aged and geriatric ($p=0.0006$) horses (Figure 2.3).

When comparing across cell types, all cell types were equally affected by donor age ($p=0.3359$), and there was no significant difference in the cellular proliferation between BM- and AT-MSCs in any of the age groups ($p>0.4$) (Figure 2.4). When comparing cell types independent of age groups, DFs had a higher cellular proliferation than BM-MSCs ($p=0.0055$) and AT-MSCs ($p=0.0177$).

As an evaluation of the study set up, no Alexa 594 background staining was detected in any of the negative control wells grown without EdU pulsing, and no study group reached a cellular proliferation of 100% (Table 2.3). Furthermore, Alexa594 staining was detected in all wells pulsed with EdU, together with DAPI staining.

Table 2.3: Cellular proliferation data of equine adipose tissue (AT)- and bone marrow (BM) derived mesenchymal stem cells (MSC) and dermal fibroblasts (DF) from horses in 5 different age groups after 24 hours of labeling with 8 µM EdU.

Age group	Cell type	n	Mean (%)	Standard deviation	Minimum (%)	Maximum (%)
0 d.	AT-MSC	4	91.87	8.07	80.00	98.02
	BM-MSC	4	89.25	3.20	85.26	92.80
	DF	4	95.16	1.63	93.13	97.00
1-2 yo.	AT-MSC	4	89.96	7.90	79.64	96.82
	BM-MSC	4	88.12	2.05	85.12	89.67
	DF	4	95.66	1.77	94.02	97.71
5-8 yo.	AT-MSC	4	90.87	5.49	82.78	94.34
	BM-MSC	4	89.10	3.12	84.48	91.26
	DF	4	93.93	1.48	92.78	95.98
12-18 yo.	AT-MSC	4	89.72	3.15	85.08	92.06
	BM-MSC	4	84.10	4.79	80.50	91.13
	DF	4	89.29	1.46	87.14	90.43
≥ 22 yo.	AT-MSC	4	67.66	6.13	61.02	75.56
	BM-MSC	4	70.91	15.14	48.58	82.16
	DF	4	79.23	4.98	73.71	84.75

**d.: days old, yo.: years old.*

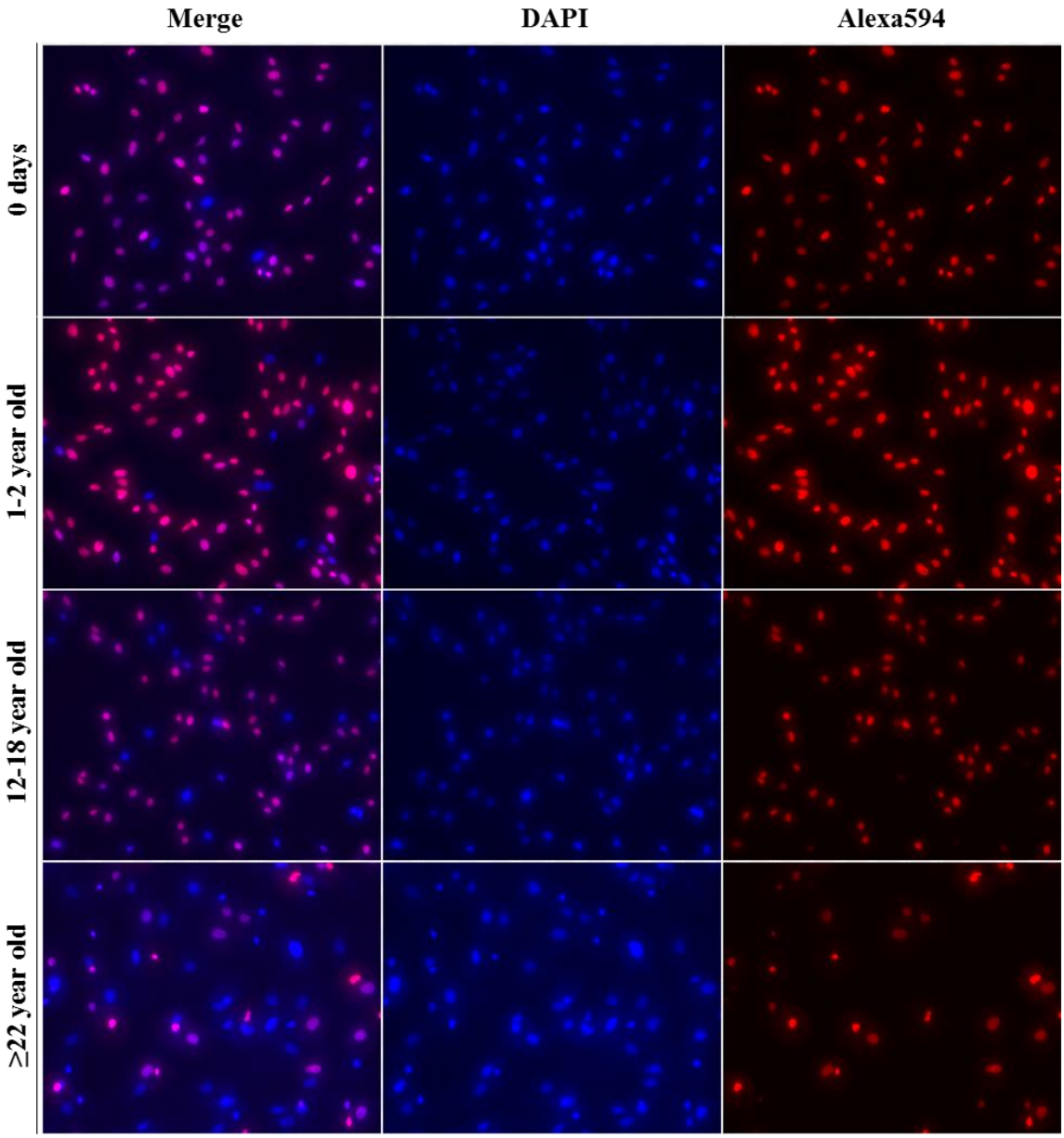

Figure 2.2: *Representative images (20X magnification) of EdU-labeled proliferating cell nuclei (Alexa594 – Red/Pink) and all cell nuclei (DAPI – Blue) from equine bone marrow derived mesenchymal stem cells in different age groups.*

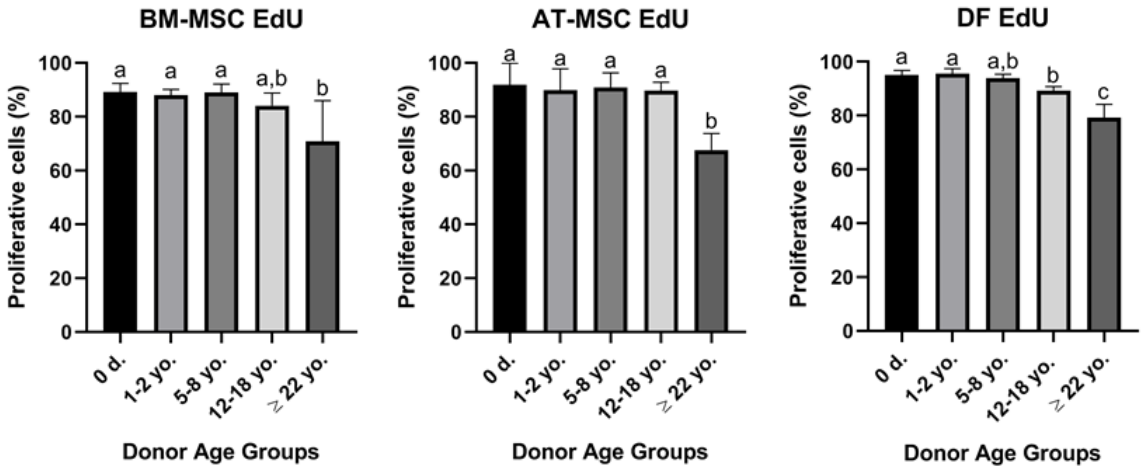

Figure 2.3: *Bar plots showing the cellular proliferation in percentage of bone marrow (BM)- and adipose tissue (AT) derived mesenchymal stem cells (MSC) and dermal fibroblasts (DF) from horses in 5 different age groups (n=4, N=60) after 24 hours of labeling with 8 µM EdU. Age groups within the same cell type not labeled with the same letter are significantly different from each other (p<0.05).*

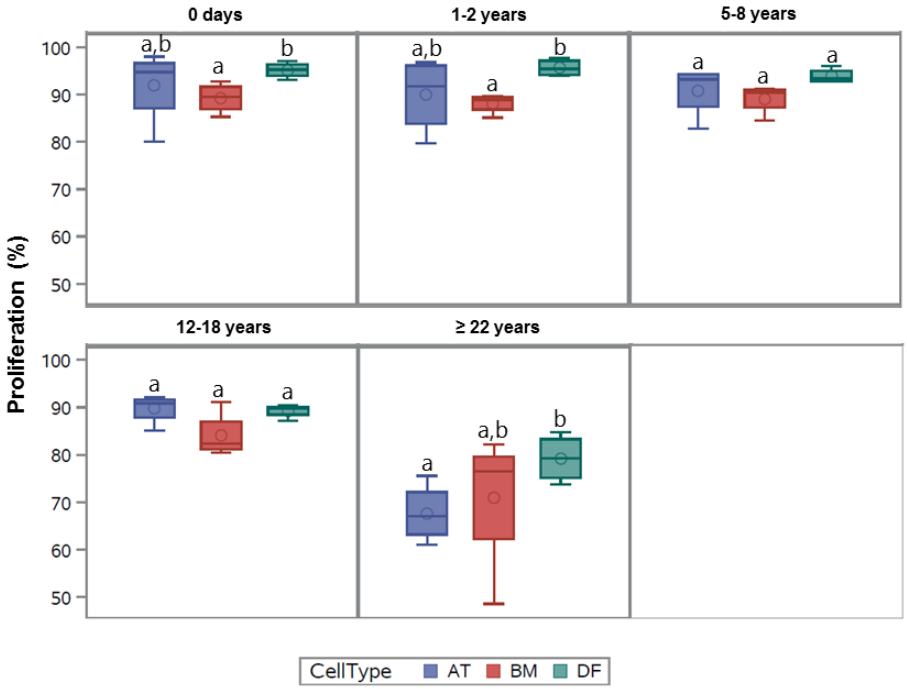

Figure 2.4: *Box plots showing the cellular proliferation (%) of equine adipose tissue (AT)- and bone marrow (BM) derived mesenchymal stem cells and dermal fibroblasts (DF) from horses in 5 different age groups (n=4 horses per age group per cell type) after 24 hours of labeling with 8 µM EdU. Cell types within the same age group not labeled with the same letter are significantly different from each other (p<0.05).*

2.3.2 Gene expression

Out of the 47 biomarkers related to proliferation and aging, gene expression was affected by donor age in 4 biomarkers (9%) in AT-MSCs, 17 biomarkers (36%) in BM-MSCs, and 15 biomarkers (32%) in DFs. Differentially expressed genes as a function of donor age within each cell type are shown in Table 2.4 and in a Venn-diagram in Figure 2.7 where intersections are visualized.

Multiple growth factors (FGF1, FGF18, GDF6, PDGFD, TGFA, and VEGFA) were up-regulated in BM-MSCs from old horses compared to young horses. On the other hand, fibroblast growth factor 5 (FGF5) were found at lower levels in BM-MSCs from geriatric horses compared to newborns ($p=0.0212$), and in higher levels in AT-MSCs compared to BM-MSCs ($p=0.0078$). Cell cycle regulators, cyclin D (CCND1) and proliferating cell nuclear antigen (PCNA), were not affected by donor age in either of the two stem cell types, but were down-regulated in DFs from geriatric horses ($p=0.0118$ and $p<0.0001$, respectively). In general, cyclin D were found at higher levels in BM-MSCs compared to AT-MSCs and DFs ($p<0.0032$), whereas PCNA was found at higher levels in DFs compared to AT-MSCs ($p<0.0001$) and BM-MSCs ($p=0.0004$). The positive regulators of cell proliferation, colony stimulating factor 2 (CSF2), were up-regulated in BM-MSCs from geriatric horses compared to all other age groups ($p<0.0005$), whereas GLI family zinc finger 3 (GLI3) were down-regulated in geriatric BM-MSCs ($p\leq0.0157$) (Figure 2.6).

For BM-MSCs, expression of the senescent marker β-galactosidase (GLB1) was significantly higher in geriatric horses compared to newborn ($p=0.0018$), yearlings ($p=0.0163$), and adult horses ($p=0.0293$), and in middle-aged compared to newborn

horses (p=0.0116). GLB1 was not affected by donor age in AT-MSCs or DFs. Higher GLB1 expression was seen in BM-MSCs compared to AT-MSCs and DFs in geriatric horses (p=0.0011 and p=0.0003, respectively) (Figure 2.6).

As shown in Figure 2.5, the tumor suppressors p16 (LOC100146270) and p21 (CDKN1A) were both up-regulated in geriatric BM-MSCs compared to newborn horses (p=0.0103 and p=0.0228, respectively). Moreover, p16 and p21 showed higher levels in BM-MSCs than in AT-MSCs ($p \leq 0.0155$) or DFs ($p \leq 0.0002$). For AT-MSCs, the tumor suppressor p53 (TP53) had higher expression in geriatric horses compared to newborn (p=0.0024) or yearlings (p=0.0075). The pro-apoptotic genes caspase 3 (CASP3) and caspase 8 (CASP8) were up-regulated in BM-MSCs from older horses ($p \leq 0.0028$).

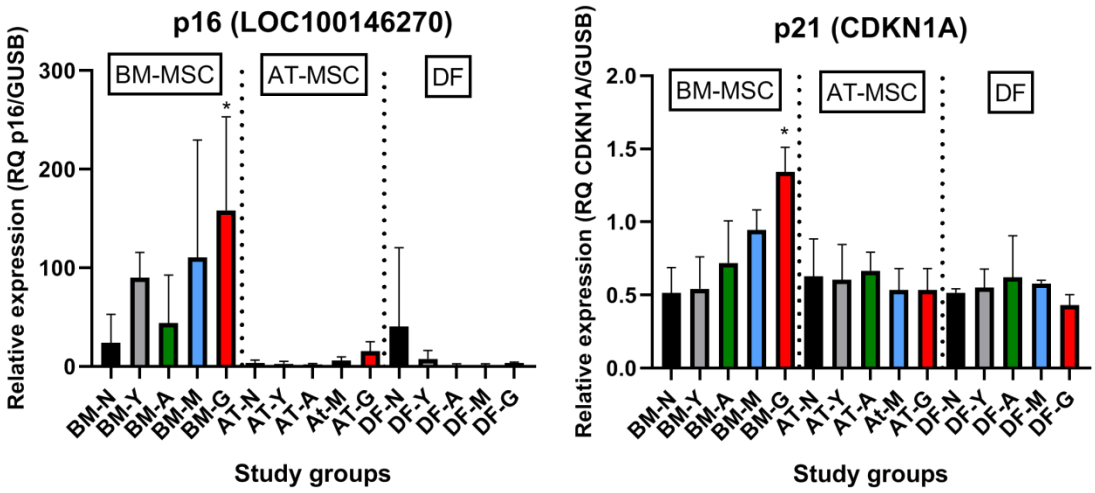

Figure 2.5: *Bar plots showing mean relative gene expression (RQ) of p16 and p21 steady state mRNA in monolayer cultures of bone marrow (BM)- and adipose tissue (AT) derived mesenchymal stem cells (MSC) and dermal fibroblasts (DF) from horses in 5 different age groups (n=4, N=60) relative to the positive control. *: indicate significant difference between geriatric and newborn age group for BM-MSCs (p<0.05). N: Newborn (black), Y: Yearling (gray), A: Adult (green), M: Middle-aged (blue), G: Geriatric (red).*

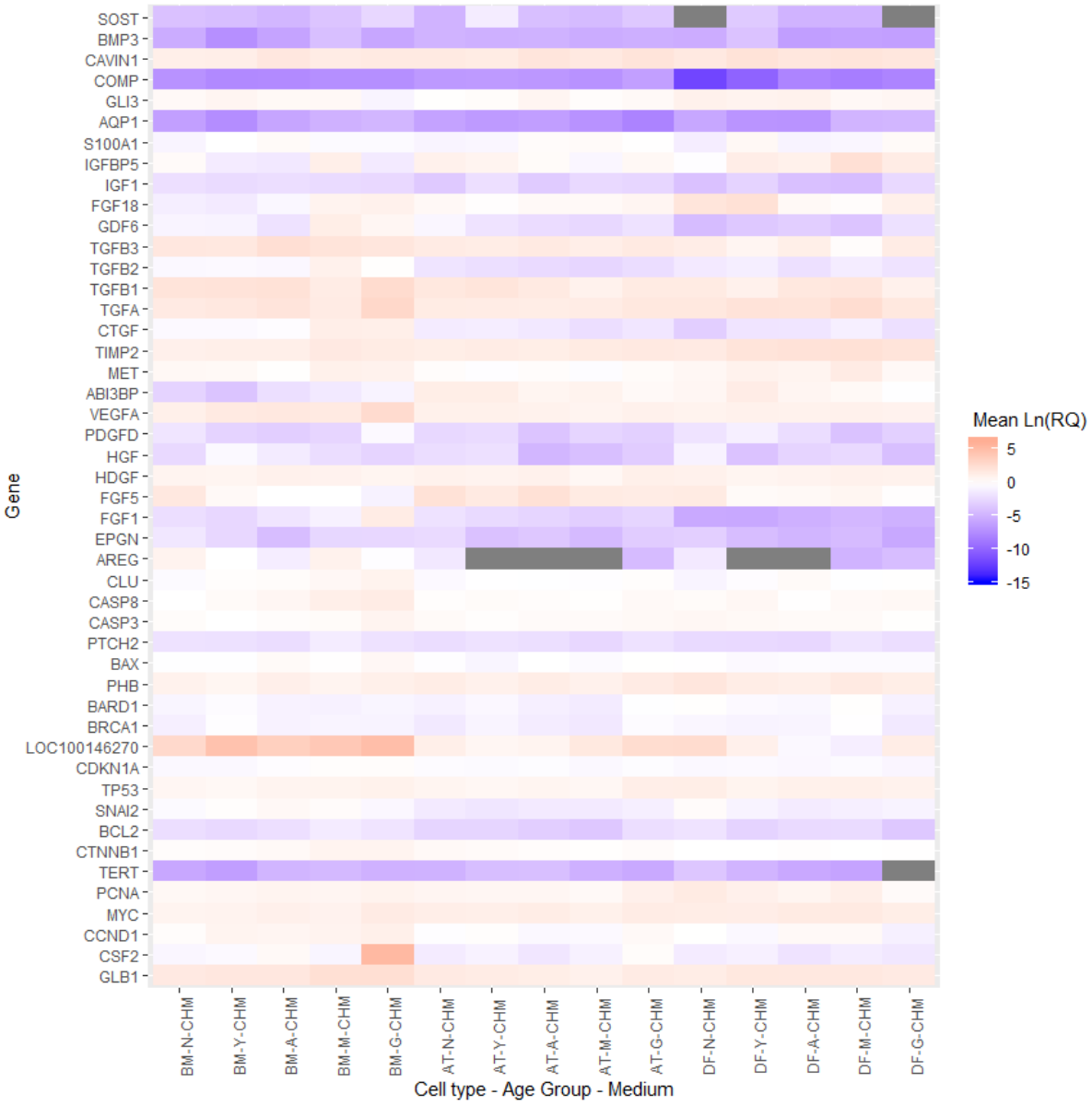

Figure 2.6: *Heatmap showing the Ln(RQ) levels of gene expression by color change between average levels in bone marrow (BM) and adipose tissue (AT) derived mesenchymal stem cells (MSCs) and dermal fibroblasts (DF) from horses in 5 different age groups (n= 4 horses per age group per cell type). Gray boxes indicate no detection of gene expression. *N: Newborn, Y: Yearling, A: Adult, M: Middle-aged, G: Geriatric, CHM: grown in T75 cm^2 culture flasks with normal expansion medium containing DMEM, 10% FBS, and 1% P/S and harvested at approximately 80% confluence.*

Table 2.4: Differentially expressed genes related to cellular proliferation as a function of donor age within adipose tissue (AT)- and bone marrow (BM) derived mesenchymal stem cells (MSC) and dermal fibroblasts (DF) from horses in 5 different age groups (n=4, N=60) after one-way ANOVA statistical analysis when significance was set to $p<0.05$.

Cell type	Gene function					
	Senescence marker	**Cell cycling**	**Growth factor**	**Anti-apoptotic**	**Tumor suppressor**	**Apoptotic**
AT-MSC		Down-regulated AQP1	Down-regulated HGF		Up-regulated TP53	Up-regulated SOST
BM-MSC	Up-regulated GLB1	Up-regulated AQP1 CSF2 CTGF	Up-regulated FGF1 FGF18 PDGFD TGFA VEGFA		Up-regulated CDKN1A GDF6 LOC100146270	Up-regulated CASP3 CASP8 SOST
		Down-regulated GLI3	Down-regulated FGF5			
DF		Up-regulated AQP1 COMP	Up-regulated FGF18 IGFBP5	Up-regulated CLU	Up-regulated GDF6	
		Down-regulated CCND1 PCNA	Down-regulated EPGN HGF PDGFD	Down-regulated BCL2	Down-regulated LOC100146270 TP53	Down-regulated CASP3

**All listed genes were significantly affected by donor age within the given cell type. Red marked genes indicate an up-regulation in gene expression with increasing donor age. Blue marked genes indicate a down-regulation in gene expression with increasing donor age.*

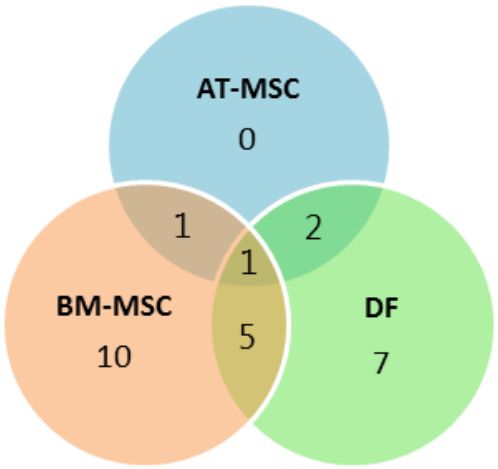

Figure 2.7: *Venn-diagram showing the distribution of differentially expressed genes as a function of donor age between adipose tissue (AT)- and bone marrow (BM) derived mesenchymal stem cells (MSC) and dermal fibroblasts (DF) from horses in 5 different age groups.*

2.4 DISCUSSION

In this study, we examined the effect of donor age on the cellular proliferation of equine BM- and AT-MSCs and DFs from horses in 5 different age groups, together with potential underlying gene expression changes in biomarkers related to proliferation and aging. Cellular proliferation *in vitro* is an essential component for MSC evaluation and expansion to therapeutically required numbers, and is furthermore positively correlated with regenerative capacity [140].

The results from the present study support the hypothesis that increasing donor age is a major variable impacting equine BM- and AT-MSCs proliferation with decreasing capacities following non-linear kinetics, which is similar to previous reports in other species [27,50,97,122,123]. Our results were furthermore supported by Schröck *et al.* who reported a heterogeneous population of equine BM-MSCs with a decreasing population of cells with maximum proliferation speed with increasing donor age [133].

Schröck's study, however, had a limited study population and was not designed to provide kinetics or clinically relevant thresholds with regards to donor age. Our study design with multiple clinically relevant age groups fills this knowledge gap, and interestingly shows that difference in equine BM- and AT-MSC cellular proliferation was only seen in pair-wise comparisons involving geriatric horses. High cellular proliferation was hence feasible in MSCs from horses below 18 years of age. This finding was supported by the gene expression data, where the majority of age related changes in expression only were seen in comparisons involving geriatric horses. However, the pair-wise comparison stands in contrast with other species where differences in proliferation were reported already in 8 year old monkeys [27] and in humans above 40 years of age [123].

On the other hand, Vidal *et al*. found no effect of donor age on the proliferative capacity of equine BM-MSCs [42]. However, Vidal's study only included horses below 5 years of age (mean 2.4 years old), and applied a less optimized manually cell doubling counting method which could explain the different conclusions. The EdU proliferation assay utilized in our study is a widely used cellular proliferation assay that provides several advantages over BrdU (5-bromo-2'-deoxyuridine) and cell doubling techniques used in previous studies [27,42,122]. Advantages includes no requirement for cell denaturation, high sensitivity, less investigator-dependent output and more time-efficient [36,132]. By using the EdU assay and automated cell counting, this study was able to determine proliferating cells that have gone through the S-phase of the cell cycle and thus were not in G0 or G1 phase arrest. The EdU assay was thereby more objective than previous approaches, and only included cells that had plastic adherence and were actively

proliferating, which is important as Yu *et al*. showed more cells in cell arrest and prolonged time in S-phase with increasing donor age [27].

The cellular proliferation of human AT-MSCs have previously been reported to be less prominently affected by donor age compared to BM-MSCs [134]. This was however not the case in the present study, where equine BM- and AT-MSCs showed similar cellular proliferation in all age groups and were equally affected by donor age. Together, this may heighten the relevance of BM-MSCs for autologous treatments as they have shown higher potential to treat cartilage and bone injuries [35,41,44]. On the other hand, less age related gene expression changes were seen in AT-MSCs with the selected biomarker panel compared to BM-MSCs and DFs. The age related changes were however all in intersection with alterations seen in BM-MSCs or DFs, and there was a consistency in up-regulation of genes suppressing proliferation and a down-regulation in genes promoting proliferation with increasing donor age. It is furthermore likely that AT-MSCs have other age related expression changes outside the selected biomarker panel as the phenotypic cellular proliferation was equal for AT- and BM-MSCs across age groups.

Our finding that DFs have a general higher cellular proliferation compared to BM-and AT-MSCs is supported by previous studies where DFs have been shown to be highly sensitive to mitogenic stimuli and readily expand in adherent monolayer cultures [36,150]. Proliferating cell nuclear antigen (PCNA), which is a cofactor for DNA polymerase δ and essential for DNA replication [151] was furthermore found at higher levels in DFs, together with less expression of the tumor suppressors p16 and p21. Compared with the two stem cell types, gene expression data from DFs showed a greater mixture of up- and down-regulated genes as a function of donor age within each

functional group. The decrease in cellular proliferation with increasing donor age for all 3 different cell types suggest that there is a general decline in the proliferative capacity of healthy equine cells with increasing donor age, which would be in accordance with Hayflick's limit [104].

The observed decrease in equine cellular proliferation with increasing donor age could e.g. be due to a decrease in growth factors and their receptors, a decrease in pro-cycling molecules, and/or an increase in cell cycle arrest genes and apoptotic factors. Similar to previous studies in other species, the tumor suppressor genes p16, p53, and p21 were up-regulated in MSCs from old donors [27,37,122–124]. p16 is a tumor suppressor that inhibits DNA replication by binding to cyclin dependent kinase 4/6 necessary for phosphorylating and inactivating Rb family members. Non-phosphorylated Rb thereby binds E2F transcription factor 1 resulting in G1-arrest [111]. An up-regulation in p16 may be due to an epigenetic de-repression of p16 reported to trigger cellular senescence [102]. p53 is a transcription factor for p21, and the growth inhibitory effect of p21 lies primarily in its ability to inhibit cyclin dependent kinases, which is necessary for the cell to progress from G1- to S-phase during the cell cycle [107]. Hence, p16 and p21 are considered markers of senescence [111,124,152]. Another function of p53 is its ability to induce transcription of apoptosis-associated genes like BAX, which leads to activation of caspase 3 [153]. Interestingly, increased p53 expression in old AT-MSCs did not result in detectable up-regulation of p21 or BAX in geriatric AT-MSCs, which e.g. can occur due to lacking phosphorylation of p53 and a resulting rapid degradation.

An increase in the apoptotic pro-factor caspase 8 can also cause up-regulation of caspase 3 [153], which is likely the reason why both CASP8 and CASP3 were up-

regulated in BM-MSCs from geriatric horses. Age related up-regulation of tumor suppressors and apoptotic factors could explain the lower cellular proliferation seen in aged horses as fewer cells would have been allowed to progress through the S-phase and get EdU incorporated. β-galactosidase (GLB1) activity is an additional marker of senescence [152], but higher gene expression in senescent cells is also reported [154]. In BM-MSCs, an age related increase in GLB1 expression was seen in geriatric horses corresponding well with a previous study showing accelerated cellular senescence with increasing donor age in human BM-MSCs [131].

In a recent study, knockdown of GLI family zinc finger 3 (GLI3) decreased stemness and cellular proliferation of cancer stem cells [155]. The observed decrease in GLI3 in BM-MSCs from geriatric horses may thus not only affect its proliferative capability but also its stemness, which has been shown to be negatively correlated with immunogenicity in allogenic transplants in an *in vivo* equine model [156]. On the other hand, multiple growth factors had higher expression in BM-MSCs from geriatric horses, which stands in contrast to the cellular proliferation finings and to previous rodent studies [97,126]. In support of the results is, however, a study by Zheng *et al.* where multiple growth factors including FGF1, PDGFA, and TGFA were up-regulated in BM-MSCs from older rats although not at significant levels [127]. Together, the gene expression data suggests that the decreased proliferation observed in BM-MSCs from geriatric horses may be more due to an up-regulation in tumor-suppressors and apoptotic factors than a decrease in growth factors or pro-cycling factors. It is moreover possible that aged BM-MSCs are less responsive to secreted growth factors, which highlights the need for more studies to investigate this further.

All of our cell lines independent of donor age were able to reach ~80% confluence at passage 4, which has also been documented in other species [50], and in an equine study reporting a decreased population doubling rate by passage 10 for BM-MSCs and by passage 20 for AT-MSCs in young horses [120]. Nevertheless, Yu *et al.* found that BM-MSCs from 12 year old rhesus macaque monkeys underwent senescence already at passage 2 and therefore could not be expanded [27]. Hillmann *et al*. also reported that the proliferation of equine adult AT-MSCs were higher at later passages compared to human adult cells [157]. Taken together with the pair-wise EdU comparison only involving geriatric horses and the majority of age related gene expression changes only involving geriatric horses, this raises the question if the cellular proliferation of equine BM- and AT-MSCs may follow a different biological aging pattern compared to other species or if the differences are due to technical variations?

All cells were collected immediately after euthanasia. This is, however, not believed to affect the translational value of the results into autologous transplantations, as no difference have been reported in MSCs from newly euthanized and anesthetized horses [133]. Collection of BM-MSCs varied for newborn and the other age groups as the newborn sternum was too cartilaginous and Jamshidi® bone marrow aspiration unfeasible. By splitting the sternum and growing the trabecular bone marrow as tissue explants, the same principles as described for foals previously were utilized [42], and the cells seeded down and followed the same expansion pattern as seen in yearlings. The newborn age group furthermore consisted only of cells from ponies, but this is believed to have minor importance as the cellular proliferation pattern and gene expression in this age group were similar to the other young age groups. The cells were collected from a

mixture of female and male horses, with both genders represented in each age group. However, there was a higher presentation of cells from female horses, but *in vitro* proliferation has been shown not to be affected by gender [50].

In conclusion, all cells independent of age group were able to be expanded to passage 4, but the cellular proliferation of equine BM- and AT-MSCs declined significantly in the geriatric age group. Furthermore, the cellular proliferation of BM- and AT-MSCs was similar in all age groups and they were equally affected by donor age. Underlying gene expression changes related to proliferation and aging showed a primary up-regulation in tumor suppressors, apoptotic genes and multiple growth factors in stem cells from old horses, and a down-regulation in some pro-cycling genes depending on cell type. AT-MSCs showed less age related expression changes in the selected biomarkers compared to BM-MSCs and DFs. Together, this highlights the importance of donor age considerations for autologous treatments in horses.

This study is the first equine study comparing the cellular proliferation potential of MSCs from horses in multiple age groups. Incorporation of 5 well-distinguished clinically relevant age groups furthermore sets it apart from most previous studies in other species where few wider age groups have been compared. The results are thus believed to be highly interpretable for clinical practice and when advising horse owners. By assessing changes in gene expression, we have identified targets to potentially improve the cellular proliferation capacity of MSCs from geriatric horses through molecular manipulations. Further transcriptome and mechanistic studies will be valuable in elucidating the exact effect of the identified biomarkers, their pathways, and how they are involved in regulating the cellular proliferation of equine MSCs as a function of

donor age. Our results showed that MSCs can be expanded *in vitro* at high rates in horses below 18 years of age, which is promising to obtain sufficient numbers for autologous treatments, but lacks to investigate how the cells proliferate *in vivo.* Furthermore, the proliferative capacity of MSCs needs to be held together with their potential to heal musculoskeletal injuries, which remains to be investigated as a function of donor age in horses. The next chapter in this dissertation will therefore focus on the effect of donor age on the chondrogenic and osteogenic differentiation potential of equine BM- and AT-MSCs in culture.

CHAPTER 3. DONOR AGE EFFECTS ON THE CHONDROGENIC AND OSTEOGENIC DIFFERENTIATION PERFORMANCE OF EQUINE MESENCHYMAL STEM CELLS IN CULTURE

3.1 INTRODUCTION

Orthopedic injuries are a major cause of lameness and morbidity in horses worldwide, leading to substantial personal and financial losses for horse owners and the horse industry [1–3]. Articular cartilage injuries are particularly problematic since cartilage has a very limited intrinsic repair capacity, believed to be due in part to a lack of vasculature and low mitotic activity of the chondrocytes. Articular cartilage is present on opposing bone surfaces in diarthrodial synovial joints, where its main functions are to distribute load and provide a smooth and lubricated surface for articulation to minimize the coefficient of friction for movement [4]. Lesions involving articular cartilage often progress and potentially involve subchondral bone, which leads to significant pain and loss of function, resulting in long periods of rest with a poor prognosis to return to full athletic function [4,5]. In the horse, evidence suggest that subchondral bone injuries can be an important etiological variable leading to the initial cartilage damage during osteoarthritis development [3,9,10]. Unlike articular cartilage, bone is vascularized and has access to progenitor cells which in general provides for healing capabilities. Nevertheless, a bone persistent reparative response with unmatched bone formation and resorption is reported in horses where architectural disruption leads to weak areas and is associated with some subchondral bone lesions and dense bone may never remodel completely. Bone persistent resorption areas are therefore believed to be one of the contributing factors to osteoarthritis in horses [3]. Consequently, there is a great need for articular cartilage and bone restoration methods as it applies to the functional unit of

diarthrodial joints. Unfortunately, none of the existing techniques have been able to fully restore articular cartilage structure and function with complete integration into the normal surrounding tissue [5,15–19].

Cell-based therapies with multipotent mesenchymal stem cells (MSCs) are an area of high scientific and clinical interest within the broad field of regenerative medicine, since MSCs have shown capacity to facilitate the repair of orthopedic injuries through differentiating, immunomodulatory, and growth factor excreting properties, in addition to managing the symptoms [17,18,21,22]. The normal function of MSCs in the body is to maintain and repair tissue from the germ layer they are derived from [158]. Clinically relevant equine tissue sources of MSCs include bone marrow (BM) and adipose tissue (AT), where published literature has reported a promising capacity to differentiate into chondrogenic and osteogenic lineages capable of restoring orthopedic lesions [38–42]. Differentiation capacity of these cells is becoming increasingly important with recent incorporation techniques of scaffolds containing MSCs to enhance retention of the cells within the injury site [61–64]. A positive correlation between *in vitro* differentiation capacity and growth factor excretion has also been reported [97].

Currently, the cell choice is mainly influenced by existing precedence, convenience of sampling, cost, and commercial interests, with BM and AT being the most commonly used sources in equine practice. The choice of MSC type, however, must also prioritize the cell type with the greatest potential for generating the injured tissue. Several studies have compared chondrogenic and osteogenic differentiation in a range of MSCs [35,38,39,41,43], and most studies report a higher potential of BM-MSCs to treat cartilage and bone injuries compared to AT-MSCs [35,41,44,45]. Presently, the

application of MSCs in equine practice is usually autologous, using cells harvested from the patient shortly after the time of injury, to avoid potential risks of immunological reactions associated with allogenic MSC treatments in equine models [92–94].

Of some concern, human, canine, and rodent studies have shown an unfortunately sharp decline in MSC quantity and quality with increasing donor age [85,97,123,125]. However, no donor age studies have been published on equine MSCs with regards to chondrogenic and osteogenic differentiation performance. A study by Asumda *et al.* found that BM-MSCs from 15 month old rats had lost their chondrogenic and osteogenic differentiation potential altogether [97], which was supported by a 76% decline in osteogenic alkaline phosphatase activity in adult human BM-MSCs [65], and a 82% decline in proteoglycan content of chondrogenic induced BM-MSC pellets from 1 year old rats compared to 1 week old rats [127].

Donor age may thus be an important variable in equine patients for orthopedic injuries treated with autologous cells, as many horses with osteoarthritis are aged. Ultimately, age-associated alterations may impact the efficacy of autologous transplanted MSCs in aged horses resulting in poorer regenerative results. The majority of MSC donor age studies in other species are made on BM-MSCs, and it is currently unclear if stem cells from different sources are equally affected by donor age, but AT-MSCs are reported to be less affected by donor age than BM-MSCs [134].

The need for regenerative medicine in equine practice is believed to increase tremendously partly due to the progressively aging equine population [143]. It is thus essential to scientifically examine how donor age affects different types of clinically

relevant equine MSCs to determine an age threshold for when a horse is no longer a suitable donor.

The studies reported in this chapter were designed to test the hypothesis that increasing donor age is a major variable impacting equine BM- and AT-MSC chondrogenic and osteogenic differentiation performance with decreasing capacities following non-linear kinetics. Specific aims were to 1) compare pellet size, histological cell morphology and proteoglycan staining in chondrogenic induced cell pellets, and to compare calcium deposits and alkaline phosphatase activity in osteogenic induced monolayer cultures, and to 2) compare the expression of targeted genes specific to articular cartilage in cell pellets and bone in monolayer cultures.

3.2 MATERIALS AND METHODS

Cells used for this study are identical as the ones described in Chapter 2 for the cellular proliferation studies.

3.2.1 Experimental samples

BM-MSCs, AT-MSCs, and dermal fibroblasts (DF) (biological negative control) were harvested immediately post-mortem from horses of mixed breeds in 5 different clinically relevant and well-distinguished age groups with 4 horses in each age group. The age groups were newborn (0 days old), yearling (1-2 year old), adult (5-8 year old), middle aged (12-18 year old), and geriatric (≥ 22 year old) horses. All horses were euthanized due to reasons unrelated to this study. The study was conducted according to the ethical guidelines of animal research at the University of Copenhagen and the University of Kentucky. A written consent was obtained from all privately-owned horses prior to collection.

Sample size was determined by power analysis. Two-sample t-test power calculations were performed in R (version 3.6.0) using pilot study data (not shown) to assess the calcium deposition of osteogenic induced BM- and AT-MSC harvested from newborn foals and geriatric horses (n=2 horses per age group per cell type) and the following equation:

$$n = 2 * \frac{(z1 - \frac{\alpha}{2} + z1 - \beta)^2}{(\delta/\sigma)^2}$$

where σ is the standard deviation for the outcome, α is the significance level, 1 – β is the power, $z1 - \frac{\alpha}{2}$ = 1.96 for α = 0.05, $z1 - \beta$ = 0.84 for 1 – β = 0.80, and δ was set to an

Alizarin Red S concentration of 1 mM as the minimum relevant difference. The estimated sample size to achieve a power of 0.80 was determined as 4 horses per age group per cell type.

3.2.1.1 Bone marrow derived MSC collection and isolation

Bone marrow/bone marrow aspirates were collected immediately post-mortem from the sternum of 12 female and 8 male horses, with the following age distribution; newborn (mean=0 days, range=0-0 days), yearling (mean=15.7 months, range=15.3-16 months), adult (mean=6.8 years, range=5-8 year), middle aged (mean=15.5 years, range=13-18 year), and geriatric (mean=25.8 years, range=22-31 year). For the newborns, BM was collected as described by Vidal *et al.* [42] with few modifications. Briefly, BM was collected from the 4^{th}-6^{th} sternebrae by sterile curettage after splitting the sternum in midline. The marrow trabecular bone was transported on ice to the laboratory in ice cold sterile Dulbecco's phosphate buffered saline (dPBS, Gibco, Cat# 14190144) with 2% (v/v) amphotericin B (Gibco, Cat# 15290026), and 2% (v/v) penicillin/streptomycin (P/S, Gibco, Cat#15070063) (isolation juice) and processed within 2 hours of collection. In the cell laboratory, the marrow trabecular bone was rinsed twice in 37^{o}C pre-warmed isolation juice and crushed before being grown as an explant culture in 2 T75 cm^2 culture flasks (Cellstar BioGreiner, VWR, Cat# 82050-856) with 12 mL/flask Dulbecco's modified Eagle's medium (DMEM, 1 g/L glucose, with phenol red, GlutaMAX, and pyruvate, Gibco, Cat# 10567-022), 10% (v/v) fetal bovine serum (FBS), 1% (v/v) P/S, and 1% amophotericin B (isolation medium). After 48 hours, BM crusts and non-adherent cells were aspirated along with the isolation medium, and the medium was changed to expansion medium containing 1 g/L DMEM, 10% FBS, and 1% P/S. The

cells were cultured at 37°C in a humidified atmosphere containing 5% CO_2 and expansion medium was changed every 2-3 days.

For the four latter age groups, BM was aspirated from the 4th-6th sternebrae as previously described [34,42]. In short, the area over the sternum was clipped and surgically prepared with 2% chlorohexidine medical scrub and 70% ethanol. A total of 20 mL of BM was collected using a 10 cm, 11 G Jamshidi® bone biopsy needle (Henry Schein Vet, Cat# DJ4011X) and two 20 mL Luer-Lock syringes preloaded with 1000 IU sodium heparin (Henry Schein Vet, Cat# 4327680) per 10 mL BM aspirate. The BM aspirate was transferred to a 50 mL falcon tube and gently inverted, before being transported on ice to the laboratory and further processed within 2 hours of collection. In the cell laboratory, the BM aspirate was layered slowly onto Ficoll-Paque® PREMIUM (GE Healthcare, Cat# 17-5442-02) in a 1:1 (v/v) manner and centrifuged for 30 minutes at 600 g. The mononuclear cell layer containing BM-MSCs was collected and washed twice in sterile dPBS and centrifuged for 5 minutes at 200 g between the washes. The supernatant was removed and the pellet was re-suspended in 24 mL isolation medium and equally divided into 2 T75 cm^2 culture flasks. After 48 hours, allowing the BM-MSCs to adhere to the bottom of the flasks, the first medium change occurred and isolation medium was replaced with expansion medium. The cells were incubated at 37°C and 5% CO_2.

3.2.1.2 Adipose tissue derived MSC collection and isolation

AT was collected from the gluteal region above the biceps femoris muscle next to the tail base of 10 female and 10 male horses as previously described [34], with the following age distribution; newborn (mean=0 days, range=0-0 days), yearling (mean=15.8 months,

range=15.3-16.1 months), adult (mean=6.8 years, range=5-8 year), middle aged (mean=14.5 years, range=13-16 year), geriatric (mean=25.8 years, range=22-31 year). Briefly, the gluteal area next to the tail base was surgically clipped and prepared as described for BM-MSCs, and 10 grams of AT was collected through a ~8 x 8 cm surgical window. The AT was transferred to a 50 mL falcon tube with ice cold isolation juice and transported on ice to the laboratory where the tissue was further processed within 2 hours of collection. In the cell laboratory, the AT was washed two times in isolation juice and dissected into smaller pieces where visible blood vessels were removed. The AT was digested in sterile filtered (0.2 µm) AT enzyme medium consisting of DMEM (1 g/L), 1% P/S, 50 µg/mL gentamycin (Sigma-Aldrich, Cat# G1264-1G), and 1 mg/mL collagenase type I (Worthington, Cat# X7H9763A) for 3 hours at 37^{o}C and 30 rpm. The enzyme medium containing released cells was transferred through a 70 µm cell strainer and the pellet with AT-MSCs was washed twice in sterile dPBS and centrifuged at 500 g for 5 minutes between the washes. The pellet was re-suspended in 24 mL isolation medium supplemented with 50 µg/mL gentamycin and distributed into 2 T75 cm^2 culture flasks. The first medium change occurred 48 hours after isolation, where fresh expansion medium was added. The cells were grown at 37^{o}C in air with 5% CO_2 with medium change every 2-3 days.

3.2.1.3 Dermal fibroblast collection and isolation

DFs were harvested from the gluteal region above the biceps femoris muscle next to the tail base of 14 female and 6 male horses as previously described [35], with the following age distribution; newborn (mean=0 days, range=0-0 days), yearling (mean=15.6 months, range=15.3-16 months), adult (mean=6 year, range=5-7 year), middle aged (mean=14.5

years, range=12-18 year), geriatric (mean=27.5 years, range=22-32 year). Briefly, 6 grams of dermal tissue was collected from the surgical window made to collect AT-MSCs. The dermis was transferred to a 50 mL falcon tube with ice cold isolation juice and transported on ice to the laboratory where the tissue was further processed within 2 hours of collection. In the cell laboratory, the dermal tissue was washed two times in isolation juice and dissected into smaller pieces. The dermis was digested in sterile filtered (0.2 µm) DF enzyme medium consisting of dPBS, 1% P/S, 1% bovine serum albumin (BSA – Sigma, Cat# A9418-10G), 50 µg/mL gentamycin, and 1 mg/mL collagenase type I for 2 hours at 37^{o}C and 30 rpm. The enzyme medium containing released cells was transferred through a 70 µm cell strainer and the pellet with DFs was washed twice in sterile dPBS and centrifuged at 1000 g for 4 minutes between the washes. The pellet was re-suspended in 24 mL isolation medium supplemented with 50 µg/mL gentamycin and distributed into 2 T75 cm^2 culture flasks and grown at 37^{o}C in air with 5% CO_2. The first medium change occurred 48 hours after isolation, where fresh expansion medium was added. Expansion medium was changed every 2-3 days.

3.2.2 Cell expansion and storage

At approximately 80% confluence, the cells were passaged with 1 mL 0.25% Trypsin/1 mM EDTA (Gibco, Cat# 11560626) per T75 cm^2 culture flask. Cell counting was performed manually using tryphan blue (Fisher Scientific, Cat# 11538886) and a hemocytometer. The cells were grown with a seeding density of 500,000 cells per T75 cm^2 culture flask. At passage 2 (P2), the cells were cryopreserved with Recovery-Cell Culture Freezing Medium® (Gibco, Cat# 11560446, containing 10% DMSO) at a concentration of 2-3 x 10^6 cells per 1 mL freezing medium in cryogenic vials (Nalgene,

Thermo Scientific, Cat# 5000-0020). The cells were thawed in 37°C pre-warmed expansion medium and washed 3 times in dPBS to remove leftover freezing medium before being grown in expansion medium and incubated at 37°C and 5% CO_2 with medium change every 2-3 days. Chondrogenic and osteogenic differentiation assays were performed at passage 4.

CHONDROGENIC ASSAYS

3.2.3 Pelleting and chondrogenic differentiation

To generate 3D cell pellets at passage 4, cells were trypsinized at passage 3, counted manually, and washed twice in dPBS before being resuspended at 500,000 cells per mL in chondrogenic induction medium as described previously [35,39,71,73,74]. The pellet was generated by centrifuging 1 mL of cell suspension at 500 g for 3 minutes in a vented 1.5 mL polypropylene microcentrifuge tube. The chondrogenic induction medium consisted of DMEM (4.5 g/L glucose – Gibco, Cat# 10569044), 1% P/S, 12.5 mg/mL BSA (Sigma, Cat# A9418-10G), 1x insulin-transferrin-selenium-sodium pyruvate (ITS-A) growth supplement (Gibco, Fisher Scientific, Cat# 51300044), 1x MEM non-essential amino acids (Gibco, Fisher Scientific, Cat# 11140050), 100 nM dexamethasone (Sigma, Cat# D4902-100MG), 50 µg/mL L-ascorbic acid-2-phosphate sesquimagnesium salt hydrate (A2P - Sigma, Cat# A8960-5G), and 10 ng/mL human recombinant transforming growth factor β_1 (rhTGFβ_1 – Sigma, Cat# T7039-50UG). A total of 15 pellets were made per cell line per biological replicate. After 24 hours, the pellets were transferred to a 1% poly 2-hydroxyethyl methacrylate (polyHEMA, Sigma, Cat# P3932) coated 24-well plate with 1 pellet per well. Coating of the wells with polyHEMA enabled suspension-culture

of the pellets by preventing adhesion of the cells to the plastic surface. After transfer, 1 mL of new chondrogenic induction medium was added to each pellet. The pellets were grown in freshly made chondrogenic induction medium for 21 days with 1 mL of complete medium change every 3 days at 37^{o}C and 5% CO_2. As a control for gene expression, P4 cells from each cell line per biological replicate were seeded at 500,000 cells in one T75 flask and grown as monolayer in expansion medium until being harvested at ~80% for RNA isolation. Six pellets from yearling BM-MSCs were grown in chondrogenic medium without TGF-β_1 and dexamethasone as a non-induced control for pellet size and proteoglycan staining.

3.2.4 Chondrogenic pellet size

Out of the 15 pellets per biological replicate, 6 were randomly chosen to be measured in size and to be histologically assessed. The remaining 9 pellets were used for RNA isolation and were not measured to prevent potential contamination. Pellets size has been shown to be positively correlated with extracellular matrix production and chondrogenesis [35,38] given that the pellets are made from the same amount of cells, which was the case for the present study where all pellets were made from 500,000 cells. In preparation for pellet measurement, the pellets were gently washed with dPBS and transferred to a 24-well plate with 0.5 mL dPBS per well and one pellet per well. 2D brightfield images of the pellets were captured at 4x using a microscope. The shortest and longest side of the pellet was measured in µm using Nikon NIS Analysis Software 4.13. The measurements were averaged per pellet and per biological replicate.

3.2.5 Histological assessments of pellets

Following pellet measurement, the pellets were fixed in 4% paraformaldehyde at 4^{o}C for 24 hours. The pellets were then pre-embedded in 2% bacto^{TM} agar (BD, Cat# 214050) /2.5% gelatin blocks as previously described to prevent folding of the pellets at sectioning [159] with 2 pellets per block. Next, the blocks were fixed in 4% paraformaldehyde for 24 hours at 4^{o}C, before being placed in 70% ethanol at 4^{o}C for batched histological processing and paraffinization. The pellets were sectioned at 5 µm at approximate midline and stained with either Hematoxylin and Eosin (H&E) for cell morphology and pellet architecture or Safranin-O to evaluate proteoglycan content and distribution. Analyses of cell morphology and staining patterns within the pellets were performed in consultation with board certified veterinary pathologist (Dr. Jennifer Janes, University of Kentucky, personal communication).

3.2.6 Proteoglycan staining of pellets and quantification

Safranin-O staining was used to measure the extracellular matrix proteoglycan content of the pellets, as an essential protein marker of chondrogenesis. Safranin-O is an orange to red stoichiometric orthochromatic dye that adheres to the sulfate groups of proteoglycan molecules in a 1:1 manner, which makes the stain semi-quantitative [82]. The redness intensity of the section staining thus represents the proteoglycan content assuming a uniform distribution of negatively charged proteoglycans across the sample. All sections were stained with Weigert's Iron Hematoxylin for 7 minutes to stain cell nuclei, and 1% Fast Green (Sigma, Cat#F7252) for 5 minutes as a background stain. Proteoglycan sulfation was identified with a 0.05% Safranin-O (Sigma, Cat# S8884) staining for 2 minutes as described previously [35]. The sections were stained in 30-slide racks in the same batch of Safranin-O and Fast Green stain to avoid inter-batch technical variation, with refreshing of the stain between every two racks. Equine articular cartilage from a 7 year old horse was included as a positive control calibrator sample with 3 randomly placed slides in each rack. Non-induced BM-MSC pellets from a yearling and epithelial tissue from a foal was incorporated as negative controls with 1 slide of each per rack. Mounted sections were imaged in brightfield with a Zeizz AX10 Imager A2 microscope at 5x using the same microscope brightness and exposure settings for all images. Images of the 0.05% Safranin-O staining used in the experiment were captured using a chamber slide as a pure red calibrator.

The redness values of the Safranin-O stained sections were measured using Fiji software in ImageJ (https://imagej.net/Fiji/Downloads) as previously described [35]. Color contributions from the background light and microscope were corrected for by

using the pure red stain as a calibrator and by subtracting the fixed background intensity measures from each individual color histogram. After red balancing and background assessment, mean red, green, and blue values were determined for all controls and pellets using the whole pellet as the focus area. The redness value of each section was calculated as follows:

$$Green_{modified} = (Green_{mean} - Green_{background})$$

$$Blue_{modified} = (Blue_{modified} - Blue_{background})$$

$$Redness\ value = Red_{mean} - \left(\frac{Green_{modified} + Blue_{modified}}{2}\right)$$

where *mean* represents the pellet value, and *background* represents the pure red value. The redness value characterizes the red color of the Safranin-O stained proteoglycan molecules, making semi-quantitative comparisons between pellets possible. The redness value of each pellet was recorded and normalized to articular cartilage control sections, and then averaged per biological replicate.

OSTEOGENIC ASSAYS

3.2.7 Monolayer cell culture and osteogenic differentiation

Passage 3 cells were trypsinized, counted, and seeded as passage 4 monolayer cells with a density of 25,000 cells per well in 6-well plates (NUNC, Fisher Scientific, Cat# 10469282). The cells were initially grown in expansion medium at 37^{o}C and 5% CO_2 and re-feed every 2-3 days. Upon ~90% confluence, expansion medium was discarded and osteogenic induction medium was added to 3 of the wells while the other 3 wells were

kept under expansion medium as a non-induced control. The osteogenic induction medium consisted of DMEM (1g/L glucose), 10% FBS, 1% P/S, 100 nM dexamethasone, 0.05 mM ascorbic acid (A2P), and 10 mM β-glycerophosphate disodium salt hydrate (Sigma, Cat# G9422) as previously described [42,86,87]. The medium in both groups were changed every 3 days with 2 mL medium per well. Four 6-well plates were made from each cell line per biological replicate, with 1 plate for day 0 RNA harvest, 1 plate for day 21 RNA harvest, 1 plate for day 7 alkaline phosphatase activity assay, and 1 plate for day 21 Alizarin Red S staining.

3.2.8 Alkaline phosphatase activity assay

After 7 days of osteogenic induction, alkaline phosphatase (ALP) activity was measured using a commercially available colorimetric kit (Abcam, Cat# ab83369) according to the manufacturer's instructions and as described previously [160]. ALP is a membrane-bound glycoprotein that catalyzes the hydrolysis of phosphates at high pH, and is an early marker of osteogenesis that enhances mineralization [90] with the highest detection for equine BM-MSCs after 6-7 days of osteogenic culture [87].

Briefly, the cell layers were washed with dPBS and harvested by 0.05% Trypsin/EDTA and cell scraping. The cell suspension from each well was transferred individually to a microcentrifuge tube, spun down, and washed to remove left over trypsin. The pellet was then resuspended in fridge cold dPBS and centrifuged. The supernatant was discarded and 200 µL assay buffer was added to each pellet before being homogenized in a QIAshredder (Qiagen, Cat# 79654) at 20,000 g for 2 minutes, followed by top speed (14000 RPM) for 15 minutes at 4^{o}C. The samples were transferred to

cryogenic vials and stored at -80^{o}C until batch ALP assays were performed. ALP activity of the cells was measured in flat-bottomed 96-well plates by adding 5 mM p-nitrophenyl phosphate substrate, which turns yellow when dephosphorylated to p-nitrophenol by ALP [160]. The cell suspension was incubated with the phosphate substrate for 60 minutes at 25^{o}C protected from light. Stop solution was added and optical density was measured at 405 nm using a microplate reader. ALP activity was calculated based on standard curve solutions incorporated in the assay and by subtracting mean blank values from the samples. All technical replicates were tested in duplicate with 3 osteogenic-induced and 3 non-induced wells per cell line. The ALP activity levels of the technical replicates were averaged per biological replicate per cell type per medium.

3.2.9 Alizarin Red S assay

After 21 days of osteogenic induction, calcium deposition was measured with a commercially available colorimetric Alizarin Red S (ARS) quantification kit (ARed-Q, ScienCell, Cat#8678) following manufacturer's protocol based on a study by Gregory *et al.* [161]. Calcium is a key component in hydroxyapatite ($Ca_{10}(PO_4)6(OH_2)_2$), which is the main inorganic component of bone. Calcium deposition thus functions as a marker of bone mineralization for osteogenic induced cells [161,162].

In short, the osteogenic medium was removed and the cells were gently washed 3 times in dPBS without calcium and magnesium (Gibco, Fisher Scientific, Cat# 14190144) before being fixed in 4% paraformaldehyde. The calcium deposits were then visualized by adding 40 mM ARS staining and incubating for 20 minutes with gentle shaking. The dye was removed and the wells were washed 5 times with milli-Q water

with 5 minute incubation between the washes to remove excess dye. The calcified minerals were extracted at low pH by means of 10% acetic acid and a cell scraper, followed by a heating process in parafilm-coated microcentrifuge tubes at 85^{o}C for 10 minutes and a cooling process on ice for 5 minutes. The solution was then neutralized with 10% ammonium hydroxide (pH between 4.1-4.5). ARS concentration was quantified by colorimetric detection at 405 nm in flat-bottomed 96-well plates using a microplate reader. The ARS concentration of the samples was calculated based on a standard curve incorporated in the assay and by subtracting the mean blank value from all samples. All technical replicates were analyzed in triplicates with 3 osteogenic-induced and 3 non-induced wells per cell line. ARS concentration was averaged per cell line per biological replicate per medium.

GENE EXPRESSION ASSAYS

3.2.10 Gene expression

3.2.10.1 RNA isolation and reverse transcription

Passage 4 cells were grown as monolayer cultures in T75 cm^2 flasks with expansion medium as a non-induced control for chondrogenesis. At approximately 80% confluence, the cells were extracted with QIAzol® (Qiagen, Cat# 79306), a guanidinium thiocynate-phenol-chloroform lysis reagent, and snap frozen in liquid nitrogen. After 21 days of culture in chondrogenic medium, 9 pellets from each cell line were washed with dPBS, and snap frozen in aliquots with 3 pellets per aliquot.

At approximately 90% confluence, cells grown in expansion medium in 6-well plates were harvested with QIAzol® as a day 0 non-induced control for osteogenesis and

snap frozen. After 21 days of culture, cells were harvested with QIAzol® from a 6-well plate with 3 wells cultured in osteogenic induction medium and 3 wells kept under expansion medium as a day 21 non-induced osteogenic control and snap frozen. All samples were stored at -80°C prior to RNA isolation.

The monolayers and pellets were homogenized in 2 mL of QIAzol® using a PowerGen 125 homogenizer (Fisher Scientific, Cat# 15120247). Total RNA was isolated using a spin column-based Qiagen RNeasy Mini Kit® (Qiagen, Cat# 74104) with modifications as previously described [144], with pooling of the technical replicates. RNA quantity was determined immediately after RNA isolation using a NanoDrop ND 1000 spectrophotometer. The samples then underwent ethanol precipitation to remove processing contaminants. Quantification of the purified RNA was performed using the Qubit BR Assay (Life Technologies, Cat# Q10210) and NanoDrop ND 1000 spectrophotometer. The quality of the purified RNA was assessed with a Bioanalyzer 2100 (Agilent Technologies, Eukaryotic Total RNA Nano & Pico Series II). All purified RNA samples met the following quality thresholds; 260/280 ratios of 1.7-2.1, 260/230 ratios of 1.8-2.28, and an Agilent RNA integrity number (RIN) of $\geq$ 7.4, with the exception of 3 samples (Appendix 1) that behaved as expected in down-stream analyses and thus were not excluded from the study.

Removal of potential genomic DNA contamination and reverse transcription of total RNA to cDNA was achieved using a commercially available kit as per manufacturer's protocol (Maxima First Strand cDNA Synthesis Kit® for RT-qPCR with dsDNase, Life Technologies, Cat# K1672). cDNA samples were diluted with nuclease-free water to 13.9 ng/uL and stored at -80°C.

3.2.10.2 Real-time quantitative PCR

Ninety-three biomarkers were selected for the gene expression panel based on functional annotation to have biological relevance important for cell proliferation, chondrogenesis, osteogenesis, or evidence in the literature of age-dependent variation. The gene expression panel e.g. included known growth factors, cell cycle regulators, articular cartilage markers, subchondral bone markers, and markers of cellular senescence (Genes and annotations are shown in Appendix 2).

Commercially available, validated equine-specific TaqMan® primer-probe sets (FAM dye-labeled MGB probes - Thermo Fisher) for all biomarkers were used to quantitate the steady state mRNA levels. Details on the primer-probe sets are listed in Table 3.1. The functionality of all primer-probe sets was tested against a positive control equine sample containing mixed cDNA consisting of a 43-sample pool of various tissue [145], day 35 whole fetus, and neonatal epiphyseal cartilage. Negative controls of RNase-free water and minus-template was incorporated, and each sample was run in duplicate.

Real-time quantitative PCR (RT-qPCR) reactions were conducted in a 384-well plate with a total reaction volume of 10 µL using 62.55 ng cDNA per reaction. A robotic ViiA™ RT-qPCR System (Thermo Fisher Scientific) was used to perform the reactions. LinRegPCR was used to measure reaction amplification efficiencies and cycle threshold (Ct) values were calculated [146]. All targets amplified with amplification efficiencies close to 2 except for the negative controls that showed no amplification (data not shown).

Three commercially available equine-specific endogenous control TaqMan® primer-probe sets were tested against all samples. The endogenous controls consisted of β-2-microglobulin (B2M), β-glucoronidase (GUSB), and ribosomal protein lateral stalk

subunit P0 (RPLP0). Using NormFinder software [147], GUSB was determined as having the most uniform performance across all cell types and age groups (data not shown).

The gene expression of the experimental samples were analyzed by RT-qPCR using the BIOMARK HD System (Fluidigm) as previously described [148]. Fluidigm is an automated nanofluidic RT-qPCR system that uses microfluidic technology in which dynamic arrays of integrated fluidic circuits are used, allowing for samples and reagents to be mixed in a variety of patterns. Hence, little sample quantity is needed to be tested against 96 targets, making it less time-consuming and more cost-effective compared to standard qPCR [148].

Briefly, experimental cDNA samples were shipped at a concentration of 13.9 ng/µL (middle of positive standard curve), together with the positive control (7 three-fold dilutions), negative controls, and primer-probe sets (including endogenous controls) to The Carver Biotechnology Center, University of Illinois, IL, USA, where the Fluidigm assay was performed. A total of 7 µL of cDNA and 25 µL of primer-probe sets were shipped per sample or target, respectively. The Fluidigm was carried out using 96.96 dynamic arrays (Fluidigm Corporation, CA, USA) according to manufacturer's instructions.

The data were analyzed with Fluidigm Real-Time PCR Analysis Software in the BIOMARK instrument (Fluidigm Corporation, CA, USA) where Ct values were calculated. Results from 5 primer-probe sets (TNF, NODAL, MATN1, HAPLN1, and MEPE) were removed from the final panel, as gene expression was below assay detection level in almost all samples, making comparisons unfeasible. Delta Ct values were

determined for each sample by subtracting the corresponding Ct value of the endogenous control (GUSB). The positive control was used as a calibrator to calculate ΔΔCt values. Relative expression (RQ) of the gene targets were calculated using the $2^{-\Delta\Delta Ct}$ method [149]. RQ levels were used for graphical bar/box plot presentations made in GraphPad Prism 8.0.1 or SAS 9.4, and Ln(RQ) values were used for heatmap and statistical analysis to linearize the data again and to avoid right-shifting of data. Gene expression heatmap visualization was done on averaged Ln(RQ) levels for each study group, grouping the samples according to cell type, donor age, and medium, and genes according to biological annotation. Heatmap was generated in RStudio 3.6.0 using the *heatmap ggplot* function.

Table 3.1: Overview of TaqMan primer-probe sets used in RT-qPCR reactions.

Gene ID	Gene name(s)	ThermoFisher Assay ID
ABI3BP	ABI family member 3 binding protein	Ec06625599_m1
ACAN	Aggrecan core protein	Ec03469667_m1
ALPL	Alkaline phosphatase	Ec06625502_g1
AQP1	Aquaporin	Ec06625425_m1
AREG	Amphiregulin	Ec06992855_m1
BARD1	BRCA1-associated RING domain 1	Ec07061151_m1
BAX	BCL2 associated X apoptosis regulator	Ec07016716_s1
BCL2	B-cell lymphoma 2	Ec07005800_g1
BGN	Biglycan	Ec03467971_m1
BMP2	Bone morphogenic factor 2	Ec06974239_m1
BMP3	Bone morphogenic factor 3	Ec07037656_m1
BMP4	Bone morphogenic factor 4	Ec03470252_s1
BMP6	Bone morphogenic factor 6	Ec03469925_m1
BMP7	Bone morphogenic factor 7	Ec04320876_m1
BRCA1	Breast cancer type 1	Ec07017862_s1
CASP3	Caspase 3	Ec03470391_m1
CASP8	Caspase 8	Ec06959413_m1
CAVIN1	Caveolae associated protein 1	Ec07036873_m1
CCND1	Cyclin D1	Ec07036996_m1
CDKN1A	p21, Cyclin-dependent kinase inhibitor 1A	Ec06955195_m1
CHADL	Chondroadherin	Ec03470206_m1
CLU	Clusterin	Ec03468575_m1
COL1A1	Collagen type 1 alpha 1	Ec03469676_m1
COL2A1	Collagen type 2 alpha 1	Ec03467411_m1
COL4A1	Collagen type 4 alpha 1	Ec06943950_m1
COL5A3	Collagen type 5 alpha 3	Ec06999559_g1
COL9A2	Collagen type 9 alpha 2	Ec03470083_m1
COL11A1	Collagen type 11 alpha 1	Ec07051918_m1
COL12A1	Collagen type 12 alpha 1	Ec03469523_m1
COMP	Cartilage oligomeric matrix protein	Ec03468062_m1
CRTAC1	Cartilage acidic protein –CEP-68	Ec07040335_g1
CRYAB	Crystalline-alpha B	Ec06997901_m1
CSF2	Colony stimulating factor 2	Ec03468208_m1
CTGF	Connective tissue growth factor	Ec06625777_gH
CTNNB1	Beta-catenin	Ec00991819_m1
DCN	Decorin	Ec03468474_m1
DMP1	Dentin matrix acidic phosphoprotein 1	Ec06992382_m1

Table 3.1: (Continued)

EBF2	Early B-cell factor 2	Ec06966528_m1
EPGN	Epithelial mitogen	Ec06992859_m1
FGF1	Fibroblast growth factor 1	Ec01092738_m1
FGF5	Fibroblast growth factor 5	Ec04656774_m1
FGF18	Fibroblast growth factor 18	Ec03248217_g1
FGFR3	Fibroblast growth factor receptor 3	Ec03470545_m1
FN1	Fibronectin 1	Ec03470760_m1
GDF6	Growth differentiation factor 6	Ec07097112_m1
GLB1	Beta-galactosidase	Ec06954363_m1
GLI3	GLI family zinc finger 3	Ec06625512_m1
HAPLN1	Hyaluronan and proteoglycan link protein 1	Ec03468716_m1
HDGF	Hepatoma-derived growth factor	Ec07037751_m1
HGF	Hepatocyte growth factor	Ec07000054_m1
IBSP	Integrin Binding Sialoprotein	Ec06625402_m1
IGF1	Insulin-like growth factor 1	Ec03468689_m1
IGFBP5	Insulin-like growth factor binding protein 5	Ec03470296_m1
LOC100146270	p16, Cyclin-dependent kinase 4 inhibitor B	Ec07037471_mH
LOC100146589	Osteocalcin, bone gamma-carboxyglutamic acid containing protein	Ec07103628_m1
MATN1	Matrilin-1	Ec06963427_m1
MEPE	Matrix extracellular phosphoglycoprotein	Ec06992377_m1
MET	MET proto-oncogene, receptor tyrosine kinase	Ec02622441_m1
MIA	CD-RAP, Cartilage-derived retinoic acid-sensitive protein	Ec03469434_m1
MMP3	Matrix metalloproteinase 3	Ec03468676_m1
MMP13	Matrix metalloproteinase 13	Ec03467796_m1
MYC	c-myc	Ec07007511_m1
NODAL	Nodal growth differentiation factor	Ec07036659_m1
OMD	Osteomodulin	Ec06625496_m1
PCNA	Proliferating cell nuclear antigen	Ec06974312_m1
PDGFD	Platelet-derived growth factor subunit D	Ec06997714_m1
PHB	Prohibitin	Ec07055990_m1
PHEX	Phosphate regulating endopeptidase homolog, X-linked	Ec07034292_s1
PTCH2	Patched 2	Ec06625424_g1
RUNX2	Runt-related transcription factor 2	Ec03469741_m1
RUNX3	Runt-related transcription factor 3	Ec06625430_g1
S100A1	S100 calcium binding protein A1	Ec03470173_g1
SMOC1	SPARC related modular calcium binding	Ec06978758_m1
SMPD3	Sphingomyelin phosphodiesterase 3	Ec06625668_m1
SNAI2	Snail family transcriptional repressor 2	Ec06625397_m1

Table 3.1: (Continued)

SOST	Scherostin	Ec07036868_m1
SOX5	SRY-box transcription factor 5	Ec01552798_m1
SOX9	SRY-box transcription factor 9	Ec03469763_s1
SP7	Osterix	Ec06625770_g1
SPARC	Osteonectin	Ec03818202_m1
SPP1	Osteopontin, Secreted phosphoprotein 1	Ec06992376_g1
TBX3	T-box 3	Ec07003300_m1
TERT	Telomerase reverse transcriptase	Ec06972692_m1
TGFA	Transforming growth factor alpha	Ec06949183_m1
TGFB1	Transforming growth factor beta 1	Ec06625477_m1
TGFB2	Transforming growth factor beta 2	Ec07074189_g1
TGFB3	Transforming growth factor beta 3	Ec00682163_m1
TIMP2	Metallopeptidase inhibitor 2	Ec03470558_m1
TNF	Tumor necrosis factor	Ec03467871_m1
TNFRSF11B	Osteoprotegerin	Ec07007303_m1
TNFSF11	RANKL, TNF superfamily member 11	Ec06625532_m1
TP53	Tumor protein 53	Ec03470648_m1
VEGFA	Vascular endothelial growth factor A	Ec03467879_m1
B2M	Beta-2-microblobulin	Ec03468699_m1
GUSB	Beta-glucoronidase	Ec03470630_m1
RPLP0	Ribosomal protein lateral stalk subunit P0	Ec04947733_g1

3.2.11 Inter-laboratory control

The study was performed in 2 different laboratories (University of Copenhagen (UCPH) and University of Kentucky (UK)). To control for potential inter-laboratory differences, inter-assay controls were included. BM-MSCs were included as an inter-assay control for the osteogenic assays, and articular chondrocytes were incorporated as an inter-assay control for the chondrogenic assays. Both samples were from yearlings, and had shown high differentiation potential in pilot and previous studies [35] to ensure a positive foreground to compare to. The two cell lines were shipped on dry-ice from UK to UCPH and tested using the same procedures in both laboratories. Plastic ware, mediums,

reagents, commercially available kits, and protocols were kept constant throughout the entire study for all samples. The osteogenic inter-laboratory control was tested using the ALP and ARS assay and by Fluidigm RT-qPCR. The chondrogenic inter-laboratory control was tested by pellet size measurement, Safranin-O staining and with Fluidigm RT-qPCR. Isolated RNA was shipped on dry-ice from UCPH to UK to allow for all RNA and cDNA samples to be analyzed on the same machines. Laboratory was furthermore added as a variable in the statistical model used for data analysis. All inter-laboratory controls showed no indication of significant differences between laboratories (data not shown).

3.2.12 Statistical analysis

The differentiation data, comparing age-groups within cell types and across cell types, were analyzed with a generalized linear mixed model using The GLIMMIX Procedure in SAS 9.4 with Tukey-Kramer's *post hoc* modifications for multiple comparisons. Gene expression data were analyzed in two steps. Initially, one-way analysis of variance (ANOVA) using SAS 9.4 was applied individually to all 88 gene targets within each cell type to look for donor age effects. Next, targets showing significant difference on the ANOVA and more than 5-fold difference between study groups on the heatmap (Figure 3.12) were analyzed using The GLIMMIX Procedure with Tukey-Kramer's *post hoc* modifications for multiple comparisons to compare across tissue types. Statistical analysis of Fluidigm RT-qPCR results was performed on individual extracted Ln(RQ) values. Genes with missing data points (as visualized on Figure 3.12) were removed from the statistical analysis for the given cell type. For the statistical analysis, pellets were

compared to T75 non-induced monolayer cultures, and osteogenic-induced cells were compared to non-induced 6-well cultures at day 21 to minimize time and well bias. To control for non-paired samples and potential inter-laboratory variables, horse number and laboratory were added to the statistical models as additional factors. Due to age-clustering within age groups, statistical linear regression analyses were not feasible and kinetics were determined based on graphical presentations. Data were considered statistically significant if the p-values were <0.05.

3.3 RESULTS

3.3.1 Cell expansion

All cell lines proliferated actively after isolation when the primary cell cultures had been established. No differences were seen in the proliferative capacity of pilot cells before and after cryopreservation (data not shown).

CHONDROGENIC DATA

3.3.2 Pellet size

No pellets disassociated during culture and it was feasible to measure all pellets. Chondrogenic induced pellet size varied from ~0.5 mm to over 1 mm in mean diameter as shown in Figure 3.2, with the following general relationship: BM-MSC > AT-MSC > DF ($p<0.006$). Representative images of pellets are shown in Figure 3.1. Non-induced control pellets made from yearling BM-MSCs had a diameter between 0.38 and 0.45 mm. No effect of donor age was seen in BM-MSC pellets. For AT-MSCs, pellets from adult horses were significantly smaller compared to newborn ($p=0.0063$) and yearlings ($p=0.0141$). Pellets from BM-MSCs were only significantly larger than AT-MSCs in yearlings ($p=0.0037$), whereas BM-MSC pellets were significantly larger compared to DF pellets in newborn (0.0206) and yearlings ($p<0.0001$) (Figure 3.2).

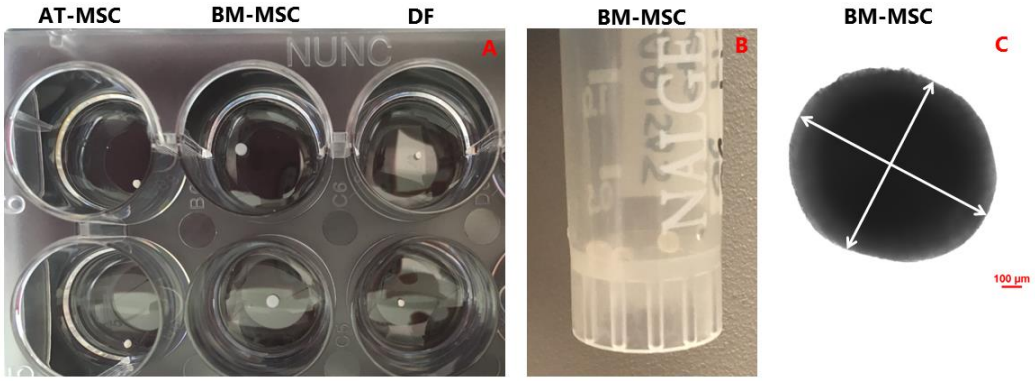

Figure 3.1: *Representative images of pellets made from the same newborn foal after 21 days of culture in chondrogenic induction medium. All pellets were generated from 5x10^5 cells. On image A, the pellets are shown in dPBS prior to pellet size measurement, as seen on the brightfield 4x magnification shown as image C. Image B, shows aliquoted BM-MSC pellets prior to snap-freezing and RNA isolation. *AT-MSC: Adipose tissue derived mesenchymal stem cell, BM-MSC: Bone marrow derived mesenchymal stem cell, DF: Dermal fibroblast.*

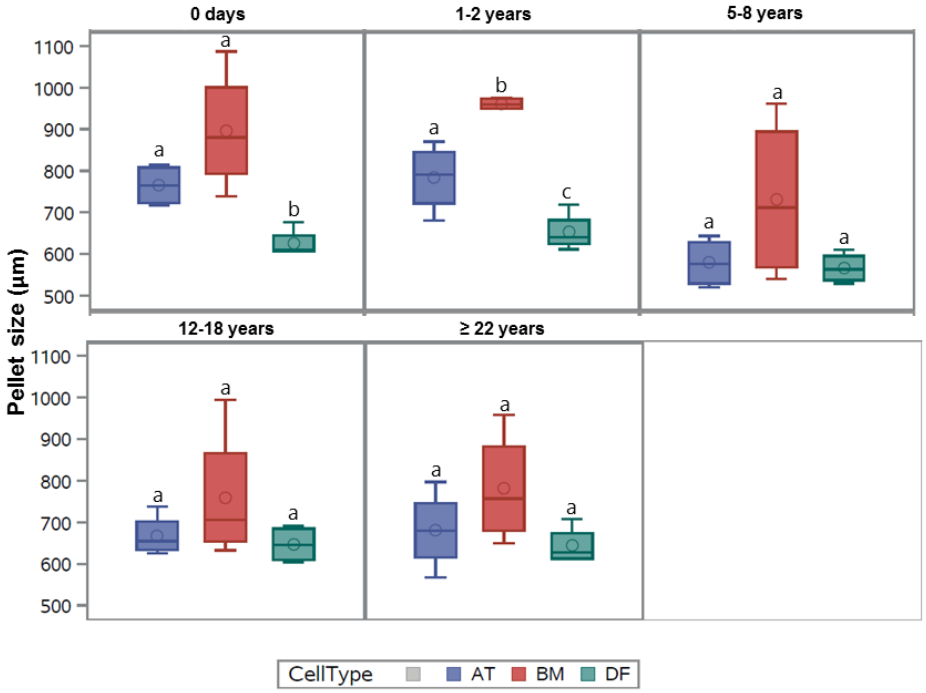

Figure 3.2**:** *Box plot showing pellet size (µm) of chondrogenic induced bone marrow (BM)- and adipose tissue (AT) derived mesenchymal stem cells and dermal fibroblasts (DF) in 5 different age groups (n= 4 horses per cell type per age group). All pellets were generated from 5x10^5 cells and cultured in chondrogenic induction medium for 21 days. Cell types within the same age group not labeled with the same letter are significantly different from each other ($p<0.05$).*

3.3.3 Morphological description of chondrogenic induced pellets

Figure 3.3, 3.4, and 3.4 show representative images of pellets made from AT-MSCs, BM-MSCs, and DFs from horses in 5 different age groups described in this section over a range of magnifications after H&E staining.

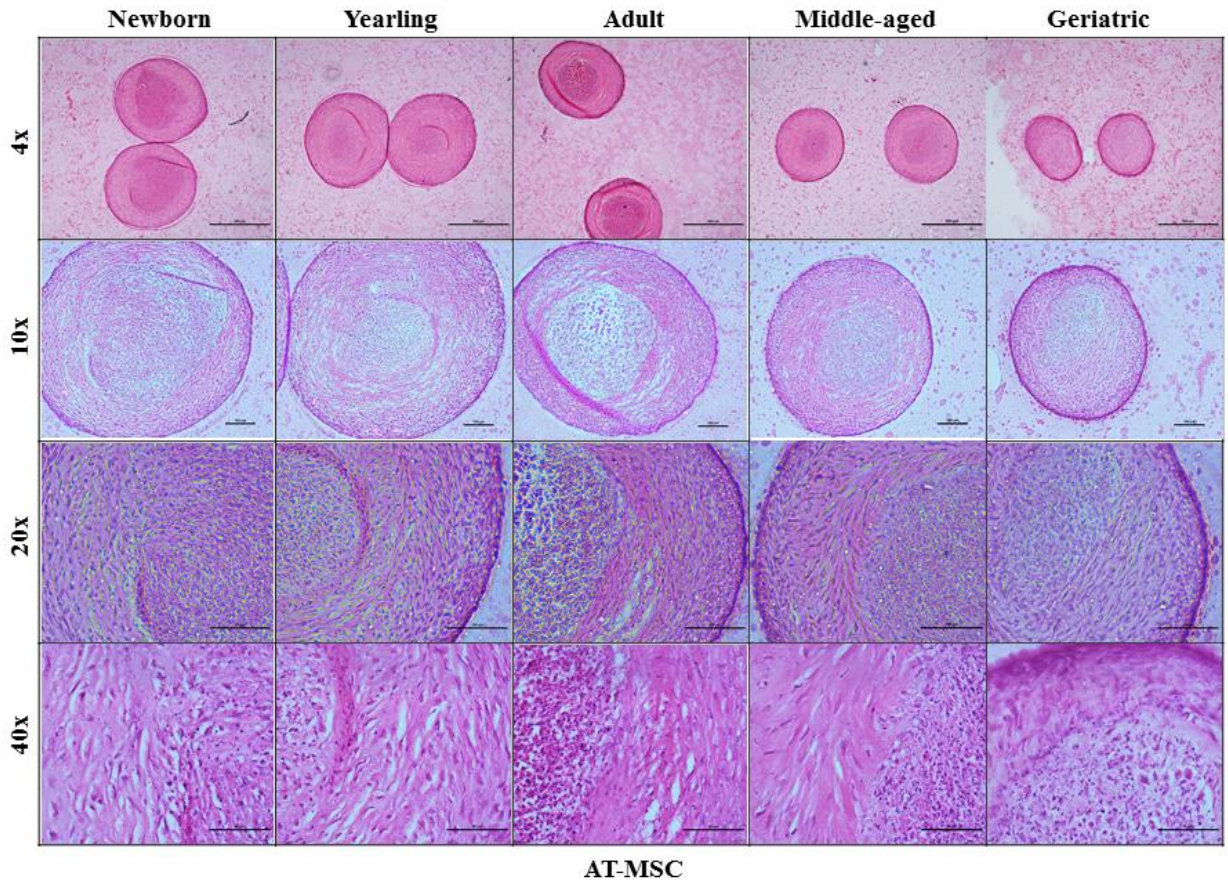

Figure 3.3: *Panel showing representative hematoxylin and eosin (H&E) stained sections of adipose tissue derived mesenchymal stem cell pellets from horses in 5 different age groups under different magnifications after 21 days of culture in chondrogenic induction medium. Size-bar on 4x magnification images is equivalent to 500 µm.*

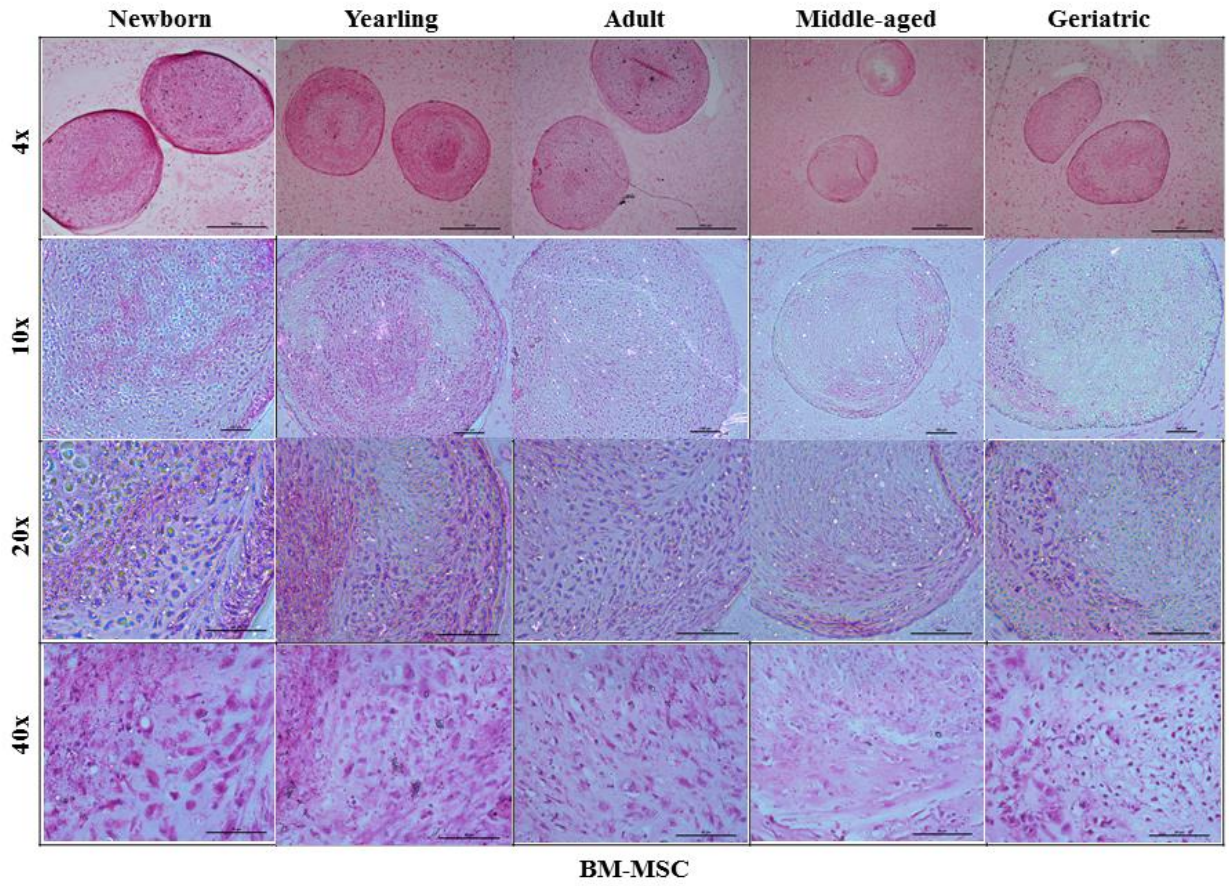

Figure 3.4: *Panel showing representative hematoxylin and eosin (H&E) stained sections of bone marrow derived mesenchymal stem cell pellets from horses in 5 different age groups under different magnifications after 21 days of culture in chondrogenic induction medium. Size-bar on 4x magnification images is equivalent to 500 µm.*

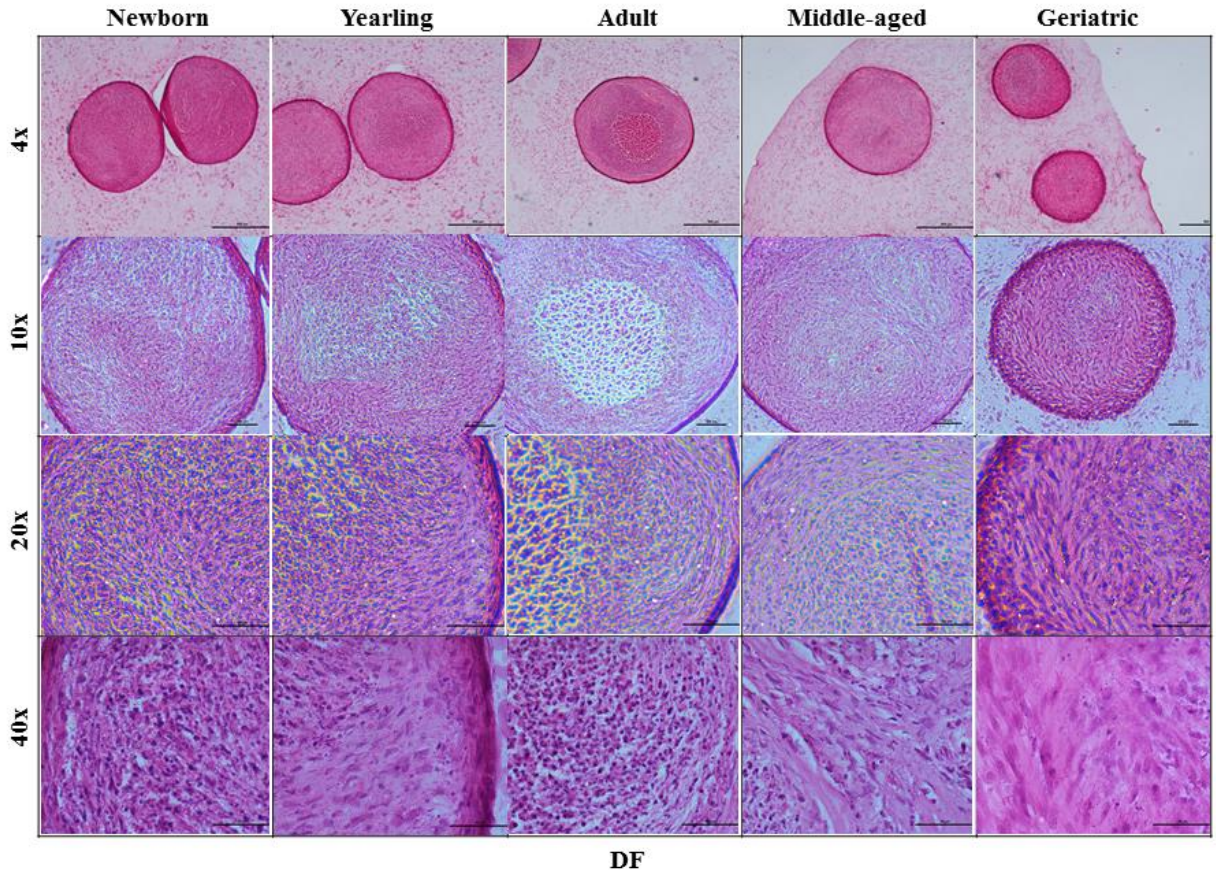

Figure 3.5: *Panel showing representative hematoxylin and eosin (H&E) stained sections of dermal fibroblast pellets from horses in 5 different age groups under different magnifications after 21 days of culture in chondrogenic induction medium. Size-bar on 4x magnification images is equivalent to 500 µm.*

Newborn bone marrow derived mesenchymal stem cell pellets (BM-N-P): The pellets were composed of polygonal cells with minimal acidophilic cytoplasm and round to oval nuclei often within lacunae separated by moderate to marked amounts of lightly basophilic matrix. There was mild variation in cell size. Along the outer rim were streams of spindle cells (4-8 cell layers thick). The spindle cells had acidophilic cytoplasm and oval nuclei, and partially to completely formed the outer rim of the pellets. Few pellets had 1-2 cores of necrotic cells and debris is the center of the pellet.

Yearling bone marrow derived mesenchymal stem cell pellets (BM-Y-P): The pellets were composed of a central accumulation of polygonal cells with minimal acidophilic cytoplasm and round to oval nuclei often within lacunae separated by moderate amounts of lightly basophilic matrix. Few necrotic cells were interspersed with this population. Mild variation was seen in cell size. The cellular population was circumferentially bordered by organized rim spindle cells (3-5 cell layers thick). The spindle cells had acidophilic cytoplasm and oval nuclei. The outermost portion of the pellets was composed of less organized polygonal cells with necrotic cells interspersed.

Adult bone marrow derived mesenchymal stem cell pellets (BM-A-P): The pellets were composed of a central accumulation of polygonal cells with minimal acidophilic cytoplasm and round to oval nuclei often within lacunae separated by moderate amounts of lightly basophilic matrix. A small core of necrotic cells were observed centrally or interspersed throughout the pellets. Mild variation was seen in cell size. The cellular population was circumferentially bordered by organized rim spindle cells several layers thick. The spindle cells had acidophilic cytoplasm and oval nuclei. The outermost portion of the pellets was composed of less organized polygonal cells with necrotic cells interspersed.

Middle-aged bone marrow derived mesenchymal stem cell pellets (BM-M-P): The pellets were composed of a central core of necrotic cells or necrotic cells interspersed throughout the pellet. Bordering the center were low numbers of polygonal cells with minimal acidophilic cytoplasm and round to oval nuclei often within lacunae separated by small to moderate amounts of lightly basophilic matrix. A rim of spindle cells formed the outermost portion of the pellets.

Geriatric bone marrow derived mesenchymal stem cell pellets (BM-G-P): The pellets were largely composed of small, polygonal cells with pyknotic nuclei (necrosis). Some pellets had margins with a small focus of polygonal cells with minimal acidophilic cytoplasm and round to oval nuclei separated by small amounts of lightly basophilic matrix.

Newborn adipose tissue derived mesenchymal stem cell pellets (AT-Y-P): The pellets were composed of a large central core of necrotic cells (approximately two-thirds the size of the pellet) bordered by fairly organized steams of spindle cells with small amounts of acidophilic cytoplasm and oval nuclei. The spindle cell layer was 3-12 cell layers thick.

Yearling adipose tissue derived mesenchymal stem cell pellets (AT-Y-P): The pellets were composed of a large central core of necrotic cells (between one and two-thirds the size of the pellet) bordered by fairly organized streams of spindle cells with small amounts of acidophilic cytoplasm and oval nuclei. The remaining of the pellets was composed of spindle cell layers.

Adult adipose tissue derived mesenchymal stem cell pellets (AT-A-P): The pellets were composed of a large central core of necrotic cells (between one to two-thirds the size of the pellet) bordered by fairly organized streams of spindle cells with small amounts of acidophilic cytoplasm and oval nuclei. Spindle cell layers comprised the remaining of the pellets.

Middle-aged adipose tissue derived mesenchymal stem cell pellets (AT-M-P): The pellets were composed of a central core of necrotic cells (approximately one-third to one-half the size of the pellet) bordered by fairly organized streams of spindle cells with small

amounts of acidophilic cytoplasm and oval nuclei. Spindle cell layers comprised the remaining of the pellets.

Geriatric adipose tissue derived mesenchymal stem cell pellets (AT-N-P): The pellets were composed of a central core of necrotic cells (approximately one-third to one-half the size of the pellet) bordered by fairly organized streams of spindle cells with small amounts of acidophilic cytoplasm and oval nuclei. Spindle cell layers comprised the remaining of the pellets.

Newborn dermal fibroblast pellets (DF-N-P): The pellets were composed of a large central core of necrotic cells (approximately one-third to four-fifth the size of the pellet) bordered by fairly organized streams of spindle cells with small amounts of acidophilic cytoplasm and oval nuclei. Spindle cell layers comprised the remaining of the pellets.

Yearling dermal fibroblast pellets (DF-Y-P): The pellets were composed of a central core of necrotic cells (approximately one-quarter to one-half the size of the pellet) bordered by fairly organized streams of spindle cells with small amounts of acidophilic cytoplasm and oval nuclei. Spindle cell layers comprised the remaining of the pellets.

Adult dermal fibroblast pellets (DF-A-P): The pellets were composed of a large central core of necrotic cells (approximately one-quarter to two-thirds the size of the pellet) bordered by fairly organized streams of spindle cells with small amounts of acidophilic cytoplasm and oval nuclei. Spindle cell layers comprised the remaining of the pellets.

Middle-aged dermal fibroblast pellets (DF-M-P): The pellets were composed of a large central core of necrotic cells (varies from one-quarter to three-quarters the size of the pellet) bordered by fairly organized streams of spindle cells with small amounts of

acidophilic cytoplasm and oval nuclei. Spindle cell layers comprised the remaining of the pellets.

Geriatric dermal fibroblast pellets (DF-G-P): The pellets were composed of a large central core of necrotic cells (varies from one-fifth to two-thirds the size of the pellet) bordered by fairly organized streams of spindle cells with small amounts of acidophilic cytoplasm and oval nuclei. Spindle cell layers comprised the remaining of the pellets.

3.3.4 Proteoglycan staining

All slides were stained on the same day using aliquots of the same staining solutions. Control articular cartilage sections from the same horse, incorporated in each staining batch, showed no significant difference between slide-position within the 30-slide staining rack or difference between batches. Representative images of BM-MSC pellets after Safranin-O staining are shown under different magnifications in Figure 3.6. Figure 3.7 shows representative images of BM-MSC pellets, AT-MSC pellets, and DF pellets from horses in 5 different age groups after Safranin-O staining. Safranin-O stains proteoglycans an orange to deep red color and showed some variation between biological replicates, but also consistent experimental group features as shown in the Redness data in Figure 3.8. Sections absent of proteoglycans presents in a turquoise blue color due to Fast Green background staining.

When comparing the Safranin-O staining with the H&E staining for the same pellets under microscopy, portions of the BM-MSC pellets with polygonal cells (especially in lacunae) and organized stream of bordering spindle cells in general stained red for proteoglycans (Figure 3.4 and 3.6). Using microscopy, no red staining was

detectable for the eye of two individual observers (Drs. Jasmin Bagge and Jennifer Janes, University of Kentucky, USA) in any of the pellets made from AT-MSCs or DFs (biological negative control) (Figure 3.7). Likewise, no redness was detected in the non-induced pellets or skin samples.

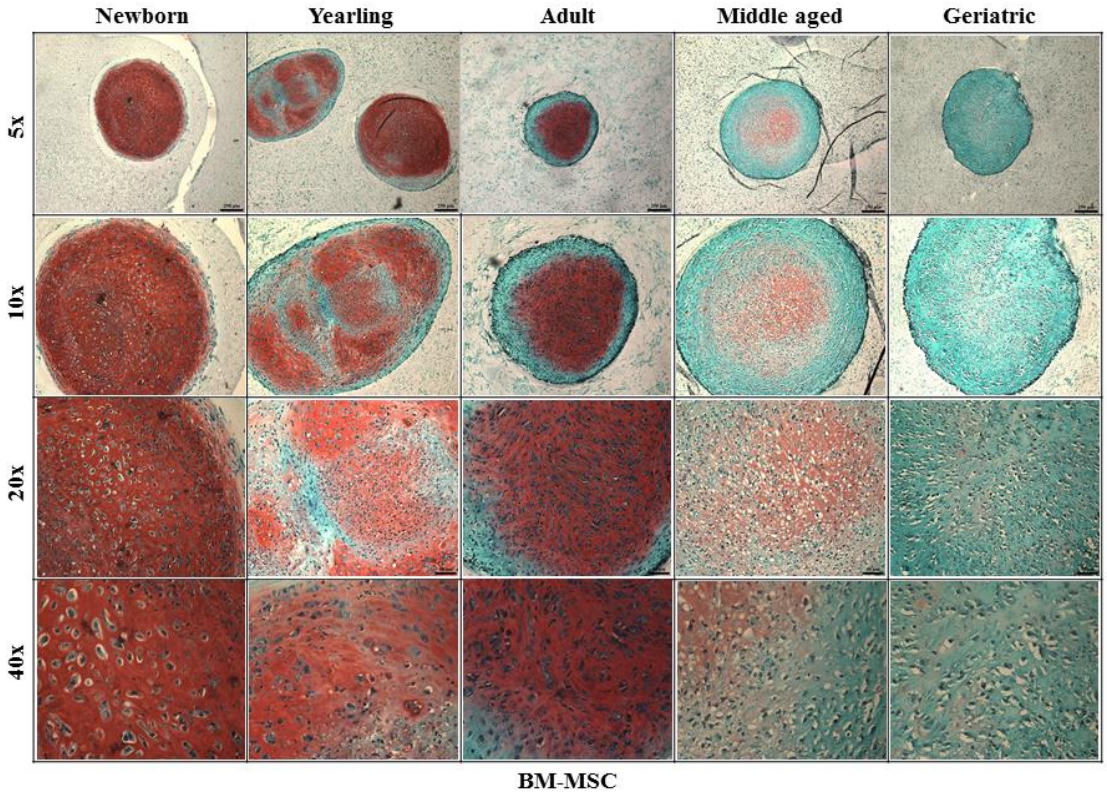

Figure 3.6: *Panel showing representative Safranin-O stained pellets of bone marrow derived mesenchymal stem cells (BM-MSCs) from horses in 5 different age groups under different magnifications after 21 days of culture in chondrogenic induction medium. Size-bar on 5x magnification images is equivalent to 250 µm.*

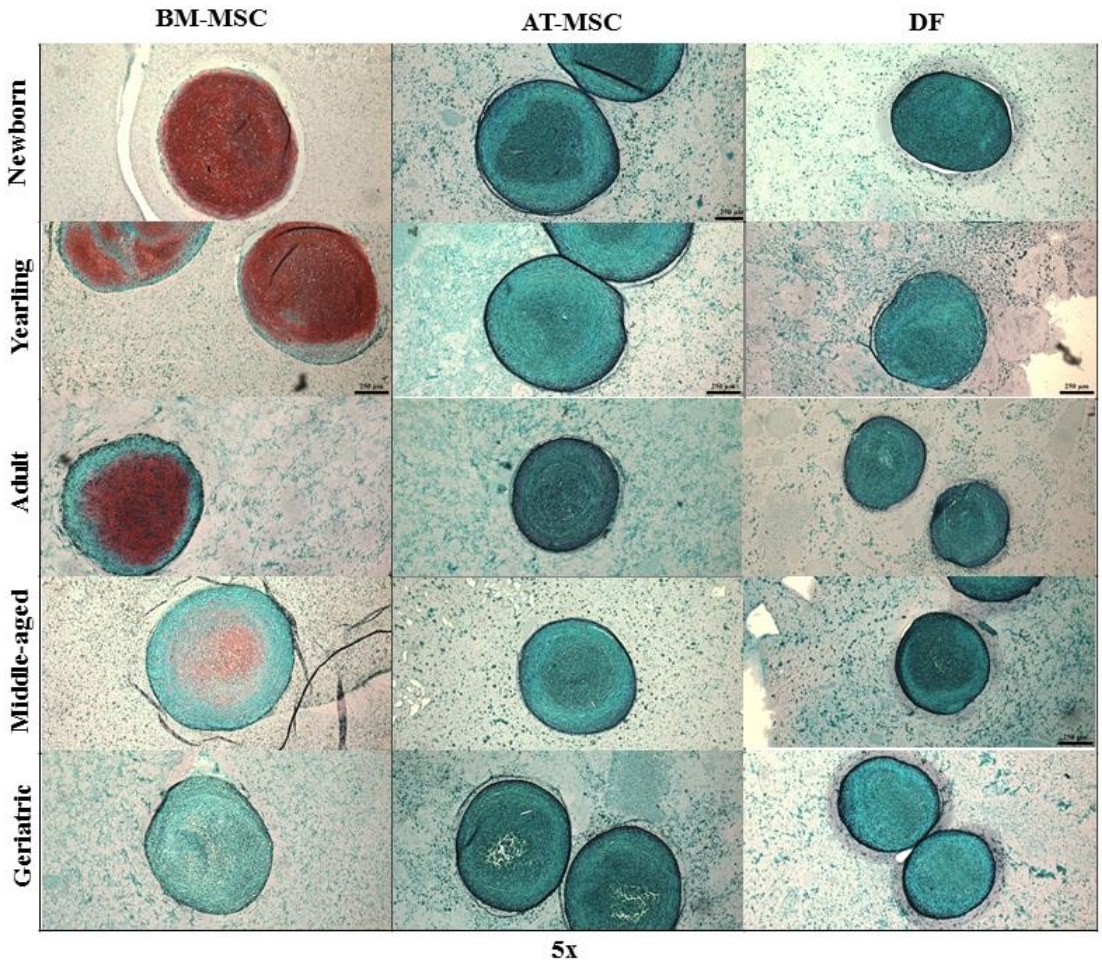

Figure 3.7: *Panel showing representative Safranin-O stained pellets of bone marrow (BM)- and adipose tissue (AT) derived mesenchymal stem cells (MSCs), and dermal fibroblasts (DF) from horses in 5 different age groups after 21 days of culture in chondrogenic induction medium. All images are taken under 5x magnifications. The size-bar on the images is equivalent to 250 µm.*

In general, BM-MSC pellets had a significantly higher proteoglycan content than pellets from AT-MSC or DF ($p<0.0001$) (Figure 3.7 and 3.8). The proteoglycan content was significantly higher in chondrogenic BM-MSC pellets compared to AT-MSC pellets in all age groups except adults (Figure 3.8).

When looking within BM-MSCs, pellets from newborn had a significantly higher proteoglycan content compared to all other age groups ($p<0.0001$), and yearlings had a significantly higher proteoglycan content compared to middle-aged horses ($p=0.0190$). For AT-MSC pellets, no statistical difference was seen in the Redness values between any of the age groups.

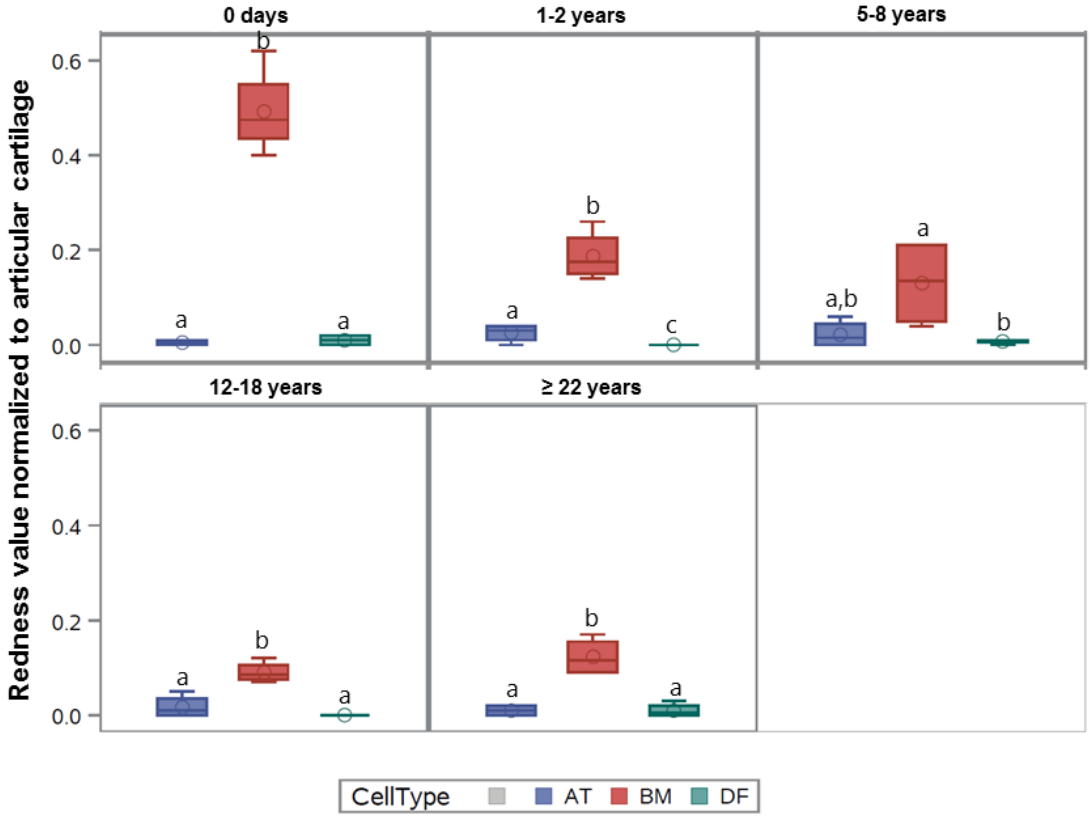

Figure 3.8**:** *Box plot showing proteoglycan Redness value of Safranin-O stained pellets of bone marrow (BM)- and adipose tissue (AT) derived mesenchymal stem cells and dermal fibroblasts (DF) (biological negative control) in 5 different age groups after normalization to articular cartilage (n=4 horses per cell type per age group). All pellets were cultured in chondrogenic induction medium for 21 days. Cell types within the same age group not labeled with the same letter are significantly different from each other ($p<0.05$).*

OSTEOGENIC DATA:

3.3.5 Alkaline phosphatase (ALP) activity

There was a significant difference in ALP activity between osteogenic induced and non-induced control BM-MSCs in newborn ($p<0.0001$), yearling ($p<0.0001$), and adult horses ($p=0.01$). No difference was seen between osteogenic induced and non-induced cells in the middle-aged or geriatric horses, or in any of the AT-MSC age groups (Figure 3.9). No statistical effect of donor age was seen in any of the pair-wise comparisons within cell types for BM-MSCs or AT-MSCs, and large inter-animal variation was seen within most age groups as indicated by the standard deviation in Figure 3.9. When comparing the 3 osteogenic induced cell types independent of age groups, the ALP activity was seen in the following order: BM-MSC > AT-MSC > DF ($p<0.0001$). When comparing across cell types within age groups, BM-MSCs had a higher ALP activity compared to AT-MSCs in yearlings only ($p=0.0155$).

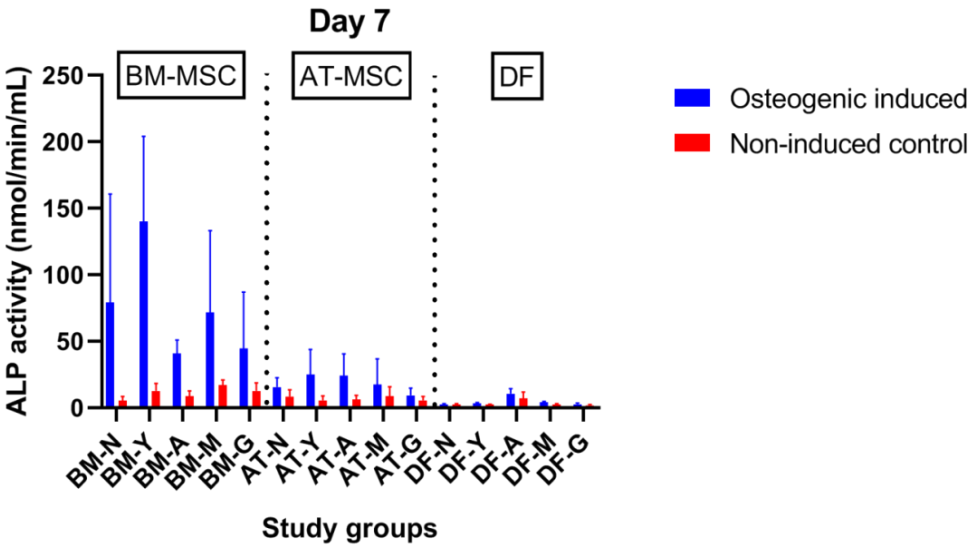

Figure 3.9: *Bar plot showing alkaline phosphatase (ALP) activity of equine bone marrow (BM)- and adipose tissue (AT) derived mesenchymal stem cells and dermal fibroblasts (DF) (biological negative control) in 5 different age groups after 7 days of culture in either osteogenic induction medium or expansion medium (non-induced control) (n=4, N=60). Error bars indicate standard deviation. *N: Newborn, Y: Yearling, A: Adult, M: Middle-aged, G: Geriatric.*

3.3.6 Alizarin Red S (ARS) concentration

There was a significantly higher ARS concentration in osteogenic induced cultures compared to non-induced controls for all BM- and AT-MSC age groups, except for middle-aged BM-MSC, and the geriatric horses of both BM- and AT-MSCs (Figure 3.11). Representative images of osteogenic induced and non-induced BM-MSCs from a newborn foal in relation to ARS staining are shown in Figure 3.10. The ARS concentration of osteogenic induced DFs (biological negative control) were significantly lower compared to both BM- and AT-MSCs ($p<0.0001$) (Figure 3.11).

As shown in Figure 3.11, there was a significant decrease in calcium deposition with increasing donor age for both BM- and AT-MSCs. Interestingly, a significant difference was seen already in pair-wise comparisons between newborn and yearlings for osteogenic induced BM-MSCs ($p=0.0003$). On the other hand, a significant difference in calcium deposition was only seen in pair-wise comparisons including geriatric horses for osteogenic induced AT-MSCs ($p<0.0001$). Nevertheless, the highest mean ARS value across all cell types were seen in BM-MSCs from newborn foals (mean ARS = 2.18 mM, SD=0.716). No sigificant difference was however detected between BM- and AT-MSCs in the newborn, adult, or geriatric age group. For yearling ($p=0.0064$) and middle-aged ($p=0.0012$) horses, AT-MSCs had a significantly higher calcium deposition compared to BM-MSCs.

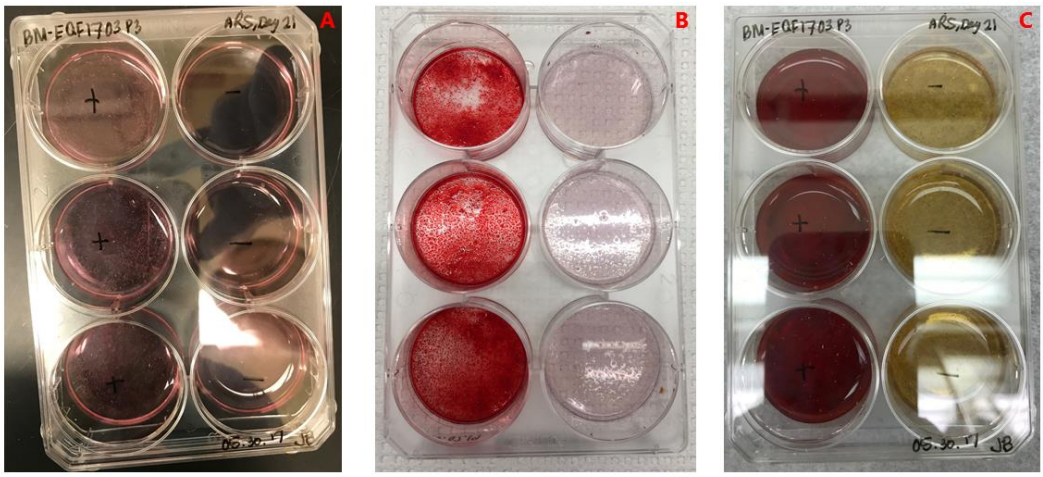

Figure 3.10: *Representative images of BM-MSCs from a newborn foal after 21 days of culture in osteogenic induction medium (+) or in expansion medium (-), where mineralized aggregates can be visualized in the (+) osteogenic induced wells (Image A). Image B shows the same cells after 40 mM Alizarin Red S staining (calcium deposits stain red). Image C shows the same cells after calcium extraction using 10% acetic acid.*

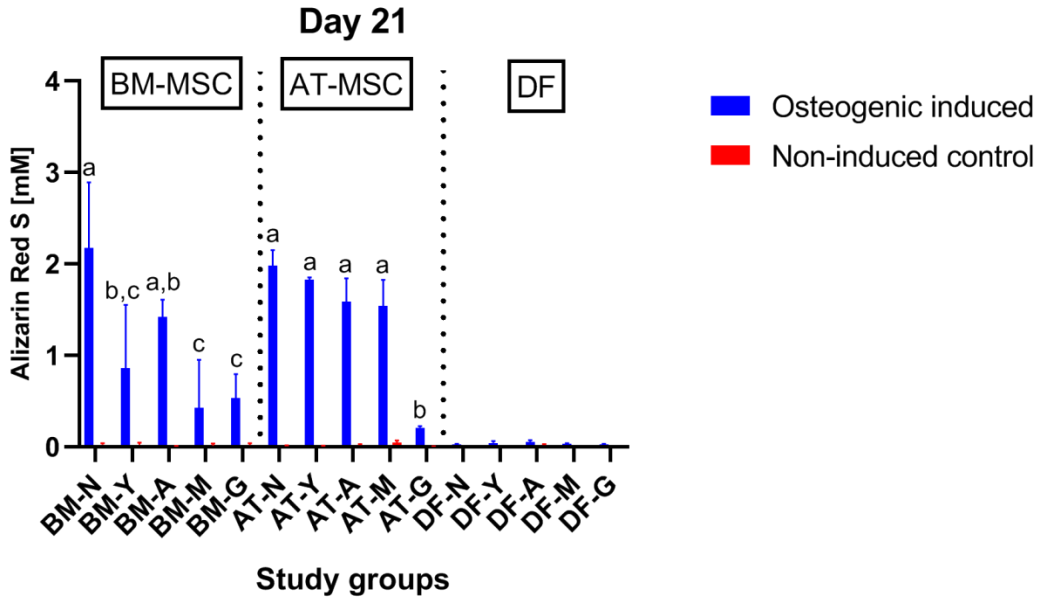

Figure 3.11: *Bar plot showing Alizarin Red S concentration (mM) as a measurement of calcium deposits of equine bone marrow (BM)- and adipose tissue (AT) derived mesenchymal stem cells and dermal fibroblasts (DF) (biological negative control) in 5 different age groups after 21 days of culture in either osteogenic induction medium or expansion medium (non-induced control) (n=4 horses per cell type per age group per medium). Age groups with in the same osteogenic induced cell type not labeled with the same letter are significantly different from each other ($p<0.05$). Error bars indicate standard deviation. *N: Newborn, Y: Yearling, A: Adult, M: Middle-aged, G: Geriatric.*

GENE EXPRESSION DATA:

3.3.7 Gene expression

After having cultured the pellets in chondrogenic induction medium for 21 days, there was a decrease in some proliferative markers like MYC (Figure 3.13) and PCNA, and a decrease in some growth factors like HDGF and FGF18 compared to non-induced monolayer cultures harvested at ~80% confluence (CHM). Following chondrogenic induction there was furthermore a general increase in expression of chondrogenic markers with most prominent rise in pellets from BM-MSCs (Figure 3.12). For the early markers of chondrogenesis, SOX5 and SOX9, there was a significantly higher gene expression of SOX5 in pellets compared to non-induced controls from BM-MSCs in all age groups ($p<0.0001$) and from AT-MSCs from horses below 8 years of age ($p\leq0.0031$). For SOX9, there was a significantly higher expression in BM-MSC pellets compared to non-induced controls in newborns and yearlings ($p\leq0.0089$), whereas no difference was seen for AT-MSCs or DFs.

The signaling and transcription factors, CTGF and TGFB3, showed no difference between pellets and non-induced controls from AT-MSCs or DFs. For BM-MSCs, TGFB3 expression was significantly higher in pellets compared to non-induced controls in all age groups ($p\leq0.0017$), whereas CTFG only showed difference in pellets versus non-induced controls in horses below 8 years of age ($p\leq0.0034$).

With regards to later markers of chondrogenesis, the same trend was seen. For MIA, there was a greater expression in chondrogenic induced BM-MSC pellets compared to non-induced controls in all age groups ($p<0.0001$), whereas no difference was seen in AT-MSCs or DFs. For the essential cartilage extracellular matrix components, COMP

and ACAN, a significant difference between pellets and non-induced controls was seen for both BM- and AT-MSCs in all age groups ($p<0.0001$). The specific marker of articular cartilage, COL2A1, was greater expressed in pellets compared to non-induced controls in BM-MSCs ($p<0.0001$) and AT-MSCs ($p\leq0.0009$) in all age groups. No difference was seen in expression of the fibrocartilage marker, COL1A1, between pellets and non-induced cells in any of the cell types. Nevertheless, the expression of COL1A1 was 1.6 fold higher (SE=0.567) in AT-MSCs pellets compared to BM-MSCs pellets, although not significant ($p=0.0924$).

When comparing the cell types independent of age group, BM-MSCs had a significantly greater expression of ACAN, COL2A1, MIA, and SOX9 than AT-MSCs or DFs ($p<0.0001$). No difference was seen between AT-MSCs and DFs for the same biomarkers.

When comparing within BM-MSCs, COMP and ACAN was significantly greater expressed in pellets from newborn compared to geriatric horses ($p=0.0138$ and $p=0.0013$, respectively). Likewise, MIA was up-regulated in newborn BM-MSC pellets compared to all other age groups ($p<0.0001$) except yearlings, who also had a higher expression compared to all older age groups ($p\leq0.0006$) (Figure 3.14).

With regards to extracellular collagens, a clear trend towards less COL2A1 expression was seen with increasing donor age in pellets from BM-MSCs. The trend was however not significant presumably due to inter-sample variation. Nevertheless, BM-MSC pellets from newborn foals had a significantly higher expression of COL11A1 compared to middle-aged ($p=0.0331$) and geriatric horses ($p=0.0003$). On the other hand, pellets from geriatric horses had a significantly higher expression of COL4A1 compared

to newborn ($p<0.0001$) and adult horses ($p=0.0186$). With regards to COL1A1, middle-aged horses had significantly lower expression compared to BM-MSC pellets from newborn ($p=0.0107$) and yearlings ($p=0.0058$). However, no difference was found in pair-wise comparisons involving geriatric horses.

Out of the 88 biomarkers included in the panel, 11 (13%) were affected by donor age in AT-MSCs, 45 (51%) in BM-MSCs, and 13 (15%) in DFs when looking at chondrogenic induced pellets (Figure 3.12 and Table 3.2). As shown in the Venn-diagram (Figure 3.15), 9 of the targets were affected by donor age in both BM- and AT-MSC pellets. Of these, 6 targets (PCNA, LOC100146270, BRCA1, BARD1, CASP8, DMP1) were up-regulated with increasing donor age in both BM- and AT-MSCs, whereas SMPD3 was down-regulated with increasing donor age in BM-and AT-MSCs. CLU and PDGFD, were up-regulated in pellets from AT-MSCs and down-regulated in pellets from BM-MSCs with increasing donor age.

Figure 3.12: *A heatmap showing the Ln(RQ) levels of gene expression by color change between average levels in bone marrow (BM) and adipose tissue (AT) derived mesenchymal stem cells and dermal fibroblasts (DF) from horses in 5 different age groups (n= 4 horses per age group per cell type per medium) grown under different conditions. Gray boxes indicate no detection of gene expression. *N: Newborn, Y: Yearling, A: Adult, M: Middle-aged, G: Geriatric, P: Pellets cultured in chondrogenic induction medium for 21 days, CHM: grown in T75 flasks with expansion medium and harvested at ~80% confluence, O0B; grown in expansion medium in 6-wells and harvested at ~90% confluence, O21A: cultured in 6-wells in osteogenic induction medium for 21 days, O21B: cultured in 6-wells in expansion medium for 21 days.*

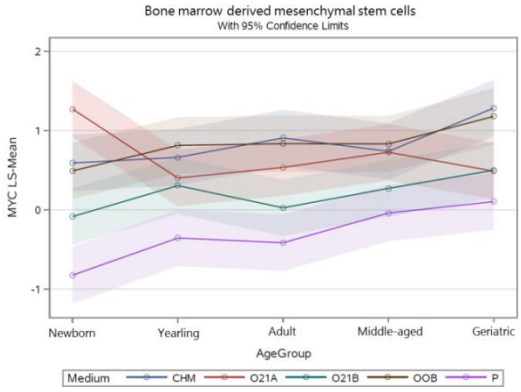

Figure 3.13: *Graphical overview of mean Ln(RQ) gene expression levels of the proliferative marker MYC from bone-marrow derived mesenchymal stem cells in 5 different age groups under different culture conditions. * CHM: grown in T75 flasks with expansion medium and harvested at ~80% confluence, O21A: cultured in 6-wells in osteogenic induction medium for 21 days, O21B: cultured in 6-wells in expansion medium for 21 days, O0B; grown in expansion medium in 6-wells and harvested at ~90% confluence, P: Pellets cultured in chondrogenic induction medium for 21 days.*

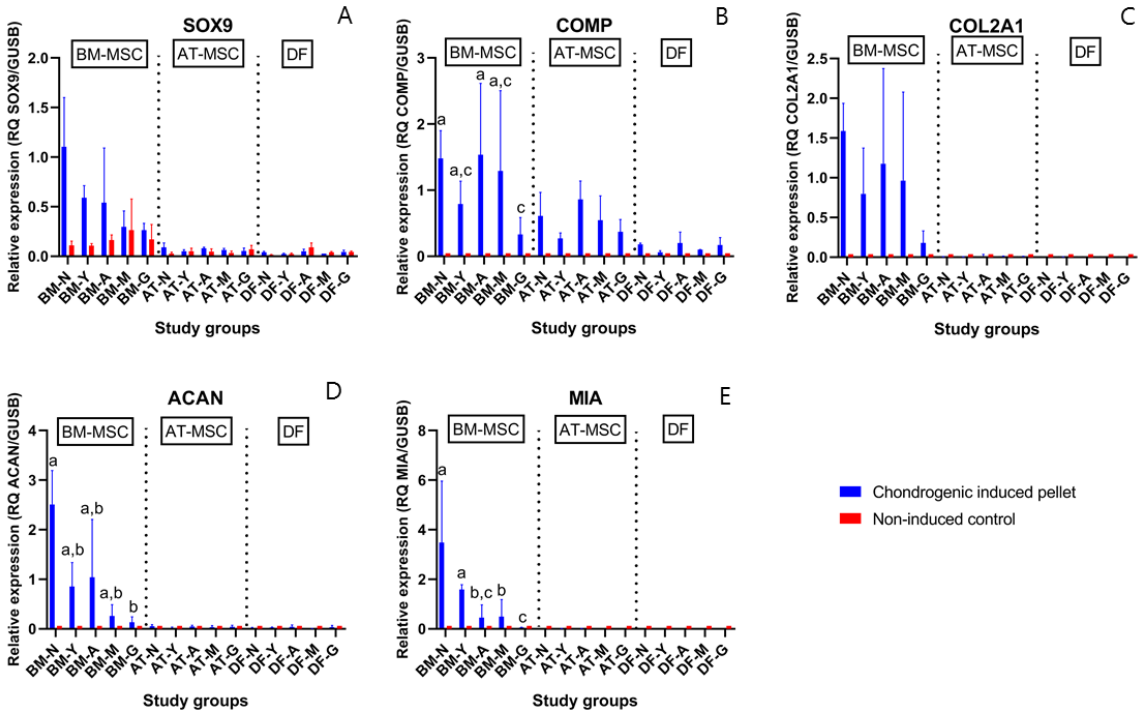

Figure 3.14: *Bar plots with standard deviation illustrating mean relative gene expression of SOX9 (A), COMP (B), COL2A1 (C), ACAN (D), and MIA (E) in chondrogenic induced pellets and non-induced monolayer controls from bone marrow (BM)- and adipose tissue (AT)- derived mesenchymal stem cells (MSCs) and dermal fibroblasts (DF) from 4 horses in 5 different age groups (n=4, N=60). Age groups within chondrogenic induced BM-MSCs not marked with the same letter are significantly different from each other ($p<0.05$). No significant donor age effect was seen for SOX9 or COL2A1. Note different y-axes. *N: Newborn, Y: Yearling, A: Adult, M: Middle-aged, G: Geriatric.*

Table 3.2: Donor age affected genes within pellets made from adipose tissue (AT)- and bone marrow (BM) derived mesenchymal stem cells (MSC) and dermal fibroblasts (DF) from 4 horses in 5 different age groups (n=4, N=60) after 21 days of culture in chondrogenic induction medium.

CELL TYPE	GENE FUNCTION			
	Proliferation regulators	**Signaling**	**Transcription factors**	**Extracellular matrix**
AT-MSCs	Up-regulated BARD1 (-) BRCA1* (-) CASP8 (-) CLU (+) LOC100146270 (-) PCNA (+) PDGFD (+)	Up-regulated MET		Up-regulated DMP1 Down-regulated CRTAC1 SMDP3*
BM-MSCs	Up-regulated BARD1 (-) BRCA1* (-) CASP8 (-) CCND1 (+) CDKN1A (-) CTNNB1 (+) GLB1* (-) HDGF (+) LOC100146270 (-) MYC (+) PCNA (+) PHB (-) TGFA (+) TP53* (-) Down-regulated BCL2 (+) CLU (+) IGF1* (+) PDGFD (+)	Up-regulated GDF6 PHEX Down-regulated ALPL* ABI3BP FGFR3 IGFBP5 MIA* S100A1 TNFRSF11B	Up-regulated BMP4 BMP7 TGFB3 Down-regulated BMP6 SNAI2*	Up-regulated COL4A1 DMP1 LOC100146589 Down-regulated ACAN CHADL COL1A1 COL9A2 COL11A1 COL12A1 COMP MMP13* SMPD3* SPARC
DFs	Down-regulated BCL2 (+) CCND1 (+) CTGF (+) HGF (+) TP53* (-)	Down-regulated GDF6 TIMP2 SMOC1	Down-regulated GLI3 RUNX3	Down-regulated ACAN COL5A3 SMPD3*

*All listed genes were significantly affected by donor age within the given cell type determined by one-way ANOVA when p<0.05. Red marked genes indicate an up-regulation in gene expression with increasing donor age. Blue marked genes indicate a down-regulation in gene expression with increasing donor age. * Categorized based on main function related to chondrogenesis, but could be categorized in more than one annotation category. (+): Enhance proliferation. (-): Inhibits proliferation.*

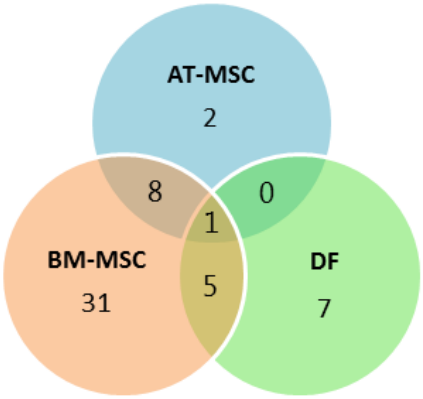

Figure 3.15: *Venn-diagram showing the distribution of differentially expressed genes as a function of donor age between chondrogenic induced pellets made from adipose tissue (AT)- and bone marrow (BM) derived mesenchymal stem cells (MSC) and dermal fibroblast (DF) from 4 horses in 5 different age groups (n=4, N=60).*

After having grown the monolayer cells in osteogenic induction medium for 21 days, there was a general decrease in some of the growth factors. FGF5 and FGF18 were lower expressed in osteogenic induced cells compared to non-induced cells at day 0 and day 21. At the same time, an increase in multiple osteogenic factors occurred in the stem cells after being cultured in osteogenic induction medium for 21 days, with the largest fold changes occurring in BM-MSCs (Figure 3.17). The early marker of osteogenesis, RUNX2, was significantly up-regulated after osteogenic induction in AT-MSCs in all age groups ($p \leq 0.0014$) and in BM-MSCs from newborn foals ($p < 0.0001$). Arcoss all age groups, RUNX2 expression followed the pattern of; BM-MSCs > AT-MSCs > DFs ($p < 0.0001$). Another early marker of osteogenesis, ALPL, also showed significantly enhanced expression after osteogenic induction in BM-MSCs ($p < 0.0001$) and AT-MSCs ($p \leq 0.0195$) in all age groups when compared to non-induced cells at day 21. When comparing cell types, osteogenic induced BM-MSCs had significantly higher ALPL gene expression compared to AT-MSCs in all age groups ($p \leq 0.0329$). BMP4 was significantly

up-regulated in osteogenic induced cells compared to non-induced day 21 cells for AT- and BM-MSCs in newborns ($p=0.0045$, and $p<0.0001$, respectively), and in BM-MSCs in yearlings ($p=0.0004$).

An up-regulation in some of the later markers of osteogenesis was also observed after osteogenic induction. For SP7, an enhanced expression in osteogenic induced versus non-induced cells was only observed in newborn ($p=0.0018$) and yearling BM-MSCs ($p=0.0092$). Across all age groups BM-MSCs had a higher expression of SP7 compared to AT-MSCs and DFs. A significant difference in LOC100146589 was also observed between osteogenic induced and non-induced cells at day 21 for AT-MSCs from horses below 8 years of age ($p\leq0.0241$) and in BM-MSCs from newborn foals ($p<0.0001$). In newborn foals, LOC100146589 was greater expressed in osteogenic induced BM-MSCs than AT-MSCs ($p=0.0441$) and DFs ($p<0.0001$). No difference was observed in LOC100146589 expression between BM- and AT-MSCs in any of the other age groups. When comparing all 3 osteogenic induced cell types independent of donor age, no difference was seen in LOC100146589 expression ($p\geq0.2414$). COL1A1 expression was higher in non-induced compared to osteogenic induced cells at day 21 for all 3 tissue types in all age-groups.

When comparing within cell types, no effect of donor age was seen on ALPL expression in osteogenic induced BM- or AT-MSCs. The same was true for RUNX2 expression in AT-MSCs, but a significant decrease in RUNX2 expression was seen with increasing donor age in BM-MSCs, specifically between newborn and adults ($p=0.0088$), and newborn and middle-aged ($p=0.0491$). With regards to later markers of osteogenesis, SP7 and COL1A1, no effect of donor age was seen in osteogenic induced AT- or BM-

MSCs. On the other hand, BM-MSCs from newborn foals had a significantly higher LOC100146589 expression compared to adult ($p=0.0006$), middle-aged ($p<0.0001$), and geriatric horses ($p=0.0242$) (Figure 3.17).

Out of the 88 biomarkers included in the panel, 15 (17%) were affected by donor age in AT-MSCs, 30 (34%) in BM-MSCs, and 32 (36%) in DFs when assessing osteogenic induced cells (Figure 3.12 and Table 3.3). As shown in the Venn-diagram (Figure 3.16), 7 of the targets were affected by donor age in both BM- and AT-MSC. Of these, 5 targets (BGN, COL11A1, CTNNB1, HGF, SMOC) were up-regulated with increasing donor age in both BM- and AT-MSCs. CASP3 and CLU, were up-regulated in osteogenic induced AT-MSCs and down-regulated in BM-MSCs with increasing donor age.

Table 3.3: Donor age affected genes within monolayer cultures of adipose tissue (AT)- and bone marrow (BM) derived mesenchymal stem cells (MSC) and dermal fibroblasts (DF) from horses in 5 different age groups (n=4, N=60) after 21 days of culture in osteogenic induction medium.

CELL TYPE	GENE FUNCTION			
	Proliferation regulators	**Signaling**	**Transcription factors**	**Extracellular matrix**
AT-MSCs	Up-regulated CASP3 (-) CLU (+)	Up-regulated CRYAB MET TNFRSF11B	Up-regulated SOX5	
	Down-regulated CTNNB1 (+) HGF (+)	Down-regulated SMOC* TNFSF11	Down-regulated BMP2 BMP4	Down-regulated BGN COL11A1 SPARC
BM-MSCs	Down-regulated AQP1 (+) BARD1 (-) CASP3 (-) CDKN1A (-) CLU (+) CTNNB1 (+) FGF5 (+) FGF18 (+) HDGF (+) HGF (+) IGF1* (+) MYC (+) PDGFD (+) TP53* (-) VEGFA (+)	Up-regulated SOST Down-regulated CAVIN1 GDF6 TIMP2 SMOC*	 Down-regulated BMP6 GLI3 RUNX2 TGFB1	Up-regulated IBSP Down-regulated ACAN BGN COL11A1 DMP1 LOC100146589
DFs	Down-regulated BCL2 (+) CASP3 (-) CDKN1A (-) FGF5 (+) HGF (+) PDGFD (+) TP53* (-) VEGFA (+)	Up-regulated ALPL CRYAB EB2F S100A1 SOST TNFRSF11B	Up-regulated BMP6 SOX9 Down-regulated BMP2 BMP4 RUNX2 RUNX3 SP7 TGFB1 TGFB2	Down-regulated BGN COL1A1 COL4A1 COL11A1 COL12A1 FN1 LOC100146589 SPARC SPP1

**All listed genes were significantly affected by donor age within the given cell type determined by one-way ANOVA when $p<0.05$. Red marked genes indicate an up-regulation in gene expression with increasing donor age. Blue marked genes indicate a down-regulation in gene expression with increasing donor age. * Categorized based on main function related to osteogenesis, but could be categorized in more than one annotation category. (+): Enhance proliferation. (-): Inhibits proliferation.*

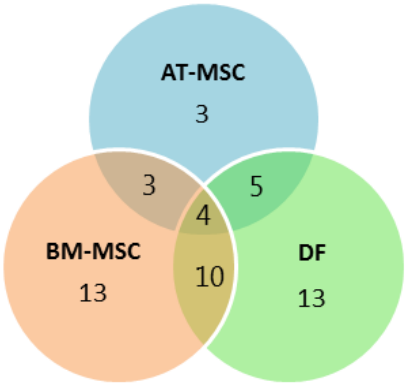

***Figure 3.16**: Venn-diagram showing the distribution of differentially expressed genes as a function of donor age between osteogenic induced adipose tissue (AT)- and bone marrow (BM) derived mesenchymal stem cells (MSC) and dermal fibroblast (DF) from horses in 5 different age groups.*

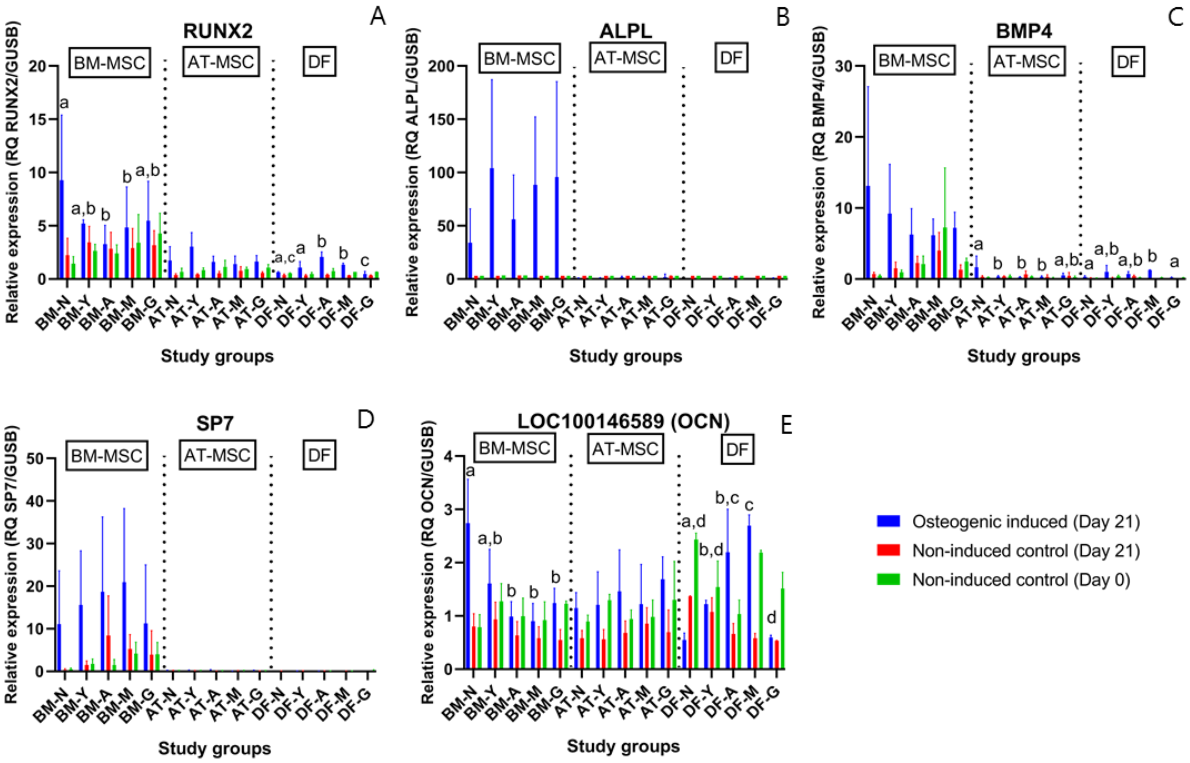

***Figure 3.17:** Bar plots with standard deviation illustrating mean relative gene expression levels of RUNX2 (A), ALPL (B), BMP4 (C), SP7 (D), and LOC100146589 (E) in osteogenic induced cells after 21 days of induction and non-induced controls at day 0 and day 21. The cells consist of bone marrow (BM)- and adipose tissue (AT) derived mesenchymal stem cells (MSCs) and dermal fibroblasts (DF) from 4 horses in 5 different age groups (n=4, N=60). Age groups within the same osteogenic induced cell type not marked with the same letter are significantly different from each other (p<0.05). Note different y-axes. *N: Newborn, Y: Yearling, A: Adult, M: Middle-aged, G: Geriatric.*

3.4 DISCUSSION

In this study, we examined the effect of donor age on the *in vitro* chondrogenic and osteogenic differentiation performance of equine BM- and AT-MSCs from horses in 5 different age groups, together with potential underlying gene expression changes in biomarkers related to differentiation and aging. Chondrogenic and osteogenic differentiation performance in culture is an important aspect of assessing stem cells potential to regenerate orthopedic injuries, as differentiation and growth factor excreting capacity has been positively linked [97], together with an increased use of scaffolds to enhance engraftment of stem cells within the injury site depending more on their direct differentiation capacity.

The results support the hypothesis that increasing donor age is a major variable impacting equine BM- and AT-MSCs chondrogenic and osteogenic differentiation performance with decreasing capacities following non-linear kinetics, which is similar to previous reports in other species [27,85,97,122–125,127]. Other research groups have however reported no age related changes in MSC differentiation potential [100,131,137], which may be caused by the lack of very young individuals in the study populations and differences in culture conditions. Stenderup *et al*. reported that age related changes in bone formation were more associated with lower MSC proliferative capacity and hence lower cell numbers than a lower function of the MSCs [131]. To control for this factor, all our assays were performed at passage 4 and all cells were plated at the same density in all steps.

The data furthermore showed that BM-MSCs have higher potential for generating cartilage under standard chondrogenic induction conditions than AT-MSCs, which is

supported by previous equine studies [35,41,69]. Nevertheless, our data showed a significant decrease in proteoglycan content with increasing donor age in pellets from BM-MSCs already in pair-wise comparisons between newborn and yearlings. This finding on protein level was supported by a decrease in ACAN gene expression with increasing donor age, as aggrecan is an essential proteoglycan in articular cartilage [4]. The higher extracellular proteoglycan content in BM-MSCs from young horses was surprisingly not reflected in pellet size where no statistical difference was detected as a function of donor age. This may be partly due to an increased number of senescent cells in BM-MSC pellets from old horses as GLB1 expression was up-regulated in aged horses, and senescent BM-MSCs are reported to have a larger cell morphology [105,131].

On a morphological level, BM-MSC pellets from newborn foals were most uniform in redness and contained similarities to native articular cartilage with areas of lacunae occupied by single cells, proteoglycan rich matrix between the cells, and minimal necrotic cells. In the older age groups, more necrotic cells appeared centrally, which was also seen in pellets from AT-MSCs and DFs in all age groups. A zonal architecture of chondrogenic induced pellets have been reported previously [35,71]. The lack of or minimal necrotic center in newborn BM-MSC pellets is particularly interesting as it suggests a cellular adaptation to lower oxygen levels. Such a characteristic would be an important feature, as articular chondrocytes live under hypoxic conditions with low oxygen levels between 1% and 10% depending on the length to the articular surface [19]. Changes in the level of necrotic core as a function of donor age and cell type may also be caused by different diffusion efficiency of oxygen and nutrients in matrices of different pellet types, which is likely as pellets from aged BM-MSC, AT-MSCs and DFs appeared

more dense with less extracellular matrix. Pellet size may also be a contributing factor, but no significant difference in pellet size was seen as a function of donor age in BM-MSCs, and the pellet size of newborn BM- and AT-MSCs was not significantly different from each other. Additionally, it is possible that equine BM-MSCs from newborns are less heterogeneous compared to the heterogeneous population described in adult horses [35,92,133], but this remains to be investigated. The lower chondrogenic potential seen already in yearlings may be highly problematic for autologous treatments of cartilage injuries if cells are not harvested and potentially cryopreserved at an early age.

It was furthermore interesting that the chondrogenic differentiation performance of AT-MSCs very closely resembled that of DFs (biological negative control) in all age groups. Additionally, AT-MSC pellets had a higher expression of COL1A1 and lower expression of COL2A1 compared to BM-MSCs. Expression of COL1A1 is documented in chondrogenic induced MSC pellets [35,38], but is considered undesirable as COL1A1 is a marker of biomechanically inferior fibrocartilage compared to hyaline cartilage with high COL2A1 content [4]. In contrast, other studies have reported a chondrogenic differentiation potential of AT-MSCs, although lower than seen for BM-MSCs [41,69,163]. The different results may be related to different culture conditions, as some of the studies used hydrogels, together with variances in chondrogenic induction formulas and assays. Together, this highlights the limitations of AT-MSCs as a therapeutic choice for cartilage regeneration.

A previous study by Asumda *et al.* [97] reported that BM-MSCs from 15 months old rats were not at all able to perform chondrogenic or osteogenic differentiation. This was partly supported by our data were only minimal chondrogenic and osteogenic

differentiation was seen in BM-MSCs from geriatric horses, with no statistical differences in ALP activity or calcium deposition between non-induced and induced cells. ALP is an early marker of osteogenesis and is highly expressed in mineralized tissue where it enzymatically degrades inhibitory pyrophosphates that bind calcium to enhance mineralization. As such, ALP is considered a hallmark of osteogenic differentiated cells in culture with highest expression 6 to 7 days after initiation of osteogenic induction [87,89,90]. The data showed the highest ALPL gene expression in BM-MSCs and no effect of donor age. This finding was supported by a protein activity assay, where APL activity was highest in osteogenic induced BM-MSCs followed by AT-MSCs and DFs with no effect of donor age in BM-MSCs. Even though no effect of donor age was shown on alkaline phosphatase activity, a trend towards decreased levels in aged horses was seen, suggesting that this part of the study might be under-powered. Interestingly, the ALP activity was significantly higher in osteogenic induced cells versus non-induced cells in BM-MSCs from horses below 8 years of age. In contrast, AT-MSCs and DFs demonstrated no difference in ALP activity between osteogenic induced and non-induced cells in any age group, highlighting the low ALP potential of osteogenic induced equine AT-MSCs.

On the other hand, Chen *et al.* [134] and Shi *et al.* [137] previously reported that human and mouse AT-MSCs osteogenic differentiation potential was less affected by donor age than BM-MSCs. This finding was partly supported by our data, where a decrease in ARS concentration of osteogenic induced BM-MSCs occurred already between newborn and yearlings, whereas calcium deposition only decreased in AT-MSCs from geriatric horses. Differences in initial calcium deposition may be a contributing

factor, as the highest ARS concentration was reported in newborn BM-MSCs although not significantly different from newborn AT-MSCs. As mineralization depends on multiple factors [89], a decrease in ARS concentration with increasing donor age is possible even though no statistical donor age effect was seen for ALP.

The data furthermore showed that BM-MSCs from young horses have higher potential for generating bone under standard osteogenic induction conditions than AT-MSCs, which is supported by previous human and equine studies [31,44,45,164,165]. Park *et al.* furthermore showed that BM-MSCs were more effective towards osteogenic differentiation under dynamic hydraulic compression than AT-MSCs [44], which may be an important feature as osteocytes have to withstand and respond to mechanical stimuli *in vivo* [166]. On the other hand, Kang *et al.* reported that osteogenic induced canine AT-MSCs had a higher ALP activity and mineralization compared to BM-MSCs after 14 days of culture, but that *in vivo* healing of bone radial defects was slightly better when using BM-MSCs [167]. Furthermore, Chung *et al*. demonstrated similar osteogenic differentiation potential between canine BM- and AT-MSCs, and found that hypoxia inhibited the proliferation of both cell types and osteogenic differentiation of AT-MSCs [168], which should be considered when using MSCs in hypoxic environments such as fractures and infections [166]. Differences in potential may be due to different species, donor age groups, and induction methods.

As expected, some of the proliferation markers were down-regulated after inducing the cells to undergo chondrogenesis as 3D pellets and osteogenesis as monolayers. Of greater interest are, however, the 6 genes all related to proliferation (except for DMP1) that were up-regulated with increasing donor age in both

chondrogenic induced BM- and AT-MSCs, as they may be markers of genes consistently affected by donor age in equine MSCs under chondrogenic induction. The tumor suppressors p16, BRCA1, and BARD1 and apoptosis factor CASP8 were all up-regulated in chondrogenic induced stem cells from aged donors. This may be related to cellular senescence or to the pelleting procedure as less oxygen is provided to the centrally located cells, which thereby would make them more prone to undergo cell death as seen on the H&E slides if not adapted to hypoxia.

Of the targets affected by donor age in both AT- and BM-MSCs, none of the targets affected under chondrogenic culture were intersecting with targets affected under osteogenic culture. This suggests that the biomarkers affected by donor age in MSCs may be influenced by culture conditions, which is likely as different transcription factors and hence pathways are provided to the cells together with pelleting versus monolayer culture. In support of this finding, a recent proteomics study by Peffers *et al.* also reported no intersection of age-affected proteins in chondrogenic and osteogenic constructs made from human BM-MSCs [85]. The highest proportion of biomarkers affected by donor age was seen in BM-MSCs. This was, however, not surprising, as BM-MSCs also had the highest chondrogenic and osteogenic potential to begin with in newborns.

On an osteogenic level, the biggest fold changes were seen in early markers of osteogenesis (e.g. RUNX2 and ALP) after 21 days of osteogenic induction. RUNX2 is an early marker of osteogenesis and an essential transcription factor for activation of osteoblast associated genes like osteocalcin and alkaline phosphatase [169]. Down-regulation in RUNX2 seen already in BM-MSCs from adult horses may very well be a

major player in the osteogenic differentiation decrease seen with increasing donor age in BM-MSCs as its expression correlated relatively well with downstream targets. Some of the later markers of osteogenesis like SP7 (osterix) and LOC100146589 (osteocalcin) were only significantly up-regulated after osteogenic induction in young horses. Osteocalcin was furthermore found at relatively high levels in day 0 DFs. Osteocalcin is specifically excreted by osteoblasts and is essential for mineralization. Low expression of osteocalcin can be partly explained by it mainly being produced by mature osteoblasts during bone mineralization [89]. Hence, it is possible that higher expression would be seen with longer culture in osteogenic medium as shown previously [87,170]. Since 2007 it has been realized that osteocalcin also plays an important role in the relationship between energy metabolism and bones, and hence are released from osteoblasts into the circulation where it targets other organs [89,171]. This may be the reason for its presence in DFs.

It has previously been reported that DFs incapable of osteogenic differentiation can produce non-apatitic spontaneous calcium deposits when cultured with more than 2 mM β-glycerophosphate [172]. This was however not demonstrated in our study, where DFs showed minimal calcium deposition after being cultured in osteogenic induction medium containing 10 mM β-glycerophosphate for 21 days. Likewise, DFs showed no chondrogenic differentiation after being cultured in chondrogenic induction medium for 21 days. The credibility of the differentiation results obtained from the MSCs are therefore strengthened, as the induction mediums were not able to produce measurable changes in cells incapable of differentiation.

All cells were collected immediately after euthanasia. This is however not believed to affect the translational value of the results into autologous transplantations, as no difference have been reported in MSCs from newly euthanized and anesthetized horses [133]. Collection of BM-MSCs varied for newborn and the other age groups as the newborn sternum was too cartilaginous and Jamshidi® bone marrow aspiration unfeasible. By splitting the sternum and growing the trabecular bone marrow as tissue explants, the same principles as described for foals previously were utilized [42]. The newborn age group furthermore consisted only of cells from ponies, but there is a lack of studies evaluating potential horse breed effects on the differentiation potential. However, the 2 ponies in the middle-aged age group performed similar to the other horses in that age group, and the newborn cells followed the same proliferation pattern as seen in yearlings. A recent study did however show different surface markers on equine BM-MSCs between Thoroughbreds and Standardbreds [173]. The cells were collected from a mixture of female and male horses, with both genders represented in each age group. However, there was a higher presentation of cells from female horses, but *in vitro* differentiation has been shown not to be affected by gender [130].

In conclusion, the chondrogenic and osteogenic differentiation performance of equine BM- and AT-MSCs decline with increasing donor age. BM-MSCs from newborn foals have the highest chondrogenic and osteogenic potential *in vitro* for regenerating cartilage and bone injuries when compared to older age groups and AT-MSCs. A decrease in chondrogenic proteoglycan content and osteogenic calcium deposition was seen already in pair-wise comparisons between newborn and yearling BM-MSCs. AT-MSCs showed minimal ability to perform chondrogenic differentiation, but was less

affected by donor age than BM-MSCs when making calcium deposits, where no difference was seen in ARS concentration in horses below 18 years of age. Gene expression alterations showed changes in regulators of proliferation and differentiation markers with increasing donor age. Together, this highlights the importance of donor age considerations and MSC tissue type selection for autologous treatments in horses.

This study is the first equine study comparing donor age effects on the chondrogenic and osteogenic differentiation performance of MSCs. Incorporation of 5 well-distinguished clinically relevant age groups furthermore sets it apart from most previous studies in other species where few wider age groups have been compared. The results are thus believed to be highly interpretable for clinical practice and when advising horse owners. By assessing changes in gene expression, we have furthermore identified targets to potentially improve the differentiation capacity of MSCs from horses with low differentiation potential as a function of age through molecular manipulations. Further transcriptome and mechanistic studies will be valuable in elucidating the exact effect of the identified biomarkers, their pathways, and how they are involved in regulating equine MSC chondrogenesis and osteogenesis as a function of donor age. Moreover, it would be interesting to test age-related changes in equine BM-MSCs sensitivity to hypoxia.

Our results showed a decrease in BM-MSC chondrogenesis and osteogenesis *in vitro* already in yearlings, which is likely problematic for autologous treatments to treat cartilage and bone injuries unless the cells are harvested at a young age and cryopreserved for potential later use. Nevertheless, the differentiation performance in culture needs to be held together with their *in vivo* potential to heal cartilage and bone injuries, which remains to be investigated as a function of donor age in horses.

CHAPTER 4. REFLECTIONS AND LOOKING AHEAD TO FUTURE STUDIES

4.1 Reflections

Research efforts in this dissertation were designed to investigate the effect of donor age on equine mesenchymal stem cells (MSCs) *in vitro* potential to treat orthopedic injuries. The specific objectives were to 1) examine the effect of donor age on the *in vitro* cellular proliferation of equine bone marrow (BM)- and adipose tissue (AT) derived MSCs, and to 2) determine the effect of donor age on the chondrogenic and osteogenic differentiation performance of equine BM- and AT- MSCs in culture.

Within the emerging field of regenerative medicine, cellular therapy of orthopedic injuries with MSCs is gaining increasing interest in equine practice, as they have shown potential to facilitate the repair of orthopedic injuries together with treating the symptoms [17,18,21,22]. As described in the previous chapters, autologous treatment is currently preferred and multiple studies in other species have shown a decline in our ability to expand the cells with increasing donor age, together with a sharp age-related reduction in their chondrogenic and osteogenic potential [27,94,97,122–124]. As both of these parameters are essential for the therapeutic efficiency of MSC therapy, it is essential to understand potential donor age effects on MSCs in horses, as the horse is an important patient population in its own right, and no direct age-conversion scale exists between horses and humans or rodents.

As presented in chapter 2, the cellular proliferation of equine BM- and AT-MSCs declined with increasing donor age, but interestingly only in pair-wise comparisons involving geriatric horses. The data hence showed that it is possible to expand MSCs *in vitro* at high rates from horses below 18 years of age, which is promising to obtain

sufficient numbers for autologous treatments, together with the fact that multiple treatments often are recommended [51]. The data furthermore showed that the cellular proliferation of BM- and AT-MSCs was equally affected by donor age, and that there was no significant difference in their proliferation performance in any of the age groups. This finding is believed to be positive for autologous treatments as BM-MSCs have shown a general higher potential to treat cartilage and bone injuries [35,41,44]. Nevertheless, it is important to remember that the frequency of MSCs is higher from adipose tissue than from bone marrow aspirates as shown previously [31,42], whereby higher cell numbers can be obtained faster for AT-MSCs. This was however not investigated as a function of donor age in the present dissertation. The data furthermore indicated that equine MSCs from geriatric donors may be more susceptible to cellular senescence, as steady state mRNA changes showed a primary up-regulation in tumor suppressors including p53, p21, and p16 with increasing donor age, which has also been proposed in previous studies leading to decreased proliferation [27,131].

In contrast to the promising age-related expansion findings in chapter 2, the data from chapter 3 showed a sharp decline in chondrogenic and osteogenic potential of BM-MSCs already in pair-wise comparisons between newborn and yearlings. Nevertheless, the chondrogenic potential of newborn BM-MSCs seems very promising for cartilage regeneration, as the chondrogenic markers and proteoglycan matrix were highly up-regulated and the cells showed additional capability to make some lacunae formation and to potentially adjust to hypoxia, which is found in articular cartilage and also documented in fetal cartilage progenitor cells after chondrogenic induction [35]. Even though the chondrogenic performance declined with increasing age, it should be noticed that the

proteoglycan content was significantly higher in chondrogenic pellets from BM-MSCs compared to the negative control (DFs) in all age groups, indicating that some (minimal) chondro-regenerative effect may be maintained. On the other hand, our data showed minimal chondrogenic performance of AT-MSCs *in vitro* in all age groups, which is critical as these cells currently are being used in clinical practice to treat cartilage injuries. Our data strongly indicate that BM-MSCs are superior compared to AT-MSCs for regenerating cartilage injuries with regards to their direct differentiation potential, and that BM-MSCs potentially should be harvested at an early age and stored for later use. These results are important to convey to equine veterinarians to improve the clinical outcome of stem cell therapies in horses, and highlights why it is important for clinical applications to be based on solid research.

Likewise, BM-MSCs in general showed superior osteogenic performance compared to AT-MSCs, but interestingly appeared to be earlier affected by donor age than AT-MSCs. The data thereby indicate that stem cell choice to treat bone injuries in older horses does not matter as much as in young horses. Furthermore, both stem cell types showed higher osteogenic potential than dermal fibroblasts.

Together this shows that even though equine MSCs can be expanded at high rates until late in life, they lose large parts of their chondrogenic and osteogenic differentiation performance earlier in life, which is discouraging for autologous treatments in older horses if the cells are harvested at the time of injury. This information is critical to convey to clinicians as autologous MSC treatment currently is being applied with various success in adult and older horses with cells harvested at the time of injury. The age of the donor and cell choice are hence believed to be critical for the clinical outcome, and can if

wrongly applied explain certain minimal benefits some clinicians complain about, although more *in vivo* studies are required.

Other suggested approaches to be advanced in old horses are instead to harvest and cryopreserve BM-MSCs from when the horse is young, find compatible allogenic MSCs or MSC derived extracellular vesicles from young horses, or to rejuvenate MSCs through molecular manipulations. More research obviously needs to be performed in these areas of which some are suggested in the future studies section below.

Limitations associated with trypsinization, tryphan blue, and cell counting techniques could potentially have affected the accuracy of cell numbers used to make pellets even though 500,000 cells were strongly attempted per pellet. Furthermore, 2D images does not account for the non-circular 3D shape seen in most pellets. Together, this could explain some of the inter-animal variances in pellet size observed within each age group. For future studies, 3D imaging and automated cell counting could be used to try to standardize the procedure even more, but in our experience automated cell counting also has limitations especially when working with cells of different sizes.

Under ideal conditions, the studies would have been performed on paired samples in the same laboratory. This was, however, not feasible due to the degree program, logistical reasons, time and economic constraints, and because some of the cells already were stored in the laboratories. Instead inter-laboratory control cells were applied together with incorporation of laboratory and animal number as factors in the statistical analyses to control for these potential effects.

Power analyses were performed on pilot data from the EdU proliferation assay and from the Alizarin Red S assay. Ideally, power analysis would have been performed on all

assays, but this was not feasible due to the study set up. A sample size of 4 horses per cell type per age group was determined based on the performed power analyses, but it appears that especially the results of the alkaline phosphatase activity assay could have benefitted from a larger sample size as it might be under-powered. That said, the study population used in this study is quite exceptional and spans over more age-groups and tissue types than seen in the majority of existing studies from newborn to geriatric.

4.2 Future studies

As with any other research, answering one question leads to more questions to be investigated. There are multiple ways to expand on the knowledge generated in this dissertation and some priority future study directions will be suggested below.

In the present work, 96 selected gene loci of interest were analyzed for their gene expression as a function of donor age. Full transcriptome analysis will be valuable to identify additional loci affected by donor age and to allow for better pathway and mechanical clustering of the effected genes and their function.

By assessing changes in gene expression as a function of donor age, targets have been identified to potentially improve the cellular proliferation and chondrogenic and osteogenic differentiation capacity of MSCs from older horses through molecular manipulations. In chapter 2, we showed an up-regulation in tumor suppressors in MSCs from geriatric horses, and it would be very interesting to see if the proliferative capacity could be regained by e.g. knocking-down p16, p53, and/or p21 using small interfering RNA (siRNA). As siRNA application *in vitro* is a transient transfection, minimal risk of tumor formation should occur after siRNA is "washed" out [174]. Nevertheless,

additional *in vitro* and *in vivo* studies would need to be conducted to assess potential oncogenic effects of down-regulating tumor suppressors in MSCs *in vitro*.

In support of the decreased proliferation capacity described in chapter 2, it would be valuable to investigate where the cells are located in the cell cycle as a function of donor age. The shown up-regulation in p16, p53, and p21 expression, suggests that a larger proportion of the cells may be arrested in G1, but this remains to be investigated in equine MSCs. Fluorescence-activated cell sorting (FACS) could be used to assess cell cycle location, and would furthermore be able to calculate the amount of apoptotic cells as apoptotic cell's DNA appear degraded on FACS histograms [110]. Knowing the exact cell cycle location of the cells as a function of donor age, would provide more information that could be used for later mechanistic approaches to see if the cell cycle location changes with e.g. siRNA manipulations as described above.

In chapter 2, it was proposed that equine MSCs from geriatric horses may be more susceptible to cellular senescence as described in other species [27,131]. To test this hypothesis in horses, additional passaging studies would need to be performed using MSCs from horses in multiple age groups and to include telomere length and β-galactosidase activity as markers of senescence.

An additional mechanistic approach would be to investigate if any of the gene loci affected by donor age have concurrent changes in DNA methylation patterns, especially in the promotor region. DNA methylation patterns in some genes have been shown to change with aging [102,103]. DNA methylation changes in the promotor region could represent a molecular mechanism for changes in gene expression as a function of donor age [102]. Additionally, Horvath demonstrated an association between DNA methylation

age and cellular proliferation in human BM-MSCs, and suggested that DNA methylation changes may be related to a decline in stem cell function with increasing age [102,175]. Interestingly, epigenetic remodeling has furthermore been shown to rejuvenate cells without affecting the cell fate [176,177]. As such, it would be of great relevance to investigate if this would be a potential area to increase expression of some of the chondrogenic and osteogenic markers down-regulated with increasing donor age, such as ACAN and RUNX2.

In chapter 3, it was enlightening to see how aged BM-MSCs and AT-MSCs showed minimal chondrogenic potential compared to young BM-MSCs under the same experimental conditions. Using the chondrogenic pellets already generated, it would thus be interesting to explore the localization of collagen type II and collagen type I as markers of hyaline- and fibrocartilage in the different cell types and age groups using immunohistochemistry. As the distribution of collagen type II and type I are of great clinical relevance, efforts in the MacLeod laboratory (M.H. Gluck Equine Research Center, University of Kentucky, USA) have previously been made to optimize immunohistochemistry on equine MSC pellets with varying success. Through the continuous development of new antibodies and commercially available kits, this may be more successful in the future. Further studies investigating the stem cells response to oxygen tension would also enhance our understanding of their cell biology, which may be especially relevant for newborn BM-MSCs that presumably showed relatively more adaptation to hypoxia.

All our donor-age related research efforts in horses have so far been conducted in culture, and we thus do not know how MSCs behave *in vivo* as a function of donor age. Based on the high chondrogenic and osteogenic *in vitro* potential of BM-MSCs from newborns, it would be interesting to see if these cells exhibited higher levels of integration and direct differentiation capacity when injected by themselves or in a scaffold into osteoarthritic joints. A study by Dressler *et al.* showed no significant difference in patellar tendon repair when treating 4 year old rabbits with autologous BM-MSCs harvested from the same animals at 1 and 4 years of age. There was, however, a trend towards higher tendon repair when using the young cells harvested at 1 year of age [178]. On the other hand, Rauscher *et al*. showed significantly better healing of atherosclerosis in mice when applying cells from young donors compared to old donors [179]. Similarly, a recent study by Khong *et al*. reported accelerated wound healing when applying allogenic MSCs from young donors [66]. A longitudinal study design similar to the rabbit study by Dressler *et al.* [178] would provide knowledge on potential donor age-related effects in horses and avoid allogenic confounding factors. It would likewise be important to compare the immunomodulatory properties as a function of donor age, together with the paracrine excretion, such as growth factors and cytokines. A study by Siegel *et al.* reported that biological age did not affect human BM-MSCs ability to suppress proliferation of activated allogenic T-cells *in vitro* [130], but this remains to be investigated in horses.

So far, our *in vitro* studies have examined the intrinsic effect of donor age on MSCs, but studies in other species have also shown an important extrinsic effect and that the age of the recipient may affect the outcome [27,105]. Extrinsic age-related effects on MSCs potential could be examined in a cross-sectional study where horses in different

age groups were treated with allogenic young cells to assess the response, or in a longitudinal study where the same animals were treated with autologous cells at various ages to avoid allogenic confounding factors.

Due to the described challenges with autologous and allogenic MSC treatments, extracellular vesicles released from MSCs have been proposed as a new treatment for orthopedic injuries. Extracellular vesicles are nanoscale particles that carry a cargo of signaling molecules from the parent cell and are believed to be responsible for the paracrine effect of MSCs [180]. It would therefore be a very natural step to investigate how donor age affects the cargo of MSC derived extracellular vesicles both *in vitro* and *in vivo* related to joint injuries.

In summary, the results of this dissertation showed that the cellular proliferation and chondrogenic/osteogenic differentiation performance of equine BM- and AT-MSCs declined with increasing donor age following non-linear kinetics. Interestingly, significant differences in the cellular proliferation were only seen in pairwise comparisons involving geriatric horses, and high proliferation rates were observed in MSCs from horses below 18 years of age. On the other hand, a decline in BM-MSCs chondrogenic and osteogenic differentiation performance occurred already in pairwise comparisons between newborn and yearlings, whereas a decline in AT-MSCs osteogenic calcium deposition only occurred in geriatric horses. BM-MSCs from newborns showed high chondrogenic and osteogenic differentiation performance. In contrast, AT-MSCs showed minimal chondrogenic potential in all age groups. This dissertation highlights the importance of donor age considerations and MSC tissue type selection for autologous

treatment of orthopedic injuries. Understanding the effect of donor age on equine MSCs has the potential to optimize autologous stem cell therapies of cartilage and bone injuries in horses, and will help advice owners on when to harvest and potentially cryopreserve the cells.

APPENDIX 1. Sample information for RT-qPCR

Sample-ID	Final concentration of cDNA (ng/uL)	260/280	260/230	RIN value
PELLETS				
BM-EQF1701-P	13,90	1,91	2,17	8,60
BM-EQF1703-P	13,90	1,97	2,15	9,00
BM-EQF1704-P	13,90	2,01	2,24	7,70
BM-EQF1705-P	13,90	1,99	1,95	9,00
BM-EQA1504-P	13,90	1,97	2,13	9,10
BM-EQA1505-P	13,90	1,70	1,98	8,60
BM-EQA1506-P	13,90	1,89	2,02	8,90
BM-EQA1507-P	13,90	2,03	2,11	8,00
BM-0115-P	13,90	1,94	1,82	8,00
BM-1607-P	13,90	1,94	2,09	9,20
BM-1608-P	13,90	1,98	2,21	7,50
BM-V1807-P	13,90	1,94	1,89	8,00
BM-1606-P	13,90	1,89	2,02	9,20
BM-1116-P	13,90	1,88	2,15	9,30
BM-S1702-P	13,90	1,85	1,98	8,00
BM-S1703-P	13,90	2,06	1,92	9,00
BM-G1801-P	13,90	1,75	2,20	8,20
BM-G1802-P	13,90	1,80	2,03	8,50
BM-0314-P	13,90	1,83	1,97	9,00
BM-G1609-P	13,90	1,86	2,03	8,20
AT-EQF1701-P	13,90	2,06	2,07	8,60
AT-EQF1703-P	13,90	1,87	2,21	8,00
AT-EQF1704-P	13,90	1,94	2,03	8,10
AT-EQF1705-P	13,90	1,76	1,87	8,10
AT-EQA1504-P	13,90	1,97	2,13	8,40
AT-EQA1505-P	13,90	1,98	2,13	9,40
AT-EQA1508-P	13,90	2,10	1,98	8,70
AT-EQA1509-P	13,90	1,98	2,06	9,30
AT-1607-P	13,90	1,94	2,06	8,00
AT-1608-P	13,90	1,93	2,19	8,30
AT-V1807-P	13,90	1,85	2,21	8,30
AT-0115-P	13,90	1,96	2,14	9,40
AT-1606-P	13,90	1,93	2,16	9,00

AT-0315-P	13,90	1,99	2,11	9,30
AT-0415-P	13,90	2,00	2,09	9,10
AT-0916-P	13,90	1,96	2,12	9,00
AT-0314-P	13,90	1,89	2,10	8,30
AT-G1609-P	13,90	1,92	2,13	8,90
AT-G1801-P	13,90	1,97	1,83	8,50
AT-G1802-P	13,90	1,86	2,07	8,70
DF-EQF1703-P	13,90	2,05	2,24	7,50
DF-EQF1704-P	13,90	1,83	2,22	9,80
DF-EQF1701-P	13,90	1,90	2,10	9,50
DF-EQF1705-P	13,90	2,00	2,05	8,90
DF-EQA1504-P	13,90	1,98	2,08	9,90
DF-EQA1505-P	13,90	1,84	2,06	7,90
DF-EQA1507-P	13,90	1,85	2,00	8,50
DF-EQA1508-P	13,90	1,98	2,03	8,90
DF-V1804-P	13,90	2,00	2,06	9,10
DF-V1805-P	13,90	2,00	2,13	8,40
DF-V1806-P	13,90	1,90	2,01	9,00
DF-V1807-P	13,90	1,92	2,08	9,10
DF-S1703-P	13,90	1,94	2,23	8,90
DF-S1702-P	13,90	1,90	1,99	8,70
DF-S1705-P	13,90	1,92	1,94	8,30
DF-S1704-P	13,90	1,87	2,00	9,00
DF-G1801-P	13,90	1,90	2,20	8,00
DF-G1802-P	13,90	2,07	1,84	8,90
DF-G1609-P	13,90	2,07	2,18	8,80
DF-G1610-P	13,90	1,99	2,18	8,60
T75 monolayer cells				
BM-EQF1701-CHM	13,90	2,03	2,06	8,60
BM-EQF1703-CHM	13,90	2,04	1,95	9,00
BM-EQF1704-CHM	13,90	2,10	2,12	8,90
BM-EQF1705-CHM	13,90	2,06	2,00	9,10
BM-EQA1504-CHM	13,90	2,03	1,96	9,10
BM-EQA1505-CHM	13,90	2,02	2,07	9,00
BM-EQA1506-CHM	13,90	2,09	2,19	8,90
BM-EQA1507-CHM	13,90	2,01	2,13	10,00
BM-0115-CHM	13,90	2,00	1,94	9,10
BM-1607-CHM	13,90	2,01	2,04	9,40
BM-1608-CHM	13,90	2,02	2,06	9,10
BM-V1807-CHM	13,90	1,93	2,08	9,60
BM-1606-CHM	13,90	2,01	2,16	9,80
BM-1116-CHM	13,90	2,24	1,83	8,00
BM-S1702-CHM	13,90	2,03	2,12	8,90

BM-S1703-CHM	13,90	2,08	2,04	8,70
BM-G1801-CHM	13,90	1,99	2,15	8,50
BM-G1802-CHM	13,90	2,04	1,98	9,00
BM-0314-CHM	13,90	2,02	1,84	8,90
BM-G1609-CHM	13,90	2,02	2,09	9,00
AT-EQF1701-CHM	13,90	2,07	2,10	9,00
AT-EQF1703-CHM	13,90	2,02	2,01	10,00
AT-EQF1704-CHM	13,90	2,00	2,08	9,80
AT-EQF1705-CHM	13,90	2,05	2,08	8,80
AT-EQA1504-CHM	13,90	2,06	2,14	9,10
AT-EQA1505-CHM	10,00	2,20	1,56	7,50
AT-EQA1508-CHM	13,90	2,04	2,11	9,00
AT-EQA1509-CHM	13,90	2,08	2,10	9,20
AT-1607-CHM	13,90	1,99	2,06	9,80
AT-1608-CHM	13,90	1,98	1,98	9,00
AT-V1807-CHM	13,90	2,02	2,00	9,30
AT-0115-CHM	13,90	2,01	2,03	9,10
AT-1606-CHM	13,90	2,05	1,99	9,00
AT-0315-CHM	13,90	2,04	2,00	9,00
AT-0415-CHM	13,90	2,00	1,93	9,30
AT-0916-CHM	13,90	2,03	2,04	9,60
AT-0314-CHM	13,90	2,02	2,02	8,80
AT-G1609-CHM	13,90	2,02	2,07	9,10
AT-G1801-CHM	13,90	2,06	2,00	9,00
AT-G1802-CHM	13,90	2,10	2,28	8,90
DF-EQF1701-CHM	13,90	2,00	2,11	9,00
DF-EQF1703-CHM	13,90	2,02	2,02	9,70
DF-EQF1704-CHM	13,90	2,05	2,17	9,50
DF-EQF1705-CHM	13,90	1,99	2,10	9,20
DF-EQA1504-CHM	13,90	2,01	2,05	9,80
DF-EQA1505-CHM	13,90	2,04	1,82	8,80
DF-EQA1507-CHM	13,90	2,05	2,10	9,00
DF-EQA1508-CHM	13,90	2,00	2,03	8,90
DF-V1804-CHM	13,90	2,03	2,11	9,40
DF-V1805-CHM	13,90	2,02	2,01	9,50
DF-V1806-CHM	13,90	1,98	2,04	9,20
DF-V1807-CHM	13,90	2,01	2,10	9,50
DF-S1702-CHM	13,90	1,97	2,00	8,90
DF-S1703-CHM	13,90	2,07	2,05	9,30
DF-S1705-CHM	13,90	1,98	2,05	9,60
DF-S1704-CHM	13,90	2,00	2,06	9,20
DF-G1801-CHM	13,90	2,00	2,02	9,70
DF-G1802-CHM	13,90	2,05	1,80	9,00

DF-G1609-CHM	13,90	2,10	2,08	10,00
DF-G1610-CHM	13,90	2,08	1,86	9,60
Osteogenic DAY 0 (O=osteogenic, 0=day 0, B=non-induced control)				
BM-EQF1701-O0B	13,90	1,97	1,83	9,00
BM-EQF1703-O0B	13,90	2,02	1,80	9,00
BM-EQF1704-O0B	13,90	2,08	2,15	9,30
BM-EQF1705-O0B	13,90	1,99	2,08	9,20
BM-EQA1504-O0B	13,90	2,01	1,87	9,40
BM-EQA1505-O0B	13,90	2,10	2,13	9,10
BM-EQA1506-O0B	13,90	2,08	2,22	9,30
BM-EQA1507-O0B	13,90	2,09	2,13	9,50
BM-0115-O0B	13,90	2,02	2,09	9,20
BM-1607-O0B	13,90	1,96	2,17	9,20
BM-1608-O0B	13,90	1,99	2,00	9,50
BM-V1807-O0B	13,90	2,00	2,03	9,10
BM-1606-O0B	13,90	2,05	2,04	9,00
BM-1116-O0B	13,90	2,07	1,86	8,90
BM-S1702-O0B	13,90	1,90	1,95	9,10
BM-S1703-O0B	13,90	2,08	2,02	9,40
BM-G1801-O0B	13,90	2,09	1,81	8,20
BM-G1802-O0B	13,90	2,06	1,96	9,00
BM-0314-O0B	13,90	2,05	1,88	8,90
BM-G1609-O0B	13,90	2,03	2,15	9,10
AT-EQF1701-O0B	13,90	2,08	1,97	9,00
AT-EQF1703-O0B	13,90	2,01	1,84	9,00
AT-EQF1704-O0B	13,90	2,04	2,05	9,50
AT-EQF1705-O0B	13,90	1,75	1,87	7,90
AT-EQA1504-O0B	13,90	1,98	1,80	8,90
AT-EQA1505-O0B	13,90	2,06	1,87	8,50
AT-EQA1508-O0B	13,90	2,08	2,09	9,30
AT-EQA1509-O0B	13,90	2,05	2,10	9,80
AT-1607-O0B	13,90	2,04	2,07	9,00
AT-1608-O0B	13,90	2,00	1,99	9,00
AT-V1807-O0B	13,90	2,02	2,11	8,90
AT-0115-O0B	13,90	2,00	1,87	8,80
AT-1606-O0B	13,90	2,05	2,08	8,90
AT-0315-O0B	13,90	2,01	1,86	9,00
AT-0415-O0B	13,90	2,03	2,04	9,60
AT-0916-O0B	13,90	2,03	2,08	9,00
AT-0314-O0B	13,90	1,97	2,08	8,70
AT-G1609-O0B	13,90	2,00	1,99	9,30
AT-G1801-O0B	13,90	1,87	1,89	8,50
AT-G1802-O0B	13,90	2,11	1,85	8,00

DF-EQF1703-O0B	13,90	1,94	1,80	8,90
DF-EQF1704-O0B	13,90	1,98	1,80	9,00
DF-EQF1705-O0B	13,90	2,05	1,88	8,90
DF-EQA1504-O0B	13,90	2,02	1,80	9,00
DF-EQA1505-O0B	13,90	2,00	1,87	9,10
DF-EQA1507-O0B	13,90	2,03	2,08	9,00
DF-EQA1508-O0B	13,90	1,99	2,05	8,90
DF-V1804-O0B	13,90	2,01	2,12	9,20
DF-V1805-O0B	13,90	2,05	2,01	9,00
DF-V1806-O0B	13,90	1,98	2,00	9,10
DF-V1807-O0B	13,90	2,00	2,01	9,50
DF-S1703-O0B	13,90	1,70	1,92	7,90
DF-S1704-O0B	13,90	1,97	2,08	8,70
DF-S1705-O0B	13,90	2,01	1,87	8,90
DF-G1609-O0B	13,90	1,98	2,03	8,90
DF-G1610-O0B	13,90	1,99	2,00	9,00
DF-G1801-O0B	13,90	2,01	1,87	9,20
DF-G1802-O0B	13,90	1,97	1,89	9,40
Osteogenic day 21 (O=osteogenic, 21=day 21, A=induced, B=non-induced control)				
BM-EQF1701-O21A	13,90	2,00	1,98	8,80
BM-EQF1701-O21B	13,90	2,01	2,02	8,90
BM-EQF1703-O21A	13,90	1,93	1,85	9,00
BM-EQF1703-O21B	13,90	1,84	1,84	8,20
BM-EQF1704-O21A	13,90	1,88	1,88	8,70
BM-EQF1704-O21B	13,90	2,03	2,10	9,40
BM-EQF1705-O21A	13,90	1,96	1,89	9,00
BM-EQF1705-O21B	13,90	2,03	1,81	9,00
BM-EQA1504-O21A	13,90	1,99	1,81	9,10
BM-EQA1504-O21B	13,90	2,02	1,80	9,40
BM-EQA1505-O21A	13,90	2,08	1,88	7,50
BM-EQA1505-O21B	13,90	2,01	2,14	9,50
BM-EQA1506-O21A	13,90	1,77	1,94	8,80
BM-EQA1506-O21B	13,90	1,96	2,08	9,50
BM-EQA1507-O21A	13,90	2,01	1,80	9,50
BM-EQA1507-O21B	13,90	2,01	2,12	9,70
BM-0115-O21A	13,90	1,80	1,80	8,80
BM-0115-O21B	13,90	2,01	2,06	9,00
BM-1607-O21A	13,90	1,99	1,88	9,30
BM-1607-O21B	13,90	2,00	2,11	9,50
BM-1608-O21A	13,90	1,98	2,08	9,10
BM-1608-O21B	13,90	2,08	1,83	8,80
BM-V1807-O21A	13,90	1,70	1,80	8,30
BM-V1807-O21B	13,90	2,03	2,09	9,20

BM-1606-O21A	13,90	1,94	1,84	8,90
BM-1606-O21B	13,90	1,99	1,87	9,30
BM-1116-O21A	10,00	1,59	1,46	7,40
BM-1116-O21B	13,90	2,06	1,86	9,20
BM-S1702-O21A	13,90	2,09	2,06	9,20
BM-S1702-O21B	13,90	2,05	2,04	9,00
BM-S1703-O21A	13,90	2,07	1,83	7,70
BM-S1703-O21B	13,90	2,07	1,95	9,40
BM-G1801-O21A	13,90	2,10	2,03	9,10
BM-G1801-O21B	13,90	1,97	1,89	8,90
BM-G1802-O21A	13,90	1,91	1,94	9,00
BM-G1802-O21B	13,90	2,04	1,90	9,00
BM-0314-O21A	10,00	2,30	1,55	7,60
BM-0314-O21B	13,90	2,01	1,88	8,70
BM-G1609-O21A	13,90	1,97	1,83	7,90
BM-G1609-O21B	13,90	2,07	1,98	9,00
AT-EQF1701-O21A	13,90	2,04	2,17	9,10
AT-EQF1701-O21B	13,90	2,03	2,15	9,80
AT-EQF1703-O21A	13,90	1,98	2,04	9,50
AT-EQF1703-O21B	13,90	1,85	1,80	8,90
AT-EQF1704-O21A	13,90	1,95	1,95	9,00
AT-EQF1704-O21B	13,90	1,93	1,80	8,60
AT-EQF1705-O21A	13,90	1,94	1,89	9,50
AT-EQF1705-O21B	13,90	2,03	1,88	8,00
AT-EQA1504-O21A	13,90	1,97	1,84	8,50
AT-EQA1504-O21B	13,90	1,98	1,80	8,60
AT-EQA1505-O21A	13,90	2,04	1,88	9,00
AT-EQA1505-O21B	13,90	1,97	1,82	8,90
AT-EQA1508-O21A	13,90	1,98	2,06	9,60
AT-EQA1508-O21B	13,90	2,07	2,13	9,20
AT-EQA1509-O21A	13,90	2,05	2,19	9,20
AT-EQA1509-O21B	13,90	2,05	2,09	9,00
AT-1607-O21A	13,90	1,96	2,15	9,10
AT-1607-O21B	13,90	2,02	2,11	9,50
AT-1608-O21A	13,90	2,03	2,13	9,40
AT-1608-O21B	13,90	2,02	2,10	9,10
AT-V1807-O21A	13,90	1,98	2,18	8,70
AT-V1807-O21B	13,90	1,98	2,13	9,40
AT-0115-O21A	13,90	1,99	2,09	9,10
AT-0115-O21B	13,90	2,05	1,98	9,00
AT-1606-O21A	13,90	2,03	2,13	8,70
AT-1606-O21B	13,90	1,99	2,07	9,00
AT-0315-O21A	13,90	1,89	1,99	8,60

AT-0315-O21B	13,90	2,01	1,92	9,00
AT-0415-O21A	13,90	2,08	2,05	8,80
AT-0415-O21B	13,90	2,01	1,89	9,00
AT-0916-O21A	13,90	1,98	1,86	9,10
AT-0314-O21A	13,90	2,00	2,08	8,60
AT-0314-O21B	13,90	1,95	1,80	9,00
AT-G1609-O21A	13,90	1,96	1,95	9,20
AT-G1609-O21B	13,90	1,97	1,81	8,70
AT-G1801-O21A	13,90	2,19	1,85	8,10
AT-G1801-O21B	13,90	2,10	1,93	8,60
AT-G1802-O21A	13,90	1,96	1,97	8,90
AT-G1802-O21B	13,90	2,02	1,82	8,30
DF-EQF1701-O21A	13,90	2,02	2,11	9,50
DF-EQF1701-O21B	13,90	2,03	2,13	9,40
DF-EQF1703-O21A	13,90	2,06	2,11	9,00
DF-EQF1703-O21B	13,90	2,01	1,82	9,10
DF-EQF1704-O21A	13,90	1,99	2,05	8,30
DF-EQF1704-O21B	13,90	2,00	2,10	8,50
DF-EQA1504-O21A	13,90	2,04	2,12	8,60
DF-EQA1504-O21B	13,90	2,08	1,88	8,40
DF-EQA1505-O21A	13,90	2,01	1,86	9,00
DF-EQA1505-O21B	13,90	2,10	1,83	9,20
DF-EQA1507-O21A	13,90	1,96	1,99	9,20
DF-EQA1507-O21B	13,90	1,97	1,88	8,70
DF-V1804-O21A	13,90	1,95	2,08	8,40
DF-V1804-O21B	13,90	2,01	1,99	7,90
DF-V1805-O21A	13,90	1,95	2,00	8,40
DF-V1805-O21B	13,90	2,04	2,01	8,60
DF-V1807-O21A	13,90	1,94	2,04	8,90
DF-V1807-O21B	13,90	2,01	2,11	9,00
DF-S1702-O21A	13,90	1,99	2,10	8,60
DF-S1702-O21B	13,90	2,01	1,92	8,40
DF-S1703-O21A	13,90	1,96	1,88	8,50
DF-S1703-O21B	13,90	1,99	1,84	8,70
DF-S1705-O21A	13,90	2,08	1,83	8,00
DF-S1705-O21B	13,90	2,07	1,88	9,20
DF-G1609-O21A	13,90	2,01	1,86	8,70
DF-G1610-O21B	13,90	2,10	1,89	8,90
DF-G1801-O21A	13,90	2,02	1,87	8,50
DF-G1801-O21B	13,90	2,03	1,82	8,50
DF-G1802-O21A	13,90	2,00	1,82	8,70
DF-G1802-O21B	13,90	2,05	1,81	9,00

APPENDIX 2. Gene list and annotation for primer-probe sets used for RT-qPCR

Gene ID	Annotation
ABI3BP	Decrease proliferation. Necessary for the switch from proliferation to differentiation in MSCs
ACAN	Proteoglycan found in articular cartilage - withstands compression
ALPL	Early marker of osteogenesis – high levels in bone (osteoblasts), bone mineralization
AQP1	Involved in chondrocyte proliferation, migration and adhesion
AREG	EGF family member. Has mitogenic effect on several cell types including epithelial cells, fibroblasts and immune cells
BARD1	Forms a heterodimer with BRCA1, which phosphorylate and stabilize p53. p53 is a transcription factor for p21, which leads to cellular arrest
BAX	Pro-apoptotic gene – belongs to the BCL2 protein family
BCL2	Anti-apoptotic. Expression affected by donor age in BM-MSCs [66]
BGN	Belongs to the leucine-rich repeat protein family. Binds to collagen fibrils. Plays a role in skeletal bone growth and remodeling
BMP2	Induces cartilage and bone formation – activates osteoblast differentiation
BMP3	Increases MSC proliferation while inducing osteogenesis
BMP4	Involved in cartilage and bone formation, specifically limb development and fracture repair. Involved in bone mineralization
BMP6	Induce the growth of bone and cartilage. Able to induce osteogenic markers in MSCs
BMP7	Plays a role in bone development. Induces ectopic bone formation and promote fracture healing
BRCA1	Up-regulate p21 and induce G1/S arrest
CASP3	Cell apoptosis
CASP8	Cell apoptosis - DNA hypermethylation is found with aging [103]
CAVIN1	Found in osteoblasts. Helps to form caveolea. Stops cell division in older cells (induce senescence)
CCND1	Cyclin 1 forms a complex with and functions as a regulatory subunit of CDK4 or CDK6, whose activity is required for cell cycle G1/S transition. Expression affected by donor age in BM-MSCs [66]
CDKN1A	Induce G1/S arrest. Increased level in senescent cells [27]
CHADL	Glycosaminoglycan. Cartilage matrix protein that mediate adhesion of chondrocytes. Promotes attachment of chondrocytes, osteoblasts, and fibroblasts
CLU	Anti-apoptotic. Inhibits BAX and p53 activation. Involved in several basic events such as cell death, tumor progression, and neurodegenerative disorders
COL1A1	Major protein component of the bone extracellular matrix and in fibrocartilage
COL2A1	Specific marker of articular cartilage
COL4A1	Extracellular glycoprotein essential in cartilage
COL5A3	Encodes an alpha chain for low abundance fibrillar collagens
COL9A2	A fibril associated collagen, that associates with COL2 and COL11 in articular cartilage (together it makes the inter-territorial matrix of AC) [4]
COL11A1	Key component of articular cartilage. Heterodimer, which forms fibrils in association with type II collagen in articular cartilage [4]. Essential for normal bone mineralization
COL12A1	Homotrimer found in association with COL1
COMP	A non-collagenous extracellular matrix protein, found in the extracellular matrix of cartilage, believed to play an important role in proliferation and apoptosis. Promotes

	proliferation by activating the Akt pathway
CRTAC1	Secreted by articular chondrocytes
CRYAB	Significantly increased in osteogenic differentiated human bone marrow MSCs in vitro
CSF2	The protein encoded by this gene is a cytokine that controls the production, differentiation, and function of hematopoietic progenitors. Affected by cellular senescence
CTGF	Promotes the proliferation and differentiation of articular chondrocytes
CTNNB1	Regulate cell growth and adhesion between cells. Expression in BM-MSCs affected by donor age [66]
DCN	Osteoprogenitor marker. A member of the small leucine-rich proteoglycan family
DMP1	Produced by osteoblasts and is found both intracellularly and extracellularly. Following osteoblast activation, DMP-1 undergoes Ca2+ mediated phosphorylation, which induces its secretion into the ECM, where it participates in mineralized bone matrix formation
EBF2	Play an important role in in a variety of developmental processes. Mouse studies suggest that this gene may be involved in osteoblast differentiation
EPGN	Ligand for the epidermal growth factor receptor and play a role in cell survival, proliferation and migration. High mitogenic activity but low affinity for its receptor
FGF1	Mitogenic and cell survical activity
FGF5	Broad mitogenic and cell survival activity
FGF18	Growth factor. Important role in cell proliferation, differentiation and migration. Required for normal ossification and bone development, and enhances chondrogenesis
FGFR3	Highly expressed in chondrocytes, negative regulator of bone growth
FN1	Encodes a glycoprotein found in the extracellular matrix. Binds to integrins (membrane spaning receptor proteins), and other extracellular matrix molecules such as collagen, fibrin and heparan sulfate proteoglycans
GDF6	This gene encodes a secreted ligand of the TGF-beta (transforming growth factor-beta) superfamily of proteins. Ligands of this family bind various TGF-beta receptors leading to recruitment and activation of SMAD family transcription factors that regulate gene expression. The encoded pre-protein is proteolytically processed to generate each subunit of the disulfide-linked homodimer. This protein is required for normal formation of some bones and joints in the limbs, skull, and axial skeleton
GLB1	Senescent marker. Overexpression and accumulation of endogenous lysosomal beta-galactosidase is seen specifically in senescent cells [154]
GLI3	Transcription factor. Controls chondrocyte proliferation and maturation
HAPLN1	Stabilizes the aggregates of proteoglycan monomers (primarily aggrecan) with hyaluronic acid in the extracellular cartilage matrix
HDGF	Mitogenic and DNA-binding activity
HGF	Regulate cell growth, cell motility and morphogenesis in numerous cell and tissue types. Secreted by mesenchymal cells. May also play a role in tissue regeneration
IBSP	Major structural protein of bone matrix, synthesized by osteoblasts
IGF1	Potent mitogen for a multitude of cells including neural progenitor-like cells and hair follicle cells. Acts as a regulator of bone growth and development. Anabolic growth factor for articular cartilage, expressed in growth plate chondrocytes. Can induce chondrogenesis in vitro. DNA methylation pattern affected by biological age [103]
IGFBP5	IGF-binding proteins
LOC100146270	Cell cycle regulator. Works in the p16/RB pathway. Biomarker of cellular senescence. Stops cell division in older cells. Increased in Senescent cells. DNA methylated [103]
LOC100146589	Secreted solely by osteoblasts, essential for mineralization of bone, binds to calcium
MATN1	Mainly expressed in cartilage. Cartilage matrix protein. Defects in Matrilin-1 leads to e.g. early onset osteoarthritis and other cartilage diseases

MEPE	Expressed in bone, where it regulates the mineralization. Secreted by osteoblasts
MET	A member of the receptor tyrosine kinase family that transduces signals from the extracellular matrix into the cytoplasm by binding to hepatocyte growth factor/HGF ligand. Regulates many physiological processes including proliferation, differentiation, scattering, morphogenesis and survival
MIA	Marker for chondrocyte differentiation. Found in equine cartilage and chondrocytes.
MMP3	Chondrogenic marker. Involved in break-down of extra cellular matrix in normal tissue remodeling and in diseases like arthtitis. MMP3 gene encodes an enzyme that degrades fibronectin, laminin, collagen III, IV, IX, X, and cartilage proteoglycans
MMP13	Chondrogenic marker
MYC	A master regulator of cellular growth regulation. C-Myc overexpression result in coordinated changes in level of expression of gene families which result in increased cellular proliferation
NODAL	Member of the TGF-Beta superfamily. Essential for mesoderm formation and subsequent organization of axial structures in early embryonic development
OMD	Implicated in biomineralization processes
PCNA	Cofactor of DNA polymerase delta. The encoded protein acts as a homotrimer and helps increase the processivity of leading strand synthesis during DNA replication
PDGFD	Mitogenic factor for cells of mesenchymal origin
PHB	Evolutionary conserved. Plays a role in senescence and tumor suppression. Anti-proliferative activity is localized to the 3' UTR region. Inhibits DNA synthesis
PHEX	A transmembrane endopeptidase that belongs to the type II integral membrane zinc-dependent endopeptidase family. Involved in bone mineralization
PTCH2	A tumor suppressor in the hedgehog signaling pathway
RUNX2	Early marker of osteogenesis – transcription factor, master switch for activation of osteoblasts
RUNX3	Tumor suppressor – member of the runt domain-containing family of transcription factors associated with BMP and TGF-beta pathways
S100A1	S100 proteins are localized in the cytoplasm and/or nucleus of a wide range of cells, and involved in the regulation of a number of cellular processes such as cell cycle progression and differentiation; Probably acts as a Ca(2+) signal transducer. Inhibits microtubule assembly
SMOC1	Plays a critical role in limb development. Found in the basement membranes. Help anchor cells to one another during embryonic development. Modulates growth factors that stimulate growth and development of tissues, especially skeletal formation. SMOC-1 protein promotes the maturation (differentiation) of osteoblasts
SMPD3	Participates in bone mineralization
SNAI2	A transcription factor; acts as a transcriptional repressor that binds to E-box motifs and is also likely to repress E-cadherin transcription; involved in EMT; has anti-apoptotic activity
SOST	Regulator of bone homeostasis. Expressed by terminally differentiated osteocytes and hypertrophic chondrocytes. Expression is induced by BMP-2, 4 and 6. Inhibited by PTH. SOST binds to BMP-2, 4 and 6 and inhibits the osteogenic differentiation induced by BMPs. SOST reduces the proliferation of MSCs and induce MSC apoptosis
SOX5	Chondrogenic marker. Essential for chondrocyte differentiation and hence cartilage formation
SOX9	Early chondrogenic marker
SP7	Later osteogenesis marker – bone specific transcription factor, required for osteoblast differentiation and bone formation
SPARC	Glycoprotein in bone, binds calcium, secreted by osteoblasts during bone formation, initiating bone mineralization – affinity for collagen type 1 and calcium

SPP1	Extracellular structural protein in bone, a linking protein, binds calcium
TBX3	Transcriptional repressor involved in developmental processes (anterior/posterior limb pattern formation). Acts as a negative regulator of PML function in cellular senescence
TERT	Catalytic subunit of teleomerase, implicated in aging and cancer. Less expression with increasing donor age and senescence. DNA methylation affected in chronological aging [102]
TGFA	Binds to the epidermal growth factor receptor, which activates a signaling pathway for cell proliferation, differentiation, and development. Expression affected by donor age in BM-MSCs [66]
TGFB1	Regulate cell activities including proliferation, differentiation, motility and apoptosis. Highly abundant in tissues that make up the skeleton, where it regulate the formation and growth of bone and cartilage. Prevent tumor growth
TGFB2	Regulate proliferation, differentiation, adhesion, migration
TGFB3	Controls the growth and proliferation of cells, differentiation, motility, and apoptosis. Keeps cells from growing and dividing too rapidly, can suppress tumor formation. Involved in regulation of bone growth and in vitro chondrogenic induction of MSCs. Increase proliferation of MSCs, while inducing chondrogenesis
TIMP2	Inhibits matrix metalloproteinases, and hence prevent degradation of extracellular matrix. Suppresses proliferation of endothelial cells
TNF	Pro-apoptotic. Involved in apoptosis, proliferation, differentiation, lipid metabolism and coagulation. Expression in BM-MSCs affected by donor age [66]. DNA hypomethylated in promotor with increasing age [103]
TNFRSF11B	Also known as osteoclastgenesis inhibitory factor. Expressed in osteoblasts. Plays a role in regulating bone density and as a decoy receptor for RANKL - hence inhibits osteoclastgenesis and bone resorption
TNFSF11	induces osteoclastgenesis by activating multiple signaling pathways in osteoclast precursor cells
TP53	Tumor suppressor. Transcription factor for p21. Induce cell cycle arrest - DNA repair or apoptosis. Increased level in senescent cells and in aged BM-MSCs [66]
VEGFA	Growth factor which induces proliferation and migration of vascular endothelial cells. Member of the PDGF/VEGF growth factor family
B2M	Encodes a serum protein found in association with MHC class I on the surface of nearly all nucleated cells
GUSB	Encodes a hydrolase that degrades glycosaminoclycans. The enzyme forms a hemotetramer that is localized to the lysosome
RPLP0	Encodes a ribosomal protein component of the 60S subunit
	*NIH, Genetics Home Reference (https://ghr.nlm.nih.gov/gene/)

REFERENCES

1. Dyson, P.K., Jackson, B.F., Pfeiffer, D.U. and Price, J.S. (2008) Days lost from training by two- and three-year-old Thoroughbred horses: A survey of seven UK training yards. *Equine Vet. J.* **40**, 650–657.
2. Murray, R.C., Walters, J.M., Snart, H., Dyson, S.J. and Parkin, T.D.H. (2010) Identification of risk factors for lameness in dressage horses. *Vet. J.* **184**, 27–36. http://dx.doi.org/10.1016/j.tvjl.2009.03.020.
3. Cruz, A.M. and Hurtig, M.B. (2008) Multiple Pathways to Osteoarthritis and Articular Fractures : Is Subchondral Bone the Culprit ? *Vet. Clin. Equine Pract.* **24**, 101–116.
4. Fox, A.J.S., Bedi, A. and Rodeo, S.A. (2009) The Basic Science of Articular Cartilage: Structure, Composition, and Function. *Sport. Heal. Orthop.* **1**, 461–468.
5. Frisbie, D.D., Auer, J.A. and Stick, J. (2006) Principles of Treatment of Joint Disease. In: *Equine Surgery*. pp 1055–1073.
6. Goldring, S.R. and Goldring, M.B. (2016) Changes in the osteochondral unit during osteoarthritis: structure, function and cartilage-bone crosstalk. *Nat. Rev. Rheumatol.* **12**, 632–644.
7. Ganguly, P., El-Jawhari, J.J., Giannoudis, P. V., Burska, A.N., Ponchel, F. and Jones, E.A. (2017) Age-related Changes in Bone Marrow Mesenchymal Stromal Cells: A Potential Impact on Osteoporosis and Osteoarthritis Development. *Cell Transplant.* **26**, 1520–1529.
8. Scanzello, C.R. (2017) Role of low-grade inflammation in osteoarthritis. *Curr Opin Rheumatol* **29**, 79–85.
9. Kawcak, C.E., McIlwraith, C.W., Norrdin, R.W., Park, R.D. and James, S.P. (2001) The role of subchondral bone in joint disease : a review. *Equine Vet. J.* **33**, 120–126.
10. Hassan, E.B., Mirams, M., Mackie, E.J. and Whitton, R.C. (2016) Role of subchondral bone remodelling in collapse of the articular surface of Thoroughbred racehorses with palmar osteochondral disease. *Equine Vet. J.* **48**, 228–233.
11. Kim, M., Kim, C., Choi, Y.S., Kim, M., Park, C. and Suh, Y. (2012) Age-realted alterations in mesenchymal stem cells related to shift in differentiation from osteogenic to adipogenic potential: implication to age-associated bone diseases and defects. *Mech. Ageing Dev.* **133**, 215–25.
12. Loeser, R.F. (2009) Aging an osteoarthritis: the role of chondrocyte senescence and aging changes in the cartilage matrix. *Osteoarthr. Cartil.* **17**, 971–979.
13. Goodrich, L. and Nixon, A. (2006) Medical treatment of osteoarthritis in the horse - A review. *Vet. J.* **171**, 51–69.
14. Caron, J.P. and Genovese, R.L. (2003) Principles and Practices of Joint Disease Treatment. In: *Diagnosis and Management of Lameness in The Horse*, 1st ed., Eds: M.W. Ross and S.J. Dyson, Saunders Elsevier Science. pp 746–764.
15. Mienaltowski, M.J., Huang, L., Frisbie, D.D., Mcilwraith, C.W., Stromberg, A.J., Bathke, A.C. and Macleod, J.N. (2009) Transcriptional profiling differences for articular cartilage and repair tissue in equine joint surface lesions. *BMC Med. Genomics* **2**, 1–14.
16. Clar, C., Cummins, E., Mcintyre, L., Thomas, S., Lamb, J., Bain, L., Jobanputra,

P. and Waugh, N. (2005) Autologous chondrocyte implantation for cartilage defects in knee joints. *Health Technol. Assess. (Rockv).* **9**.
17. Zayed, M., Adair, S., Ursini, T., Schumacher, J. and Misk, N. (2018) Concepts and challenges in the use of mesenchymal stem cells as a treatment for cartilage damage in the horse. *Res. Vet. Sci.* **118**, 317–323. https://doi.org/10.1016/j.rvsc.2018.03.011.
18. McIlwraith, C.W., Frisbie, D.D., Rodkey, W.G., Kisiday, J.D., Werpy, N.M., Kawcak, C.E. and Steadman, J.R. (2011) Evaluation of Intra-Articular Mesenchymal Stem Cells to Augment Healing of Microfractured Chondral Defects. *Athroscopy J. Arthrosc. Relat. Surg.* **27**, 1552–1561. http://dx.doi.org/10.1016/j.arthro.2011.06.002.
19. Demoor, M., Ollitrault, D., Gomez-leduc, T., Bouyoucef, M., Hervieu, M., Fabre, H., Lafont, J., Denoix, J., Audigié, F., Mallein-gerin, F., Legendre, F. and Galera, P. (2014) Cartilage tissue engineering : Molecular control of chondrocyte differentiation for proper cartilage matrix reconstruction. *Biochim. Biophys. Acta* **1840**, 2414–2440. http://dx.doi.org/10.1016/j.bbagen.2014.02.030.
20. Wernecke, C., Braun, H.J. and Dragoo, J.L. (2015) The Effect of Intra-articular Corticosteroids on Articular Cartilage. *Orthop. J. Sport. Med.* **3**.
21. Pfeiffenberger, M., Bartsch, J., Hoff, P., Ponomarev, I., Buttgereit, F., Gaber, T., Barnewitz, D., Tho, C. and Id, A.L. (2019) Hypoxia and mesenchymal stromal cells as key drivers of initial fracture healing in an equine in vitro fracture hematoma model. *PLoS One* **April**, 1–20.
22. Frisbie, D.D. and Smith, R.K.W. (2010) Clinical update on the use of mesenchymal stem cells in equine orthopaedics. *Equine Vet. J.* **42**, 86–89.
23. Agung, M., Ochi, M., Yanada, S., N., A., Izuta, Y., Yamasaki, T. and Toda, K. (2006) Mobilization of bone marrow-derived mesenchymal stem cells into the injured tissues after intraarticular injection and their contribution to tissue regeneration. *Knee Surg Sport. Traumatol Arthrosc* **14**, 1307–1314.
24. Friedstein, A.J., Chailakhjan, R.K. and Laykina, K.S. (1970) The development of fibroblast colonies in monolayer cultures of guinea-pig bone marrow and spleen cells. *Cell Tissue Kinet.* **3**, 393–403.
25. Friedstein, A.J. (1990) Osteogenic Stem Cells in Bone Marrow. In: *Bone and Mineral Research*, Eds: J.N.M. Heersche and J.A. Kanis, Elsevier, Amsterdam. pp 243–272.
26. Caplan, A.I. (1991) Mesenchymal Stem Cells. *J. Orthop. Res.* **9**, 641–650.
27. Yu, J.M., Wu, X., Gimble, J.M., Guan, X., Freitas, M.A. and Bunnell, B.A. (2011) Age-related changes in mesenchymal stem cells derived from rhesus macaque bone marrow. *Aging Cell* **10**, 66–79.
28. Koch, T.G., Thomsen, P.D. and Betts, D.H. (2009) Improved isolation protocol for equine cord blood-derived mesenchymal stromal cells. *Cytotherapy* **11**, 443–447. http://dx.doi.org/10.1080/14653240902887259.
29. Spaas, J.H., Schauwer, C. De, Cornillie, P., Meyer, E., Soom, A. Van and Walle, G.R. Van de (2013) Culture and characterisation of equine peripheral blood mesenchymal stromal cells. *Vet. J.* **195**, 107–113. http://dx.doi.org/10.1016/j.tvjl.2012.05.006.
30. Kasashima, Y., Ueno, T., Tomita, A., Goodship, A.E. and Smith, R.K.W. (2011)

Optimisation of bone marrow aspiration from the equine sternum for the safe recovery of mesenchymal stem cells. *Equine Vet. J.* **43**, 288–294.
31. Vidal, M.A., Kilroy, G.E., Lopez, M.J., Johnson, J.R., Moore, R.M. and Gimble, J.M. (2007) Characterization of equine adipose tissue-derived stromal cells: Adipogenic and osteogenic capacity and comparison with bone marrow-derived mesenchymal stromal cells. *Vet. Surg.* **36**, 613–622.
32. Dominici, M., Blanc, M. Le, Mueller, I., Slaper-Cortenbach, I., Marini, F., Krause, D., Deans, R., Keating, A., Prockop, D.J. and Horwitz, E. (2006) Minimal criteria for defining multipotent mesenchymal stromal cells. The International Society for Cellular Therepy position statement. *Cytotherapy* **8**, 315–317.
33. Schauwer, C. De, Meyer, E., Walle, G.R. Van de and Soom, A. Van (2011) Markers of stemness in equine mesenchymal stem cells: A plea for uniformity. *Theriogenology* **75**, 1431–1443. http://dx.doi.org/10.1016/j.theriogenology.2010.11.008.
34. Bundgaard, L., Stensballe, A., Elbæk, K.J. and Berg, L.C. (2018) Mapping of equine mesenchymal stromal cell surface proteomes for identification of specific markers using proteomics and gene expression analysis: An in vitro cross-sectional study. *Stem Cell Res. Ther.* **9**, 1–10.
35. Adam, E.N., Janes, J., Lowney, R., Lambert, J., Thampi, P., Stromberg, A. and MacLeod, J.N. (2019) Chondrogenic differentiation potential of adult and fetal equine cell types. *Vet. Surg.* **48**, 375–387.
36. Thampi, P., Dubey, R., Lowney, R., Adam, E.N., Janse, S., Wood, C.L. and Macleod, J.N. (2019) Effect of Skeletal Paracrine Signals on the Proliferation of Interzone Cells. *Cartilage* 1–13. https://doi.org/10.1177/1947603519841680.
37. Choudhery, M.S., Khan, M., Mahmood, R., Mehmood, A., Khan, S.N. and Riazuddin, S. (2012) Bone marrow derived mesenchymal stem cells from aged mice have reduced wound healing, angiogenesis, proliferation and anti-apoptosis capabilities. *Cell Biol. Int.* **36**, 747–753.
38. Berg, L.C., Koch, T.G., Heerkens, T., Besonov, K., Thomsen, P.D. and Betts, D.H. (2009) Chondrogenic potential of mesenchymal stromal cells derived from equine bone marrow and umbilical cord blood. *Vet Comp Orthop Traumatol* **22**, 363–370.
39. Barberini, D.J., Pereira, N., Freitas, P., Magnoni, M.S., Maia, L., Listoni, A.J., Heckler, M.C., Sudano, M.J. and Golim, M.A. (2014) Equine mesenchymal stem cells from bone marrow , adipose tissue and umbilical cord : immunophenotypic characterization and differentiation potential. *Stem Cell Res. Ther.* **5**, 1–11.
40. Barrachina, L., Romero, A., Zaragoza, P., Rodellar, C. and Vázquez, F.J. (2018) Practical considerations for clinical use of mesenchymal stem cells : From the laboratory to the horse. *Vet. J.* **238**, 49–57. https://doi.org/10.1016/j.tvjl.2018.07.004.
41. Vidal, M.A., Robinson, S.O., Lopez, M.J., Paulsen, D.B., Borkhsenious, O., Johnson, J.R., Moore, R.M. and Gimble, J.M. (2008) Comparison of chondrogenic potential in equine mesenchymal stromal cells derived from adipose tissue and bone marrow. *Vet. Surg.* **37**, 713–724.
42. Vidal, M.A., Kilroy, G.E., Johnson, J.R., Lopez, M.J., Moore, R.M. and Gimble, J.M. (2006) Cell growth characteristics and differentiation frequency of adherent equine bone marrow-derived mesenchymal stromal cells: Adipogenic and

osteogenic capacity. *Vet. Surg.* **35**, 601–610.
43. Schauwer, C. De, Goossens, K., Piepers, S., Hoogewijs, M.K., Govaere, J.L.J., Smits, K., Meyer, E., Soom, A. Van and Walle, G.R. Van De (2014) Characterization and profiling of immunomodulatory genes of equine mesenchymal stromal cells from non-invasive sources. *Stem Cell Res. Ther.* **5**, 1–13. Stem Cell Research & Therapy.
44. Park, S.H., Sim, W.Y., Min, B.H., Yang, S.S., Khademhosseini, A. and Kaplan, D.L. (2012) Chip-Based Comparison of the Osteogenesis of Human Bone Marrow- and Adipose Tissue-Derived Mesenchymal Stem Cells under Mechanical Stimulation. *PLoS One* **7**, 1–11.
45. Burk, J., Ribitsch, I., Gittel, C., Juelke, H., Kasper, C., Staszyk, C. and Brehm, W. (2013) Growth and differentiation characteristics of equine mesenchymal stromal cells derived from different sources. *Vet. J.* **195**, 98–106. http://dx.doi.org/10.1016/j.tvjl.2012.06.004.
46. Frisbie, D.D., Kisiday, J.D., Kawcak, C.E., Werpy, N.M. and McIlwraith, C.W. (2009) Evaluation of adipose-derived stromal vascular fraction or bone marrow-derived mesenchymal stem cells for treatment of osteoarthritis. *J. Orthop. Res.* **27**, 1675–1680.
47. Korchunjit, W., Laikul, A., Taylor, J., Watchrarat, K., Ritruechai, P., Supokawej, A. and Wongtawan, T. (2019) Characterization and Allogeneic Transplantation of Equine Bone Marrow–Derived Multipotent Mesenchymal Stromal Cells Collected From Cadavers. *J. Equine Vet. Sci.* **73**, 15–23. https://doi.org/10.1016/j.jevs.2018.11.004.
48. Shojaee, A. and Parham, A. (2019) Strategies of tenogenic differentiation of equine stem cells for tendon repair : current status and challenges. *Stem Cell Res. Ther.* **10**, 1–13.
49. Turinetto, V., Vitale, E. and Giachino, C. (2016) Senescence in human mesenchymal stem cells: Functional changes and implications in stem cell-based therapy. *Int. J. Mol. Sci.* **17**, 1–18.
50. Katsara, O., Mahaira, L.G., Iliopoulou, E.G., Moustaki, A., Antsaklis, A., Loutradis, D., Stefanidis, K., Baxevanis, C.N., Papamichail, M. and Perez, S.A. (2011) Effects of Donor Age, Gender, and In Vitro Cellular Aging on the Phenotypic, Functional, and Molecular Characteristics of Mouse Bone Marrow-Derived Mesenchymal Stem Cells. *Stem Cells Dev.* **20**, 1549–1561.
51. Hatsushika, D., Muneta, T., Nakamura, T., Horie, M., Koga, H., Nakagawa, Y., Tsuji, K., Hishikawa, S., Kobayashi, E. and Sekiya, I. (2014) Repetitive allogeneic intraarticular injections of synovial mesenchymal stem cells promote meniscus regeneration in a porcine massive meniscus defect model. *Osteoarthr. Cartil.* **22**, 941–950. http://dx.doi.org/10.1016/j.joca.2014.04.028.
52. Matas, J., Orrego, M., Amenabar, D., Infante, C., Tapia-Limonchi, R., Cadiz, M.I., Alcayaga-Miranda, F., González, P.L., Muse, E., Khoury, M., Figueroa, F.E. and Espinoza, F. (2019) Umbilical Cord-Derived Mesenchymal Stromal Cells (MSCs) for Knee Osteoarthritis: Repeated MSC Dosing Is Superior to a Single MSC Dose and to Hyaluronic Acid in a Controlled Randomized Phase I/II Trial. *Stem Cells Transl. Med.* **8**, 215–224.
53. Smith, R.K.W., Korda, M., Blunn, G.W. and Goodship, A.E. (2003) Isolation and

implantation of autologous equine mesenchymal stem cells from bone marrow into the superficial digital flexor tendon as a potential novel treatment. *Equine Vet. J.* **35**, 99–102.
54. Wilke, M.M., Nydam, D.V. and Nixon, A.J. (2007) Enhanced Early Chondrogenesis in Articular Defects following Arthroscopic Mesenchymal Stem Cell Implantation in an Equine Model. *J. Orthop. Res.* **25**, 913–925.
55. Lamo-Espinosa, J.M., Mora, G., Blanco, J.F., Granero-Moltó, F., Nuñez-Córdoba, J.M., Sánchez-Echenique, C., Bondía, J.M., Aquerreta, J.D., Andreu, E.J., Ornilla, E., Villarón, E.M., Valentí-Azcárate, A., Sánchez-Guijo, F., Cañizo, M.C., Valentí-Nin, J.R. and Prósper, F. (2016) Intra-articular injection of two different doses of autologous bone marrow mesenchymal stem cells versus hyaluronic acid in the treatment of knee osteoarthritis: Multicenter randomized controlled clinical trial (phase I/II). *J. Transl. Med.* **14**, 1–9.
56. Bruder, S.P., Kraus, K.H., Goldberg, V.M. and Kadiyala, S. (1998) The effect of implants loaded with autologous mesenchymal stem cells on the healing of canine segmental bone defects. *J. Bone Jt. Surg. - Ser. A* **80**, 985–996.
57. Muschler, G.F. and Midura, R.J. (2002) Connective tissue progenitors: Practical concepts for clinical applications. *Clin. Orthop. Relat. Res.* **1**, 66–80.
58. Huurne, M. ter, Schelbergen, R., Blattes, R., Blom, A., Munter, W. De, Grevers, L.C., Jeanson, J., Casteilla, L., Jorgensen, C., Berg, W. Van Den and Lent, P.L.E.M. Van (2012) Antiinflammatory and Chondroprotective Effects of Intraarticular Injection of Adipose-Derived Stem Cells in Experimental Osteoarthritis. *Arthritis Rheum.* **64**, 3604–3613.
59. Grady, S.T., Britton, L., Hinrichs, K., Nixon, A. and Watts, A.E. (2019) Persistance of fluorescent nanoparticle-labelled bone marrow mesenchymal stem cells in vitro and after intra-articular injection. *J. Tissue Eng. Regen. Med.* **13**, 191–202.
60. Lopez, M.J. and Jarazo, J. (2015) State of the art : Stem cells in equine regenerative medicine. *Equine Vet. J.* **47**, 145–154.
61. Colbath, A.C., Frisbie, D.D., Dow, S.W., Kisiday, J.D., Mcilwraith, C.W. and Goodrich, L.R. (2016) Equine Models for the Investigation of Mesenchymal Stem Cell Therapies in Orthopaedic Disease. *Oper. Tech. Sports Med.* **25**, 41–49.
62. Xu, T., Binder, K.W., Albanna, M.Z., Dice, D., Zhao, W., Yoo, J.J. and Atala, A. (2013) Hybrid printing of mechanically and biologically improved constructs for cartilage tissue engineering applications. *Biofabrocation* **5**, 1–10.
63. Kim, H., Lee, J. and Im, G. (2010) Chondrogenesis using mesenchymal stem cells and PCL scaffolds. *J. Biomed. Mater. Res. Part A* **92**, 659–666.
64. Prabha, R.D., Nair, B.P., Ditzel, N., Kjems, J., Nair, P.D. and Kassem, M. (2019) Strontium functionalized scaffold for bone tissue engineering. *Mater. Sci. Eng. C* **94**, 509–515.
65. D'Ippolito, G.D., Schiller, P.C., Ricordi, C., Roos, B.A. and Howard, G.A. (1999) Age-Related Osteogenic Potential of Mesenchymal Stromal Stem Cells from Human Vertebral Bone Marrow. *J. Bone Miner. Res.* **14**, 1115–1122.
66. Khong, S.M.L., Lee, M., Kosaric, N., Khong, D.M., Dong, Y., Hopfner, U., Aitzetmüller, M., Duscher, D., Schäfer, R. and Gurtner, G.C. (2019) Single-Cell Transcriptomics of Human Mesenchymal Stem Cells Reveal Age-Related Cellular

Subpopulation Depletion and Impaired Regenerative Function. *Stem Cells* **37**, 240–246.
67. Borjesson, D.L. and Peroni, J.F. (2011) The Regenerative Medicine Laboratory : Facilitating Stem Cell Therapy for Equine Disease. *Clin. Lab. Med.* **31**, 109–123. http://dx.doi.org/10.1016/j.cll.2010.12.001.
68. Arnhold, S.J., Goletz, I., Klein, H., Stumpf, G., Beluche, L.A., Rohde, C., Addicks, K. and Litzke, L.F. (2007) Isolation and characterization of bone marrow- derived equine mesenchymal stem cells. *Am. J. Vet. Res.* **68**, 1095–1105.
69. Kisiday, J.D., Kopesky, P.W., Evans, C.H., Grodzinsky, A.J., Mcilwraith, C.W. and Frisbie, D.D. (2008) Evaluation of Adult Equine Bone Marrow- and Adipose-Derived Progenitor Cell Chondrogenesis in Hydrogel Cultures. *J. Orthop. Res.* 322–331.
70. Martinello, T., Bronzini, I., Maccatrozzo, L., Iacopetti, I., Sampaolesi, M., Mascarello, F. and Patruno, M. (2010) Cryopreservation does not affect the stem characteristics of multipotent cells isolated from equine peripheral blood. *Tissue Eng. Part C Methods* **16**, 771–781.
71. Watts, A.E., Ackerman-yost, J.C. and Nixon, A.J. (2013) A Comparison of Three-Dimensional Culture Systems to Evaluate In Vitro Chondrogenesis of Equine Bone Marrow-Derived Mesenchymal Stem Cells. *Tissue Eng.* **19**, 2275–2283.
72. Grogan, S., Reiser, F., Winkelmann, V., Berardi, S. and Mainil-Varlet, P. (2003) A static, closed and scaffold-free bioreactor system that permits chondrogenesis in vitro. *Osteoarthr. Cartil.* **11**, 403–411.
73. Worster, A.A., Nixon, A.J., Brower-toland, B.D. and Williams, J. (2000) Effect of transforming growth factor β 1 on chondrogenic differentiation of cultured equine mesenchymal stem cells. *Am J Vet Res* **61**, 1003–1010.
74. Jakobsen, R.B., Østrup, E., Zhang, X., Mikkelsen, T.S. and Brinchmann, J.E. (2014) Analysis of the Effects of Five Factors Relevant to In Vitro Chondrogenesis of Human Mesenchymal Stem Cells Using Factorial Design and High Throughput mRNA-Profiling. *PLoS One* **9**.
75. Johnstone, B., Hering, T.M., Caplan, A.I., Goldberg, V.M. and Yoo, J.U. (1998) In Vitro Chondrogenesis of Bone Marrow-Derived Mesenchymal Progenitor Cells. *Exp. Cell Res.* **238**, 265–272.
76. Coricor, G. and Serra, R. (2016) TGF-β regulates phosphorylation and stabilization of Sox9 protein in chondrocytes through p38 and Smad dependent mechanisms. *Nat. Sci. REports* **6**, 1–11.
77. Giovannini, A., Brehm, W., Mainil-varlet, P. and Nesic, D. (2008) Multilineage differentiation potential of equine blood-derived fibroblast-like cells. *Differentiation* **76**, 118–129. http://dx.doi.org/10.1111/j.1432-0436.2007.00207.x.
78. Stewart, A.A., Byron, C.R., Pondenis, H.C. and Stewart, M.C. (2008) Effect of dexamethasone supplemantation on chondrogenesis of equine mesenchymal stem cells. *Am. J. Vet. Res.* **69**, 1013–1021.
79. Tsai, T., Manner, P. and Li, W. (2013) Regulation of mesenchymal stem cell chondrogenesis by glucose through protein kinase C/transforming growth factor signaling. *Osteoarthr. Cartil.* **21**, 368–376.
80. Temu, T.M., Wu, K.Y., Gruppuso, P.A. and Phornphutkul, C. (2010) The mechanism of ascorbic acid-induced differentiation of ATDC5 chondrogenic cells.

Am J Physiol Endocrinol Metab **299**, 325–334.
81. Ichinose, S., Tagami, M., Muneta, T. and Sekiya, I. (2005) Morphological examination during in vitro cartilage formation by human mesenchymal stem cells. *Cell Tissue Res.* **322**, 217–226.
82. Rosenberg, L. (1971) Chemical basis for the histological use of safranin O in the study of articular cartilage. *J Bone Jt. Surg Am.* **53**, 69–82.
83. Schmitz, N., Laverty, S., Kraus, V.B. and Aigner, T. (2010) Basic methods in histopathology of joint tissues. *Osteoarthr. Cartil.* **18**, S113–S116.
84. Rigueur, D. and Lyons, K.M. (2014) Whole-Mount Skeletal Staining. *Methods Mol. Biol.* **1130**, 113–121.
85. Peffers, M.J., Collins, J., Loughlin, J., Proctor, C. and Clegg, P.D. (2016) A proteomic analysis of chondrogenic , osteogenic and tenogenic constructs from ageing mesenchymal stem cells. *Stem Cell Res. Ther.* **7**, 1–17. http://dx.doi.org/10.1186/s13287-016-0384-2.
86. Jaiswal, N., Haynesworth, S.E., Caplan, A.I. and Bruder, S.P. (1997) Osteogenic differentiation of purified, culture-expanded human mesenchymal stem cells in vitro. *J. Cell Biochem.* **64**, 295–312.
87. Glynn, E.R.A., Londono, A.S., Zinn, S.A., Hoagland, T.A. and Govoni, K.E. (2013) Culture conditions for equine bone marrow mesenchymal stem cells and expression of key transcription factors during their differentiation into osteoblasts. *J. Anim. Sci. Biotechnol.* **4**, 1–10.
88. Langenbach, F. and Handschel, J. (2013) Effects of dexamethasone, ascorbic acid and β-glycerophosphate on the osteogenic differentiation of stem cells in vitro. *Stem Cell Res. Ther.* **4**, 117.
89. McKee, M.D. and Cole, W.G. (2012) Bone Martix and Mineralization. In: *Pediatric Bone*, 2nd ed., Ed: Elsevier. pp 9–37.
90. Golub, E.E. and Boesze-Battaglia, K. (2007) The role of alkaline phosphatase in mineralization. *Curr Opin Orthop* **18**, 444–448.
91. Ryan, J.M., Barry, F.P., Murphy, J.M. and Mahon, B.P. (2005) Mesenchymal stem cells avoid allogeneic rejection. *J. Inflamm.* **2**, 1–11.
92. Schnabel, L. V, Pezzanite, L.M., Antczak, D.F., Felippe, M.J.B. and Fortier, L.A. (2014) Equine bone marrow-derived mesenchymal stromal cells are heterogeneous in MHC class II expression and capable of inciting an immune response in vitro. *Stem Cell Res. Ther.* **5**, 1–13.
93. Pezzanite, L.M., Fortier, L.A., Antczak, D.F., Cassano, J.M., Brosnahan, M.M., Miller, D. and Schnabel, L. V (2015) Equine allogeneic bone marrow-derived mesenchymal stromal cells elicit antibody responses in vivo. *Stem Cell Res. Ther.* **6**, 1–11.
94. Joswig, A., Mitchell, A., Cummings, K.J., Levine, G.J., Gregory, C.A., Smith III, R. and Watts, A.E. (2017) Repeated intra-articular injection of allogeneic mesenchymal stem cells causes an adverse response compared to autologous cells in the equine model. *Stem Cell Res. Ther.* **8**, 1–11.
95. Hailey, E. (2018) Medical Advantages of Allogeneic vs Autologous Stem Cell Transplants as Treatment in Blood Related Cancer Patients. *Acad. Festiv.* **131**, 1–22.
96. Frisbie, D.D., McCarthy, H.E., Archer, C.W., Barrett, M.F. and Mcilwraith, C.W.

(2015) Evaluation of articular cartilage progenitor cells for the repair of articular defects in an equine model. *J Bone Jt. Surg Am.* **97**, 484–493.
97. Asumda, F.Z. and Chase, P.B. (2011) Age-related changes in rat bone-marrow mesenchymal stem cell plasticity. *BMC Cell Biol.* **12**, 44. http://www.biomedcentral.com/1471-2121/12/44.
98. Sampogna, G., Guraya, S.Y. and Forgione, A. (2015) Regenerative medicine: Historical roots and potential strategies in modern medicine. *J. Microsc. Ultrastruct.* **3**, 101–107.
99. Wang, Y., Chen, X., Cao, W. and Shi, Y. (2014) Plasticity of mesenchymal stem cells in immunomodulation: Pathological and therapeutic implications. *Nat. Immunol.* **15**, 1009–1016.
100. Justesen, J., Stenderup, K., Eriksen, E.F. and Kassem, M. (2002) Maintenance of Osteoblastic and Adipocytic Differentiation Potential with Age and Osteoporosis in Human Marrow Stromal Cell Cultures. *Calcif. Tissue Int.* **71**, 36–44.
101. Rumman, M., Majumder, A., Harkness, L., Venugopal, B., Vinay, M.B., Pillai, M.S., Kassem, M. and Dhawan, J. (2018) Induction of quiescence (G0) in bone marrow stromal stem cells enhances their stem cell characteristics. *Stem Cell Res.* **30**, 69–80.
102. Horvath, S. and Raj, K. (2018) DNA methylation-based biomarkers and the epigenetic clock theory of ageing. *Nat. Rev. Genet.* **19**, 371–384.
103. Jung, M. and Pfeifer, G.P. (2015) Aging and DNA methylation. *BMC Biol.* **13**, 1–8.
104. Shay, J.W. and Wright, W.E. (2000) Hayflick , his limit , and cellular ageing. *Nat. Rev. Mollecular Cell Biol.* **1**, 72–76.
105. Sethe, S., Scutt, A. and Stolzing, A. (2006) Aging of mesenchymal stem cells. *Ageing Res. Rev.* **5**, 91–116.
106. Lange, T. de, Shiue, L., Myers, R.M., Cox, D.R., Naylor, S.L. and Varmus, H.E. (1990) Structure and variability of human chromosome ends. *Mol. Cell Biol.* **10**, 518–527.
107. Beauséjour, C.M., Krtolica, A., Beause, C.M., Galimi, F., Narita, M., Lowe, S.W., Yaswen, P. and Campisi, J. (2003) Reversal of human cellular senescence : roles of the p53 and p16 pathways. *EMBO J.* **22**, 4212–4222.
108. Campisi, J. (2001) From cells to organisms: can we learn about aging from cells in culture? *Exp. Gerontol.* **36**, 607–618.
109. Harley, C.B., Futcher, B. and Greider, C.W. (1990) Telomeres shorten during ageing of human fibroblasts. *Nature* **345**, 458–460.
110. Alberts, B., Johnson, A., Lewis, J., Morgan, D., Raff, M., Roberts, K. and Walter, P. (2015) The Cell Cycle. In: *Molecular Biology of THE CELL*, 6th ed., Garland Science. pp 963–1020.
111. Romagosa, C., Simonetti, S., López-Vicente, L., Mazo, A., Lleonart, M.E., Castellvi, J. and Cajal, S.R. (2011) p16 Ink4a overexpression in cancer : a tumor suppressor gene associated with senescence and high-grade tumors. *Oncogene* **30**, 2087–2097.
112. Jayasurya, R., Sathyan, K.M., Lakshminarayanan, K., Abraham, T., Nalinakumari, K.R., Abraham, E.K., Krishnan Nair, M. and Kannan, S. (2005) Phenotypic alterations in Rb pathway have more prognostic influence than p53 pathway

proteins in oral carcinoma. *Mod. Pathol.* **18**, 1056–1066.
113. Fujisawa, M., Tanaka, H., Tatsumi, N., Okada, H., Arakawa, S. and Kamidono, S. (1998) Telomerase activity in the testis of infertile patients with selected causes. *Hum. Reprod.* **6**, 1476–1479.
114. Thomson, J.A., Itskovitz-Eldor, J., Shapiro, S.S., Waknitz, M.A., Swiergiel, J.J., V.S., M. and Jones, J.M. (1998) Embryonic stem cell lines derived from human blastocysts. *Science (80-.).* **282**, 1145–1147.
115. Ostenfeld, T., Caldwell, M.A., Prowse, K.R., Linskens, M.H., Jauniaux, E. and C.N., S. (200AD) Human neural precurssor cells express low levels of telomerase in vitro and show diminishing cell proliferation with extensice axonal outgrowth following transplantation. *Exp. Neurol.* **164**, 215–226.
116. Chiu, C.., Dragowska, W., Kim, N.W., Vaziri, H., Yui, J., T.E., T., Harley, C.B. and Lansdorp, P.M. (1996) Differential expression of telomerase activity in hematopoietic progenitors from adult human bone marrow. *Stem Cells* **14**, 239–248.
117. Izadpanah, R., Trygg, C., Patel, B., Kriedt, C., Dufour, J., Gimble, J.M. and Bunnell, B.A. (2006) Biological Properties of Mesenchymal Stem Cells Derived From Bone Marrow and Adipose Tissue. *J. Cell Biochem.* **99**, 1285–1297.
118. Zimmerman, S., Voss, M., Kaiser, S., Krapp, U., Waller, C.F. and Martens, U.M. (2003) Lack of telomerase activity in human mesenchymal stem cells. *Leukemia* **17**, 1146–1149.
119. Wilson, B., Novakofski, K.D., Donocoff, R.S., Liang, Y.X.A. and Fortier, L.A. (2014) Telomerase Activity in Articular Chondrocytes Is Lost after Puberty. *Cartilage* **5**, 215–220.
120. Vidal, M.A., Walker, N.J., Napoli, E. and Borjesson, D.L. (2012) Evaluation of Senescence in Mesenchymal Stem Cells Isolated from Equine Bone Marrow, Adipose Tissue, and Umbilical Cord Tissue. *Stem Cells Dev.* **21**, 273–283.
121. Herranz, N. and Gil, J. (2018) Mechanisms and functions of cellular senescence. *J. Clin. Invest.* **128**, 1238–1246.
122. Zhou, S., Greenberger, J.S., Epperly, M.W., Goff, J.P., Adler, C., Leboff, M.S. and Glowacki, J. (2008) Age-related intrinsic changes in human bone-marrow- derived mesenchymal stem cells and their differentiation to osteoblasts. *Aging Cell* 335–343.
123. Stolzing, A., Jones, E., Mcgonagle, D. and Scutt, A. (2008) Age-related changes in human bone marrow-derived mesenchymal stem cells : Consequences for cell therapies. *Mech. Ageing Dev.* **129**, 163–173.
124. Choudhery, M.S., Badowski, M., Muise, A., Pierce, J. and Harris, D.T. (2014) Donor age negatively impacts adipose tissue-derived mesenchymal stem cell expansion and differentiation. *J. Transl. Med.* **12**, 1–14.
125. Guercio, A., Bella, S. Di, Casella, S., Marco, P. Di, Russo, C. and Piccione, G. (2013) Canine mesenchymal stem cells (MSCs): characterization in relation to donor age and adipose tissue-harvesting site. *Cell Biol. Int.* **37**, 789–798.
126. Wilson, A., Shehadeh, L.A., Yu, H. and Webster, K.A. (2010) Age-related molecular genetic changes of murine bone marrow mesenchymal stem cells. *BMC Genomics* **11**, 1–14.
127. Zheng, H., Martin, J.A., Duwayri, Y., Falcon, G. and Buckwalter, J.A. (2007)

Impact of Aging on Rat Bone Marrow-Derived Stem Cell Chondrogenesis. *J. Geriontology* **62A**, 136–148.
128. Alvarez-Veijo, M., Menedez, Y., Bionco-Galeaz, M.A., Ferrero-Gutierrez, A., Fernandez-Rodriguez, J., Gala, J. and Otero-Hernandez, J. (2013) Quantifying Mesenchymal Stem Cells in the Mononuclear Cell Fraction of Bone Marrow Samples Obtained for Cell Therapy. *Transplation Proc.* **45**, 434–439.
129. Mazini, L., Rochette, L., Amine, M. and Malka, G. (2019) Regenerative Capacity of Adipose Derived Stem Cells (ADSCs), Comparison with Mesenchymal Stem Cells (MSCs). *Int. J. Mol. Sci.* **20**, 2523.
130. Siegel, G., Kluba, T., Hermanutz-Klein, U., Bieback, K., Northoff, H. and Schäfer, R. (2013) Phenotype, donor age and gender affect function of human bone marrow-derived mesenchymal stromal cells. *BMC Med.* **11**, 1–20.
131. Stenderup, K., Justesen, J., Clausen, C. and Kassem, M. (2003) Aging is associated with decreased maximal life span and accelerated senescence of bone marrow stromal cells. *Bone* **33**, 919–926.
132. Salic, A. and Mitchison, T.J. (2008) A chemical method for fast and sensitive detection of DNA synthesis in vivo. *PNAS* **105**, 2415–2420.
133. Schröck, C., Eydt, C., Geburek, F., Kaiser, L., Felicitas, P., Burk, J., Pfarrer, C. and Staszyk, C. (2017) Bone marrow-derived multipotent mesenchymal stromal cells from horses after euthanasia. *Vet. Med. Sci.* **3**, 239–251.
134. Chen, H., Lee, M., Chen, C. and Chuang, S. (2012) Proliferation and differentiation potential of human adipose-derived mesenchymal stem cells isolated from elderly patients with osteoporotic fractures. *J. Cell. Mol. Med.* **16**, 582–592.
135. Wu, W., Niklason, L. and Steinbacher, D.M. (2013) The effect of age on human adipose-derived stem cells. *Plast. Reconstr. Surg.* **131**, 27–37.
136. Kretlow, J.D., Jin, Y., Liu, W., Zhang, W.J., Hong, H., Zhou, G., Baggett, L.S., Mikos, A.G. and Cao, Y. (2008) Donor age and cell passage affects differentiation potential of murine bone marrow-derived stem cells. *BMC Biol.* **9**, 1–13.
137. Shi, Y.Y., Nacamuli, R.P., Salim, A. and Longaker, M.T. (2005) The osteogenic potential of adipose-derived mesenchmal cells is maintained with aging. *Plast. Reconstr. Surg.* **116**, 1686–1696.
138. Bailey, C J., Reid, S W J., Hodgson, D R., Rose, R.J. (1999) Impact of injuries and disease on a cohort of two- and three-year-old thoroughbreds in training. *Vet. Rec.* **145**, 487–493.
139. Schnabel, L. V, Lynch, M.E., Meulen, M.C.H. van der, Yeager, A.E., Kornatowski, M.A. and Nixon, A.J. (2009) Mesenchymal Stem Cells and Insulin-Like Growth Factor-I Gene- Enhanced Mesenchymal Stem Cells Improve Structural Aspects of Healing in Equine Flexor Digitorum Superficialis Tendons. *J. Orthop. Res.* 1392–1398.
140. Dexheimer, V., Frank, S. and Richter, W. (2012) Proliferation as a Requirement for In Vitro Chondrogenesis of Human Mesenchymal Stem Cells. *Stem Cells Dev.* **21**, 2160–2169.
141. Escacena, N., Quesada-Hernández, E., Capilla-Gonzalez, V., Soria, B. and Hmadcha, A. (2015) Bottlenecks in the efficient use of advanced therapy medicinal products based on mesenchymal stromal cells. *Stem Cells Int.* **2015**.

142. Whitworth, D.J. and Banks, T.A. (2014) Stem cell therapies for treating osteoarthritis : Prescient or premature ? *Vet. J.* **202**, 416–424.
143. USDA (2005) *Equine Report 2005. Part II: Changes in the U.S. Equine Industry, 1998-2005*. https://www.aphis.usda.gov/animal_health/nahms/equine/downloads/equine05/Equine05_dr_PartII.pdf.
144. Mienaltowski, M.J., Huang, L., Stromberg, A.J. and Macleod, J.N. (2008) Differential gene expression associated with postnatal equine articular cartilage maturation. *BMC Musculoskelet. Disord.* **9**, 1–14.
145. Hestand, M.S., Kalbfleisch, T.S., Coleman, S.J., Zeng, Z., Liu, J., Orlando, L. and Macleod, J.N. (2015) Annotation of the Protein Coding Regions of the Equine Genome. *PLoS One* 1–13. http://dx.doi.org/10.1371/journal.pone.0124375.
146. Ramakers, C., Ruijter, J.M., Lekanne, R.H. and Moorman, A.F.M. (2003) Assumption-free analysis of quantitative real-time polymerase chain reaction (PCR) data. *Neoroscience Lett.* **339**, 62–66.
147. Andersen, C.L., Jensen, J.L. and Ørntoft, T.F. (2004) Normalization of Real-Time Quantitative Reverse Transcription-PCR Data: A Model-Based Variance Estimation Approach to Identify Genes Suited for Normalization, Applied to Bladder and Colon Cancer Data Sets. *Cancer Res.* **64**, 5245–5250.
148. Olwagen, C.P., Adrian, P. V and Madhi, S.A. (2019) Performance of the Biomark HD real-time qPCR System (Fluidigm) for the detection of nasopharyngeal bacterial pathogens and Streptococcus pneumoniae typing. *Sci. Rep.* 1–11. http://dx.doi.org/10.1038/s41598-019-42846-y.
149. Livak, J.K. and Schmittgen, T.. (2001) Analysis of Relative Gene Expression Data Using Real-Time Quantitative PCR and the 2−ΔΔCT Method. *Methods* **25**, 404–408.
150. Kalluri, R. (2016) The biology and function of fibroblasts in cancer. *Nat. Rev. Cancer* **16**, 582–598. http://dx.doi.org/10.1038/nrc.2016.73.
151. Strzalka, W. and Ziemienowicz, A. (2011) Proliferating cell nuclear antigen (PCNA): a key factor in DNA replication and cell cycle regulation. *Ann. Bot.* **107**, 1127–1140.
152. Wagner, W., Bork, S., Lepperdinger, G., Joussen, S., Ma, N. and Koch, C. (2010) How to track cellular aging of mesenchymal stromal cells ? *Aging (Albany. NY).* **2**, 224–230.
153. Jesenberger, V. and Jentsch, S. (2002) DEADLY ENCOUNTER : UBIQUITIN MEETS APOPTOSIS. *Nat. Rev. Mollecular Cell Biol.* **3**, 112–121.
154. Lee, B.Y., Han, J.A., Im, J.S., Morrone, A., Johung, K., Goodwin, C., Kleijer, W.J., Dimaio, D. and Hwang, E.S. (2006) Senescence-associated β -galactosidase is lysosomal β -galactosidase. *Aging Cell* **5**, 187–195.
155. Rodrigues, M., Miguita, L., Andrade, N.P.D.E., Heguedusch, D., Rodini, C.O., Moyses, R.A., Toporcov, T.N., Gama, R.R., Tajara, E.E. and Nunes, F.D. (2018) GLI3 knockdown decreases stemness , cell proliferation and invasion in oral squamous cell carcinoma. *Int. J. Oncol.* **53**, 2458–2472.
156. Rowland, A.L., Xu, J.J., Joswig, A.J., Gregory, C.A., Antczak, D.F., Cummings, K.J. and Watts, A.E. (2018) In vitro MSC function is related to clinical reaction in vivo. *Stem Cell Res. Ther.* **9**, 1–9.

157. Hillmann, A., Ahrberg, A.B., Brehm, W., Heller, S., Josten, C., Paebst, F. and Burk, J. (2016) Comparative Characterization of Human and Equine Mesenchymal Stromal Cells : A Basis for Translational Studies in the Equine Model. *Cell Transplant.* **25**, 109–124.
158. Caplan, A.I. (2007) Adult Mesenchymal Stem Cells for Tissue Engineering Versus Regenerative Medicine. *J. Cell. Physiol.* **213**, 341–347.
159. Jones, M. V and Calabresi, P.A. (2007) Agar-gelatin for embedding tissues prior to paraffin processing. *Biotechniques* **42**, 569–570.
160. Taghiyar, L., Hosseini, S., Hesaraki, M. and Sayahpour, F.A. (2018) Isolation , Characterization and Osteogenic Potential of Mouse Digit Tip Blastema Cells in Comparison with Bone Marrow-Derived Mesenchymal Stem Cells In Vitro. *Cell J.* **19**, 585–598.
161. Gregory, C.A., Gunn, W.G., Peister, A. and Prockop, D.J. (2004) An Alizarin red-based assay of mineralization by adherent cells in culture: comparison with cetylpyridinium chloride extraction. *Anal. Biochem.* **329**, 77–84.
162. Wu, L.N., Ishikawa, Y., Sauer, B.R., Genge, F., Mwale, F., Mishima, H. and Wuthier, R.E. (1995) Morphological and biochemical characterization of mineralizing primary cultures of avian growth plate chondrocytes: evidence for cellular processing of Ca2+ and Pi prior to matrix mineralization. *J. Cell Biochem.* **57**, 218–237.
163. Braun, J., Hack, A., Weis-Klemm, M., Conrad, S., Treml, S., Kohler, K., Walliser, U., Skutella, T. and Aicher, W.K. (2010) Evaluation of the osteogenic and chondrogenic differentiation capacities of equine adipose-tissue-derived mesenchymal stem cells. *Am. J. Vet. Res.* **71**, 1228–1236.
164. Toupadakis, C.A., Wong, A., Genetos, D.C., Cheung, W.K., Borjesson, D.L., Ferraro, G.L., Galuppo, L.D., Leach, J.K., Owens, S.D. and Yellowley, C.E. (2010) Comparison of the osteogenic potential of equine mesenchymal stem cells from bone marrow, adipose tissue, umbilical cord blood, and umbilical cord tissue. *Am. J. Vet. Res.* **71**, 1237–1245.
165. Shafiee, A., Seyedjafari, E., Soleimani, M., Ahmadbeigi, N., Dinarvand, P. and Ghaemi, N. (2011) A comparison between osteogenic differentiation of human unrestricted somatic stem cells and mesenchymal stem cells from bone marrow and adipose tissue. *Biotechnol. Lett.* **33**, 1257–1264.
166. Liao, H.-T. and Chen, C.-T. (2014) Osteogenic potential: Comparison between bone marrow and adipose-derived mesenchymal stem cells. *World J. Stem Cells* **6**, 288–295.
167. Kang, B.J., Ryu, H.H., Park, S.S., Koyama, Y., Kikuchi, M., Woo, H.M., Kim, W.H. and Kweon, O.K. (2012) Comparing the osteogenic potential of canine mesenchymal stem cells derived from adipose tissues, bone marrow, umbilical cord blood, and Wharton's jelly for treating bone defects. *J. Vet. Sci.* **13**, 299–310.
168. Chung, D.J., Hayashi, K., Toupadakis, C.A., Wong, A. and Yellowley, C.E. (2012) Osteogenic proliferation and differentiation of canine bone marrow and adipose tissue derived mesenchymal stomal cells and the influence of hypoxia. *Res. Vet. Sci.* **92**, 66–75.
169. Ducy, P., Zhang, R., Geoffroy, V., Ridall, A.L. and Karsenty, G. (1997) Osf2 / Cbfa1 : A Transcriptional Activator of Osteoblast Differentiation. *Cell* **89**, 747–

754.
170. Koo, K., Lee, S.W., Lee, M., Kim, K.H., Jung, S.H. and Kang, Y.G. (2014) Time-dependent expression of osteoblast marker genes in human primary cells cultured on microgrooved titanium substrata. *Clin. Oral Implants Res.* **25**, 714–722.
171. Lee, N.K., Sowa, H., Hinoi, E., Ferron, M., Ahn, J.D., Confavreux, C., Dacquin, R., Mee, P.J., Mckee, M.D., Jung, D.Y., Zhang, Z., Kim, J.K., Mauvais-jarvis, F., Ducy, P. and Karsenty, G. (2007) Endocrine Regulation of Energy Metabolism by the Skeleton. *Cell* **130**, 456–469.
172. Chung, C.H., Golub, E.E., Forbes, E., Tokuoka, T. and Shapiro, I.M. (1992) Mechanism of action of β-glycerophosphate on bone cell mineralization. *Calcif. Tissue Int.* **51**, 305–311.
173. Kamm, J.L., Parlane, N.A., Riley, C.B., Gee, E.K., Dittmer, E. and Mcilwraith, C.W. (2019) Blood type and breed-associated differences in cell marker expression on equine bone marrow-derived mesenchymal stem cells including major histocompatibility complex class II antigen expression. *PLoS One* **14**, 1–16. http://dx.doi.org/10.1371/journal.pone.0225161.
174. Lee, S.H. and Sinko, P.J. (2006) siRNA — Getting the message out. *Eur. J. Pharm. Sci.* **27**, 401–410.
175. Horvath, S. (2013) DNA methylation age of human tissues and cell types. *Genome Biol.* **14**, R115.
176. Ocampo, A., Reddy, P., Martinez-redondo, P., Guillen, I., Guillen, P., Ocampo, A., Reddy, P., Martinez-redondo, P., Platero-luengo, A., Hatanaka, F., Campistol, J.M., Guillen, I., Guillen, P., Carlos, J. and Belmonte, I. (2016) In Vivo Amelioration of Age-Associated Hallmarks by Partial Reprogramming. *Cell* **167**, 1719–1733.
177. Mendelsohn, A.R. and Larrick, J.W. (2019) Epigenetic Age Reversal by Cell-Extrinsic and Cell-Intrinsic Means. *Rejuvenation Res.* **22**.
178. Dressler, M.R., Butler, D.L. and Boivin, G.P. (2005) Effects of age on the repair ability of mesenchymal stem cells in rabbit tendon. *J. Orthop. Res.* **23**, 287–293.
179. Rauscher, F.M., Goldschmidt-Clermont, P.J., Davis, B.H., Wang, T., Gregg, D., Ramaswami, P., Pippen, A.M., Annex, B.H., Dong, C. and Taylor, D.A. (2003) Aging, Progenitor Cell Exhaustion, and Atherosclerosis. *Circulation* **108**, 457–463.
180. Li, J., Hosseini-Beheshti, E., Grau, G., Zreiqat, H. and Little, C. (2019) Stem Cell-Derived Extracellular Vesicles for Treating Joint Injury and Osteoarthritis. *Nanomaterials* **9**, 261.

VITA

Jasmin Bagge

Place of Birth: Copenhagen, Denmark

EDUCATION

2015 – Present	*Dual Degree PhD Candidate*, Department of Veterinary Clinical Sciences, University of Copenhagen, Denmark, and Department of Veterinary Science, University of Kentucky, USA
2012 – 2015	*Doctor of Veterinary Medicine (DVM)*, University of Copenhagen, Denmark
2009 – 2012	*Bachelor of Science in Veterinary Medicine*, University of Copenhagen, Denmark

PROFESSIONAL POSITIONS

2015 – Present	*Graduate Research Assistant*, Department of Veterinary Science, University of Kentucky, USA
2015	*Scientific Assistant*, Department of Large Animal Sciences, Faculty of Health and Medical Sciences, University of Copenhagen
2014	*Veterinary Student Assistant*, Højelse Hestepraksis (equine veterinary clinic and stud farm), Denmark

SCHOLASTIC AND PROFESSIONAL HONORS

2018	Hubbard Award of Excellence, University of Kentucky, USA
2018	2nd place in 3 Minute Thesis Competition, University of Kentucky, USA
2008	Lektor Einar Rønnau og Lektor Adolph Rønnau's Grant for academic excellence, Frederiksberg Gymnasium, Denmark
2006	Winner of the Microbiologists Galathea 3 Expedition Competition
2005	Valedictorian, Kirkebjerg Folkeskole, Denmark

PROFESSIONAL PUBLICATIONS

Journal articles

Bagge, J. (2017): Internationalt forskningssamarbejde om stamceller og ledskader. *Ridehesten, Hippologisk i Avl og Sport*, Vol. 6, pp. 38-42.

Bagge, J., A. Tnibar, S.S. Nielsen and R. Buhl: Evaluation of surgical treatments of equine sarcoids – A multicenter international retrospective study. *Journal of Equine Veterinary Science*. Submitted July 2019.

Manuscripts under preparation

Bagge, J., L.C. Berg, J. Janes, S.L. Buchardt, E. Melcher and J.N. MacLeod: The effect of donor age on the chondrogenic and osteogenic differentiation performance of equine mesenchymal stem cells in culture.

Bagge, J., J.N. MacLeod and L.C. Berg: Donor age effects on equine mesenchymal stem cells proliferative potential in culture.

Peer – reviewed abstracts

Bagge, J., J.N. Macleod and L.C. Berg (2019): The Effect of Donor Age on the Proliferative and Osteogenic Differentiation Potential of Bone Marrow Derived Mesenchymal Stem Cells in Culture, *Danish Stem Cell Society (DASCS) Conference 2019*, Vejle, Denmark

Bagge, J., L.C. Berg and J.N. MacLeod (2019): Donor Age Effects on the Proliferative and Osteogenic Differentiation Potential of Equine Bone Marrow Derived Mesenchymal Stem Cells in Culture, *8th Annual International Symposium on Regenerative Rehabilitation*, Charlottesville, VA, USA

Written interviews

Pence, T., J. Bagge, L. Berg and J.N. MacLeod (2016): University of Copenhagen Team Up for Dual PhD Program, *TheHorse.com*, Dec. 23, 2016.

Oral presentations

2019	*Poster presentation* at the 8th Annual International Symposium on Regenerative Rehabilitation, Charlottesville, VA, USA, with the title: Donor Age Effects on the Proliferative and Osteogenic Differentiation Potential of Equine Bone Marrow Derived Mesenchymal Stem Cells in Culture
2019	*Poster presentation* at the Danish Stem Cell Society Conference, Vejle, Denmark, with the title: Effect of Donor Age on the Proliferative and Osteogenic Differentiation Potential of Equine Bone Marrow Derived Mesenchymal Stem Cells in Culture
2019	*Departmental seminar* at Department of Veterinary Clinical Sciences, University of Copenhagen, Denmark, with the title: Donor Age Effects on Equine Mesenchymal Stem Cells
2018	*3 Minute Thesis Competition*, Gluck Equine Research Center, University of Kentucky, USA, with the title: Donor age Effects on Stem Cells Potential to Treat Osteoarthritis in Horses
2018	*Veterinary Science Seminar* at Gluck Equine Research Center, Kentucky, USA, with the title: The Effect of Donor Age on Equine Mesenchymal Stem Cells
2017	*Veterinary Science Seminar* at Gluck Equine Research Center, Kentucky, USA, with the title: The Importance of Donor Age on the Proliferation and Chondrogenic/Osteogenic Differentiation Performance of Equine Mesenchymal Stem Cells in culture
2016	*Departmental seminar* at the Department of Large Animal Sciences, University of Copenhagen Denmark, with the title: Mesenchymal stem cells for the treatment of cartilage and bone injuries in horses